

Aus dem Departement Innere Medizin  
Klinik für Innere Medizin IV: Nephrologie und Allgemeinmedizin  
des Universitätsklinikums Freiburg im Breisgau

**Characterization of zebrafish lines with mutations in the nephronophthisis-associated  
genes *nphp1*, *nphp2*, *nphp4* and *nphp8***

INAUGURAL-DISSERTATION

zur

Erlangung des Medizinischen Doktorgrades  
der Medizinischen Fakultät  
der Albert-Ludwigs-Universität Freiburg im Breisgau

Vorgelegt 2022

von Nicolas Michel Kayser  
geboren in Esch-sur-Alzette, Luxemburg

Dekan: Prof. Dr. med. Lutz Hein

1. Gutachter: Prof. Dr. med. Gerd Walz

2. Gutachter: Prof. Dr. med. Martin Moser

Jahr der Promotion: 2023

## Table of contents

<b>Abstract.....</b>	<b>6</b>
<b>1. Introduction.....</b>	<b>7</b>
1.1 Kidney function and dysfunction .....	7
1.2 Kidney development in vertebrates: pronephros, mesonephros, metanephros .....	8
1.2.1 Kidney development in zebrafish .....	10
1.3 Nephronophthisis (NPH).....	11
1.4 Zebrafish as a model organism.....	13
1.5 Development of cloaca cysts in zebrafish .....	14
1.6 Development of kidney cysts in the zebrafish pronephros .....	14
1.7 Development of other ciliopathy associated phenotypes in zebrafish .....	15
1.8 NPHP genes and gene products .....	16
1.8.1 Nphp1 .....	16
1.8.2 Invs/Nphp2 .....	17
1.8.3 Nphp4 .....	19
1.8.4 Rpgrp1-1L/Nphp8 .....	21
1.9 Gene modification techniques .....	22
1.9.1 ENU mutagenesis .....	22
1.9.2 Morpholino oligonucleotide (MO)-induced knock-down .....	23
1.9.3 CRISPR/Cas9 system .....	25
1.10 Aims of this work.....	29
<b>2. Materials and Methods.....</b>	<b>30</b>
2.1 Materials.....	30
2.1.1 Chemicals.....	30
2.1.2 Enzymes and biological reagents .....	31
2.1.3 Bacteria.....	31
2.1.4 Kits.....	31
2.1.5 Consumables.....	31
2.1.6 Solutions .....	32
2.1.7 Primers for PCR and sequencing.....	34
2.1.8 Oligonucleotides for sgRNA construction .....	35
2.1.9 Morpholino oligonucleotides.....	35
2.1.10 Hardware .....	35
2.1.11 Software.....	36
2.2. Housing and mating conditions of adult zebrafish.....	36
2.2.1 Housing conditions .....	37
2.2.2 Mating of the zebrafish.....	37

2.3 Embryo collection and maintenance .....	37
2.3.1 Embryo collection.....	37
2.3.2 Embryo maintenance .....	38
2.4 Microinjection technique.....	38
2.4.1 MO injections .....	38
2.5. Zebrafish lines.....	39
2.5.1 Transgenic lines.....	39
2.5.2 Mutant lines and their transgenic outcrosses.....	39
2.6 Lysis of zebrafish embryos or after fin clipping .....	40
2.7 Polymerase chain reaction (PCR) .....	40
2.7.1 Standard PCR .....	41
2.7.2 Gradient PCR.....	42
2.7.3 PCR in the sgRNA construction process.....	42
2.7.4 PCR on PCR.....	43
2.7.5 Colony PCR.....	43
2.8 Agarose gel electrophoresis .....	44
2.9 Purification of PCR products .....	45
2.10 DNA sequencing (Sanger sequencing) .....	45
2.11 sgRNA construction for CRISPR/Cas9 gene editing method.....	45
2.12 Crispr/Cas9 Injections.....	47
2.13 TOPO Cloning.....	48
2.14 Transformation .....	48
2.15. Clone selection.....	48
2.16 Plasmid DNA preparation – Mini preparation .....	49
2.17 <i>In situ</i> hybridization .....	49
2.18 Microscopy.....	51
2.19 Statistical analysis .....	51
<b>3. Results .....</b>	<b>52</b>
3.1 Ciliopathy phenotypes in zebrafish mutant lines with defined point mutations – an intergenerational comparison .....	52
3.1.1 Point mutations in <i>invs/nphp2</i> .....	54
3.1.2 Point mutations in <i>nphp4</i> .....	57
3.1.3 Point mutations in <i>rpgrip11/nphp8</i> .....	62
3.2 <i>nphp4</i> morpholino-oligonucleotide (MO)-induced knockdown .....	67
3.2.1 <i>nphp4<sup>sa41188</sup></i> MO knockdown .....	67
3.2.2 <i>nphp4<sup>sa38686</sup></i> MO knockdown.....	69
3.3 Ciliopathy phenotypes in zebrafish mutant lines with large deletions.....	71
3.3.1 <i>nphp4-ex1-del5</i> .....	71

3.3.2 <i>nphp1-ex15-del4</i> .....	76
3.4 Generation of a new <i>invs/nphp2</i> mutant line by CRISPR/Cas9.....	77
<b>4. Discussion.....</b>	<b>82</b>
4.1 Zebrafish lines with defined <i>nphp</i> point mutations show no consistent genotype-phenotype correlation in F1 .....	82
4.2 Intergenerational compensation of phenotypes in zebrafish lines with defined point mutations .....	86
4.3 Resistance to MO-induced knockdown in <i>nphp4</i> mutants.....	88
4.4 Ciliopathy phenotypes in zebrafish mutant lines with large deletions.....	91
4.3.1 <i>nphp4-ex1-del5</i> .....	92
4.3.2 <i>nphp1-ex15-del4</i> .....	93
4.4 The CRISPR/Cas9 method can be used to generate new loss-of-function mutants.....	94
4.5 Conclusion.....	96
<b>5. German summary / Zusammenfassung .....</b>	<b>97</b>
<b>6. Acknowledgments .....</b>	<b>98</b>
<b>7. References .....</b>	<b>99</b>
<b>8. Publication .....</b>	<b>111</b>
<b>9. Apendix .....</b>	<b>112</b>
9.1 Abbreviations.....	112
9.2 List of tables .....	113
9.3 List of figures .....	114
<b>Lebenslauf.....</b>	<b>115</b>
<b>Eidesstattliche Versicherung.....</b>	<b>116</b>
<b>Erklärung zum Eigenanteil.....</b>	<b>117</b>

## Abstract

Nephronophthisis (NPH) is a rare autosomal recessive genetic kidney disease. It is the most common genetic cause of end-stage renal failure in children and young adults and is characterized by its phenotypic and genotypic heterogeneity. To this date, mutations in more than 25 different NPHP genes have been associated with NPH. Most of these genes encode proteins that localize to the cilium and mutations in these genes affect ciliary function. Thus, NPH is considered a ciliopathy.

I used zebrafish, a well-established model system in biomedical research, to characterize chemically induced point mutations in the *nphp1*, *nphp2*, *nphp4*, and *nphp8* genes. Two successive generations of mutant fish were assessed for typical ciliopathy-associated phenotypes, including glomerular cysts formation, cloaca malformation, aberrant heart-looping, heart edema, hydrocephalus and abnormal body curvature. Recently, discrepancies between phenotypes caused by morpholino oligonucleotides (MO)-mediated target gene depletion, and mutants with defined mutations have uncovered the ability of zebrafish to compensate defective gene functions. Although still poorly understood, several concepts including transcriptional adaptation triggered by mRNA decay have been implicated to explain this phenomenon of “genetic robustness”. We questioned whether this acquired compensation is passed down to the progeny of mutant zebrafish. We observed that typical ciliopathy phenotypes (i.e. glomerular cysts and cloaca malformation) were further reduced between F1 and F2 generations, suggesting evolutionary compensation. The second (F2) generation of maternal zygotic mutant fish allowed the assessment of the lack of maternal RNA contribution. Zebrafish lines carrying more severe mutations and displaying stronger phenotypes in F1 tended to compensate the loss of protein function more successfully in F2. Mutations in the *nphp8* gene, which are associated with severe human disease, seem less capable to compensate than zebrafish with mutations in the *nphp4* gene. Genetic compensation could be confirmed in *nphp4*-deficient mutants *via* MO-induced knockdown of the *nphp4* gene, since these F2 mutants became largely refractory to additional gene depletion.

Not only do zebrafish, carrying defined point mutations in *nphp1* and *nphp4*, display reduction of ciliopathy-related phenotypes between F1 and F2, but so do mutant lines with larger CRISPR/Cas9-mediated deletions, further revealing partial compensation in the maternal zygotic F2 zebrafish. Finally, CRISPR/Cas9 was used in this work to generate a new loss-of-function *nphp2* mutation. Simultaneous use of two sgRNAs, targeting the first and the last exon respectively, successfully deleted most of the genes' open-reading frame, creating a new model to study *nphp2* function in zebrafish in further experiments.

# 1. Introduction

## 1.1 Kidney function and dysfunction

The kidney is a very complex organ commissioned with various tasks. It is the body's central organ of excretion and plays a crucial role in homeostasis in the blood milieu. It regulates electrolyte levels, pH, fluid balance and the elimination of proteins, toxins, nitrogenous metabolic waste products and other solutes (Veelken and Ditting, 2018a). In addition to these excretory functions, the kidney also acts as an exocrine organ by releasing various hormones and enzymes: Renin, one of the main components of the renin-angiotensin-aldosterone system, which plays an important role in the blood pressure regulation; Erythropoietin, which stimulates the production and maturation of erythrocyte progenitor cells in the bone marrow; Thrombopoietin, which induces the production of thrombocytes and 1,25-Dihydroxyvitamin D<sub>3</sub>, which is important for correct calcium and phosphate level maintenance (Veelken and Ditting, 2018a).

The kidney is comprised of functional working units called nephrons. The human adult kidney accounts for more than a million nephrons (Bertram et al., 2011). All nephrons comprise the same fundamental organization into three specialized segments: the glomerulus, the tubule, and the collecting duct at the distal end. Blood plasma filtration takes place at the glomerulus, which contains a capillary tuft with fenestrated endothelial cells covered with podocytes. The primary urine is then modified in the subsequent tubule, which can be divided into different subsegments (proximal, intermediate and distal), each characterized by their individual epithelial cell types, which are specialized in different secretion or reabsorption processes (Lüllmann-Rauch and Asan, 2019). The urine is conveyed through the proximal tubule, with its convoluted and straight part followed by the intermediate tubule, with its descending and ascending limb, the distal convoluted tubule, and the connecting tubule, until it is finally channeled away into the collecting duct (Fig.1). The collecting ducts, which collect urine from numerous nephrons, merge into constantly bigger ducts, all converging in an arbor-like manner into the centralized drainage system of the kidney (Lüllmann-Rauch and Asan, 2019). The complexity of the nephron becomes more evident, when considering that more than 20 different specialized cell types have been identified so far to be required for its physiological functions (Al-Awqati and Oliver, 2002). It is only by combining the functions of all these different cell types, that the nephrons assure the tasks of the kidneys, namely the regulation of fluid balance, osmolarity and pH regulation as well as the removal of metabolic waste (Wingert and Davidson, 2008). The acquired loss of nephrons, due to acute or chronic injuries, or the malformation and malfunction of nephrons, due to a congenital disease, constitutes a risk factor for renal failure (Hoy et al., 2008). The loss of nephrons is irreversible in humans.

After the nephrogenesis period, which lasts until the 36<sup>th</sup> week of gestation in human fetuses, no new nephrons can be generated to compensate for an eventual nephron loss (Ahmadi et al., 2020). Congenital abnormalities of the kidney and the urinary tract (CAKUT) are listed among the most common birth defects (Airik and Kispert, 2007). Chronic kidney disease (CKD) affects around 10% of the European population, making it a major concern of public health and scientific research (Kelly et al., 2021). If the renal function is impaired, a characteristic set of symptoms occurs, which can be deduced by the kidneys' physiological functions; in earlier stages polydipsia and polyuria, as manifestations of the loss of the kidneys' concentrating abilities occur. The subsequent loss of different solutes might lead to disturbed acid-base balance and/or abnormal electrolyte concentration levels. Both are crucial for a multitude of physiological processes, like the electrophysiological activity of muscles, nerves, or the conduction system of the heart (Veelken and Ditting, 2018b). In more advanced stages of kidney failure, as nephron loss can no longer be compensated by remaining functional units, water and electrolytes are retained and general edema, heart insufficiency, hypertension or arrhythmias might occur (Veelken and Ditting, 2018b). The accumulation of toxic metabolic waste products, like urea, uric acid, and creatine, a consequence of impaired excretion, can cause uremia, uremic coma, or ultimately leads to death. Patients with uremic syndrome present specific and unspecific symptoms, like uremic fetor, pruritus, general and increasing weakness, nausea, vomiting, confusion, seizures or even stupor and coma (Baumgaertel et al., 2014). The loss of the kidney's exocrine functions might lead to anemia (loss of erythropoietin), hypotension (loss of renin) and unbalanced calcium and phosphate levels (loss of 1,25-Dihydroxyvitamin D<sub>3</sub>), which in turn leads to osteodystrophy (Veelken and Ditting, 2018b).

## **1.2 Kidney development in vertebrates: pronephros, mesonephros, metanephros**

The development of the kidneys in higher vertebrates is characterized by the evolutionary succession of three distinct excretory organs arising from the intermediate mesoderm: the pronephros as the earliest and most primitive form, followed by the mesonephros with improved functionality and complexity and representing the adult kidney for lower vertebrates such as fish or amphibians; and ultimately the metanephros, the definitive mature kidney for higher vertebrates such as humans or other mammals (Drummond, 2003). All three evolutionary kidney stages, even though different in terms of temporal and spatial organization, share the same fundamental organization into three main segments: the glomerulus for blood-filtration, the tubule for secretion and reabsorption of different solutes and ions, followed by the collecting duct, for final adjustments and transportation of the filtrate to the distal urinary tract's collection system (Wingert and



Davidson, 2008) Kidney development in humans starts approximately in the 4<sup>th</sup> and lasts until the 34-37<sup>th</sup> week of gestation (Lindström et al., 2018).

Organogenesis of the kidney, arising from the intermediate mesoderm, can be subdivided into the formation of the collection system on one hand and the formation of the nephrons as filtration units on the other hand (Costantini and Kopan, 2010). Cells in the dorsal intermediate mesoderm form the epithelialized nephric duct, also called Wolffian duct, while cells in the ventral intermediate mesoderm are at the origin of the nephrogenic cord. Together, these two structures form the primitive renal tubules of the transient pronephros and mesonephros (Costantini and Kopan, 2010; Dressler, 2006). The formation of the final metanephric kidney starts with the caudal region of the intermediate mesoderm differentiating into the metanephric mesenchyme. Signals from metanephric mesenchymal progenitor cells induce the branching process of the uretric bud, which is an outgrowth of the distal nephric duct. This branching process results in the arbor-like drainage system of the kidney (Costantini, 2006; Lindström et al., 2018). Reciprocally, inductive signals from the tip of the uretric bud, engender the differentiation of the mesenchymal progenitor cells. This pool of mesenchymal progenitor cells gives rise to two different tissues; the mesenchymal cells, which undergo a mesenchyme-to-epithelial transition and form all the nephron comprising segments, like the glomerulus, the proximal or distal tubule. Other mesenchymal cells differentiate to form the interstitial stroma (Dressler, 2006). As a new nephron forms at the tip of every uretric-bud-derived branch, after 12 generations of branching, an enormous number of functional units in the metanephric kidney, which even doubles again after branching ceases, arises (McMahon, 2016). The distal end of the nephric duct, extends caudally until it fuses with the epidermal layer, opening to the exterior for waste excretion (Drummond, 2003). Finally, the formation of the capillary tuft by ingrowing endothelial cells, completes the formation of the nephron and marks the beginning of nephron function by connecting it to the blood circulation (Dressler, 2006).

After the pronephros and mesonephros are gradually removed during embryogenesis, parts of the mesonephros remain and form elements of the male reproductive system. The mesonephric ducts (Wolffian ducts) form primary male genital organs, like the epididymis, the vas deferens and the seminal vesicles under the influence of testosterone (Hannema and Hughes, 2007).

This brief description of kidney development leaves no room for mentioning the discovery of numerous intricate signaling pathways, necessary for mesenchymal-epithelial interactions and cell fate determination of different progenitor cell pools during kidney organogenesis (Khoshdel Rad et al., 2020). Many kidney defects and renal diseases could possibly be explained, if the mechanisms controlling these intricate processes of kidney morphogenesis, requiring sequential tissue interactions, cell differentiation, cell migration and many more would be better understood.

Unfortunately, these mechanisms still remain hardly uncovered and therefore represent a much-investigated field of developmental biology.

### **1.2.1 Kidney development in zebrafish**

In Zebrafish, the pronephros is not only a transient and non-functional precursor of the adult kidney, but it is indeed functional during their early life and used to maintain osmoregulation. (Drummond, 2003). The formation of the zebrafish pronephros occurs early in embryonic development, considering its beginning at approximately 12 hours post-fertilization (hpf) (Serluca and Fishman, 2001) leading to a functional pronephros by 48 hpf (Drummond et al., 1998). The onset of glomerular filtration in zebrafish was determined by fluorescent dextran injections and set to around 40-48 hpf (Drummond et al., 1998). The pronephric kidney in zebrafish is composed of a bilateral pair of nephrons fused at the midline, which share one common capillary tuft filtering from the dorsal aorta. The segment patterning of the zebrafish pronephric nephrons shows a high degree of structural conservation of mammalian metanephric nephrons (Fig.1) (Wingert and Davidson, 2008). The segmental organization of each nephron consists of a glomerulus, followed by a neck section, connecting it to a proximal convoluted tubule, which continues into a proximal straight tubule. The adjacent distal tubule, divided in a “distal early” and a “distal late” segment, contains the corpuscle of Stannius, an endocrine organ playing a role in calcium hemostasis. A pronephric duct forms the caudal end of the nephron (Wingert and Davidson, 2008). The bilateral pronephric ducts fuse at their caudal end to form the cloaca and thereby to become patent to the exterior by 24 hpf (Drummond et al., 1998). The main difference between the zebrafish pronephric and the mammalian metanephric nephron is the lack of the descending and ascending thin limb of the intermediate duct, also known as Loop of Henle. As freshwater fish have no need to concentrate the primary urine in order to retain water as much as vertebrates living on land do, this nephron segment is not necessary to zebrafish (Wingert and Davidson, 2008). Even though the pronephros is a functional organ in the early days of life of a zebrafish, it is eventually replaced by a mesonephros, counting several hundred nephrons, which take over physiological tasks of the kidneys after around 2 weeks post fertilization (Diep et al., 2015). Unlike mammalian metanephros, which cannot regenerate lost nephrons, the adult zebrafish mesonephros is able to form new nephrons from renal progenitor cells as the fish grows or after kidney injury (Gerlach and Wingert, 2013).

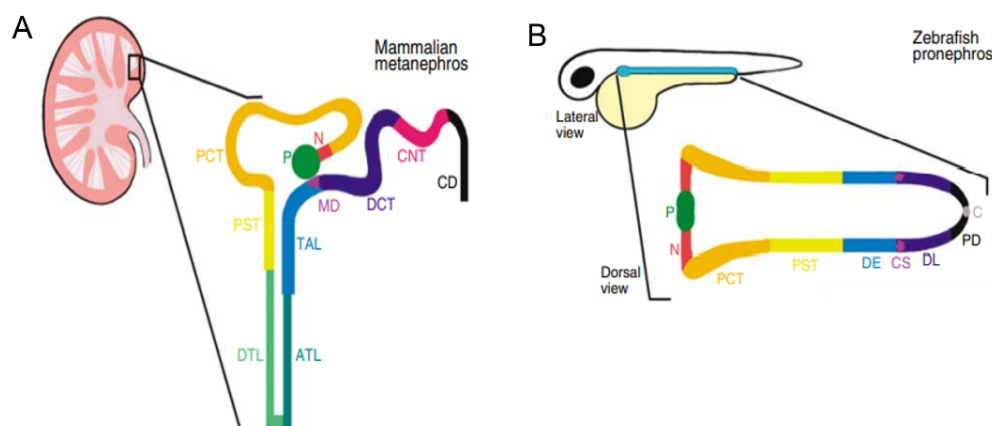


**Figure 1: Metanephric and pronephric nephrons share a similar segmentation pattern** (adapted from Wingert and Davidson, 2008).

**A)** Mammalian metanephric kidney, with enlargement depicting the segmental organization of a single nephron.

**B)** Zebrafish embryo, shown in a lateral view, with the pronephros depicted in blue. Enlargement shows a dorsal view of the pronephros, with the segmental organization of each nephron as indicated. Abbreviations: ATL, ascending thin limb; C, cloaca; CD, collecting duct; CNT, connecting tubule; CS, corpuscle of Stannius; DCT, distal convoluted tubule; DE, distal early; DL, distal late; DTL, descending thin limb; G, glomus; MD, macula densa; N, neck; P, podocytes of renal corpuscle; PCT, proximal convoluted tubule; PD, pronephric duct; PE, proximal early; PL, proximal late; PST, proximal straight tubule; T, tubule; TAL, thick ascending limb (Wingert and Davidson, 2008).

### 1.3 Nephronophthisis (NPH)

Nephronophthisis (NPH) is a rare autosomal recessive hereditary polycystic kidney disease, predominantly affecting children and young adults. It has an estimated incidence of 1 in 100,000 in the United-States (Luo and Tao, 2018). Causing up to 15% of end-stage renal disease (ESRD) in the first three decades of life, nephronophthisis is the leading monogenetic cause of ESRD in childhood and youth (Hildebrandt et al., 1993).

According on the age at which the ESRD occurs, nephronophthisis is categorized into three clinical subtypes: infantile, juvenile and adolescent. Infantile NPH can present itself even before birth with oligohydramnios alongside the consequent limb contractures and pulmonary hypoplasia, or postnatally with rapidly deteriorating renal functions, leading to ESRD before the third year of life (Stokman et al., 2016). The juvenile form of NPH, with variable onset of ESRD, is the most frequent one and accounts for 5-10% of ESRD in children (Tory et al., 2009). Early symptoms in children with juvenile NPH include polyuria, polydipsia, nocturia or secondary enuresis, as effects of the kidneys' reduced concentrating abilities and/or other symptoms of chronic kidney disease like growth retardation, anemia or chronic persistent fatigue (Stokman et al., 2016). The adolescent NPH form is clinically close to the juvenile form, the main difference being the later onset of ESDR at a median age of 19 years, compared to 13 years in juvenile nephronophthisis (Luo and Tao, 2018). Because of the highly variable and nonspecific symptoms, NPH is diagnosed on average only 3.5 years after onset of symptoms (Soliman et al., 2012). Histologically, NPH is characterized by cyst formation at the cortico-medullary junction, diffuse interstitial fibrosis, interstitial inflammation, and renal tubular cell atrophy with thickened and disrupted tubular

basement membrane, all driving kidney failure (Gupta et al., 2021). Unlike other polycystic kidney diseases, the kidneys in NPH patients do not seem enlarged on ultrasound but appear of normal or even reduced size, with increased echogenicity (Wolf and Hildebrandt, 2011). In 10-20% of patients, nephronophthisis is associated with extrarenal manifestations, of which retinal degeneration is the most frequent one (Luo and Tao, 2018).

Despite being the most common genetic cause for ESRD in children and young adults, the pathomechanisms of NPH have remained obscure for decades. Up to this point, mutations in more than 25 different genes have been implicated in the pathogenesis of nephronophthisis, making it not only a highly phenotypically heterogeneous but also a genetically heterogeneous disease (McConnachie et al., 2021). Most of these NPH genes, encode proteins (nephrocystins) (Nphps), which localize to cilia (primary/non-motile or motile cilia) or its associated structures and are essential to normal ciliogenesis and ciliary function (Luo and Tao, 2018). Almost all mammalian cells have primary cilia, being microtubular hairlike organelles protruding from their surface, and which are essential for sensory processes, such as chemo-, mechano-, or photoreception. They connect external stimuli to intracellular changes, such as epithelial cell polarity processes or cell-cycle control (Goetz and Anderson, 2010). Motile cilia on epithelial cells of different organs, create a fluid-flow by actively beating in a coordinated way, which plays an important role in multiple developmental processes as well as physiological functions in mature organs (Kramer-Zucker et al., 2005). Structurally or functionally defective nephrocystins cause ciliary dysfunction, and thereby make nephronophthisis part of a heterogeneous group of human genetic disorders with partly overlapping clinical features, called “ciliopathies” (Hildebrandt and Zhou, 2007). Other ciliopathies are syndromes like the lethal Meckel-Gruber syndrome (MKS), Joubert Syndrome (JBS), Senior-Løken syndrome (SLS) or Bardet-Biedl (BBS) syndrome, characterized by diverse and partly coinciding phenotypes with varying severity. Multiple organ systems can be affected, resulting for example in renal cystic dysplasia, cerebellar vermis hypoplasia, polydactyly, liver fibrosis, retinal degeneration, situs inversus, cardiac malformations or many more developmental and/or degenerative deficiencies (Cardenas-Rodriguez and Badano, 2009; Hildebrandt and Zhou, 2007). No specific therapy for NPH is available to this date. The clinical management is supportive only and focuses on controlling the concomitant symptoms and complications. Renal transplantation is the only curative option for patients diagnosed with NPH (Stokman et al., 2016).

#### **1.4 Zebrafish as a model organism**

The Zebrafish (*Danio rerio*) is a freshwater fish, who has his native origins in South Asia, more precisely on the Indian subcontinent and the Himalayan region (Parichy, 2015). He owes his name to his horizontal linear body pigmentation, giving him a zebra-like appearance. The adult fish measures up to 4 cm in length and has a life expectancy of about 2-3 years (Spence et al., 2008). It is a well-established popular translational research model organism with an increasingly important role in the study of vertebrate development and physiology over the last 80 years (Adamson et al., 2018). The zebrafish has some significant advantages, making it a valuable model to study embryologically or genetically tractable diseases: Firstly the zebrafish larvae perform a rapid development ex-utero and remain translucent during the first 24 hours post fertilization (hpf), a characteristic which may be further upheld, by treating the embryos with 1-phenyl 2-thiourea (PTU) (Karlsson et al., 2001). This enables the in vivo observation of early developmental stages and developing pathologies *via* simple non-invasive imagery (Lieschke and Currie, 2007). Secondly, the husbandry of zebrafish is relatively easy and cost-efficient, as the fish are small, robust, easy to maintain, reach fertility at around 3 months and have a high reproduction rate alongside a reasonably short generation time, predisposing the zebrafish for large-scale high-throughput genetic and therapeutic screening (Song et al., 2016). Large-scale forward-genetic screens alongside with a fully sequenced zebrafish genome, have led to the identification and characterization of numerous disease-causing mutations in zebrafish genes, which have human orthologues (Amsterdam and Hopkins, 2006). Several studies have shown that zebrafish, being a lower vertebrate, express a genetic structure and follow conserved developmental pathways similar to higher vertebrates, like humans. Approximately 70% of genes of the human genome have at least one orthologue gene in zebrafish, making zebrafish a convenient and effective model system, to study gene function and model human genetic diseases (Howe et al., 2013). Zebrafish were used extensively to investigate mutations, which affect embryogenesis and thereby led to the discovery of a multitude of new genes playing a role in vertebrate development (Adamson et al., 2018; Haffter et al., 1996a).

Important for this work, zebrafish pronephros have become a valuable model to study renal development, as they represent a simplified model of nephron development, which still shares structural and developmental similarities with mammalian nephrons (Drummond, 2000).

### **1.5 Development of cloaca cysts in zebrafish**

The cloaca in zebrafish is the common body opening of the urinary and gastrointestinal tracts and is formed around 24 hours post fertilization (hpf) (Drummond et al., 1998). Caudal-ventral elongation of the pronephric duct *via* directed cell migration, constitutes an essential process in renal development and cloacal morphogenesis. It was shown that nephrocystin-4 (Nphp4), the gene product of the *nphp4* gene, was essential for these migratory and cellular rearrangement processes (Burcklé et al., 2011). In zebrafish deficient of Nphp4, cells at the distal end of the pronephric duct failed to connect to the ectodermal cells and because of the missing selective apoptosis of these cells no cloaca was formed. Consequentially, the pronephric duct remained without opening to the outside and this obstruction resulted in cloaca cyst formation (Slanchev et al., 2011). With no patency of the pronephric duct at its distal end to the outside of the fish, the urinary excretion is impaired, and the resulting pondage of urine can contribute to tubular dilatation and proximal cyst formation as well (Kramer-Zucker et al., 2005). Early inductive events influencing cell fate for proper cloaca formation later on, were shown to be dependent on sustained bone morphogenetic protein (Bmp) signaling during early developmental stages. If Bmp signaling is disrupted, the pronephric tubules fail to connect to the outside of the body because of missing regulated apoptosis in the proctodeal region (Pyati et al., 2006). Activated CaMK-II, a mediator of intracellular calcium downstream of PKD-2, was shown to ensure proper cloacal morphogenesis and stabilization of cloacal cilia as CaMK-II suppression resulted in gradually disassembling cloacal cilia and incorrect cloaca formation (Rothschild et al., 2011). Formation but also preservation of the integrity and appearance of the pronephric ducts relies on cell-polarity, which in turn depends on cell junctions. If cell adhesions are disturbed, for example by depletion of *chd17* in zebrafish embryos, pronephric ducts become irregular in diameter and fail to properly fuse at the cloaca (Horsfield et al., 2002). In short, cloaca formation in zebrafish relies on an elaborate orchestration of different processes like directed cell migration, tissue rearrangements, selective apoptosis, and tissue maintenance, all of which can result in cystic malformation if they are impaired.

### **1.6 Development of kidney cysts in the zebrafish pronephros**

The zebrafish pronephros consists of only one central capillary tuft, which is connected to two pronephric ducts. These ducts run along the body axis on both sides and fuse at their caudal end, forming the cloaca (Drummond, 2003). The pronephric ducts are formed by polarized epithelial cells, which feature multiple motile cilia at their apical membrane. By beating in an efficient and coordinated way, these cilia create a fluid flow alongside the pronephric duct to excrete urine through the cloaca (Kramer-Zucker et al., 2005). If their function is impaired, the alterations in the fluid flow result in duct dilation and formation of pronephric cysts as soon as the glomerular

filtration is established (Kramer-Zucker et al., 2005). Studies on *Pkd1* and *Pkd2*, the genes which are linked to autosomal dominant polycystic kidney disease (ADPKD), have shown that primary non-motile cilia were involved in cystic kidney deformation as well. They were attributed a mechano-sensory role, detecting fluid flow, which leads to cilium deflection and subsequent fluctuations in intracellular calcium levels. This connection between the extracellular stimuli and intracellular processes seems essential for kidney tissue development and maintenance (Nauli et al., 2003; Praetorius and Spring, 2001). Mechanical obstruction of the cloaca is also closely related to pronephric cyst formation due to fluid backup (Kramer-Zucker et al., 2005). Studying morphogenesis of the zebrafish pronephros could help to investigate vital information behind kidney birth defects and diseases in humans, as the embryonic (pronephric) nephrons in zebrafish show a segmental organization similar to adult (metanephric) human nephrons (Wingert and Davidson, 2008). By identifying and characterizing the genes that are crucial for kidney development and thus potentially involved in congenital malformation and cystic kidney disease, new diagnostic and therapeutic strategies could be developed.

### **1.7 Development of other ciliopathy associated phenotypes in zebrafish**

Ciliary dysfunction of primary/non-motile or motile cilia, leads to a broad spectrum of disorders, given the multiple and diverse functions of cilia in different tissues (Huang et al., 2009). During embryonic development, primary cilia regulate various signaling pathways, while motile cilia create directional fluid flow. If defective, nearly all tissues can be affected, and organogenesis can be impaired (McConnachie et al., 2021). On that account, dysfunctional cilia, as the common underlying etiology of different cystic kidney diseases like NPH, MKS and JBTS can also cause phenotypes other than kidney and cloaca cysts. If the structure or motility of cilia is impaired, not only the fluid flow essential for urine excretion along the pronephric ducts is disrupted, but also the fluid flow in other organs, such as the heart or the brain. The accumulation of fluid can cause pericardial heart edema or hydrocephalic distention of the ventricles (Kramer-Zucker et al., 2005). Furthermore, the zebrafish's laterality organ, named Kupffer's vesicle causes the left-right body axis determination in early embryogenesis. Multiple motile cilia protruding from the epithelial cells of the Kupffer's vesicle, create a counterclockwise fluid flow, which is essential of the lateralization process, hence being the earliest process linked to ciliary function (Kramer-Zucker et al., 2005). This lateralization process and hence ciliary function can be assessed in zebrafish embryos by analyzing the orientation of the heart loop (Smith and Uribe, 2021). In addition, abnormal body curvature of zebrafish embryos has also been related to ciliary dysfunction (Song et al., 2016).

## 1.8 NPHP genes and gene products

Hitherto, 25 genes have been identified through positional cloning to be involved in the pathogenesis of nephronophthisis (McConnachie et al., 2021). Functional characterization of the proteins these genes encode for, called nephrocystins (Nphps), have led to the characterization of nephronophthisis, with its vast range of nonspecific symptoms and often concomitant diverse syndromes, as a ciliopathy. Nphps locate to the cilium or its surroundings, regulate cilium assembly, ciliary protein trafficking, access to the ciliary compartment and many more processes, which are essential for correct ciliary function (Luo and Tao, 2018). They have been associated with processes not involving cilia as well, such as cell adhesion, cell migration and cell polarization (Srivastava et al., 2018). With the progression in identification of new genes and the discovery of an increasing number of Nphps over the years, interactions between different Nphps have been described. Due to physical and functional interactions, Nphps have been grouped into protein modules, for example the Nphp1-4-8, the NPHP2-3-9/AHI1 the Nphp5-6/Ataxin10 and the MKS module (Sang et al., 2011).

Characterization of a still growing number of Nphps and their interactions has helped to gain considerable insights in the fundamental mechanisms involved in cyst formation and other cilia-associated disorders. Unfortunately, an estimated two-thirds of nephronophthisis cases still remain genetically unknown and further research is needed for more *nphp* genes to be discovered (Luo and Tao, 2018). Because Nphps are highly conserved proteins through evolution, animal models like zebrafish can be used to gain further insights into their regulation, interaction and function and thereby develop future therapeutic approaches.

### 1.8.1 Nphp1

Mutations in the *nphp1* gene have been the first mutations to be put into relation with the development of nephronophthisis (NPH). Twenty-five years ago, Hildebrandt et al. identified in Freiburg, mutations in the *nphp1* gene, which codes for the protein nephrocystin (Nphp1), to cause juvenile NPH (Hildebrandt et al., 1997a). To this day, mutations in the *nphp1* gene remain by far the most common cause of NPH, being found in 21% of patients, while mutations in the other *nphp* genes count for no more than 3% each (Hildebrandt et al., 2009). Among patients with juvenile nephronophthisis, 67 to 75% carry large homozygous deletions in the *nphp1* gene locus (Hildebrandt et al., 1997a). Nphp1 localizes to the transition zone of primary cilia (Fliegauf et al., 2007). It plays a role in cell-cell and cell-matrix contacts, both important for the maintenance of polarized epithelial tissues. It was discovered that Nphp1 contains an Src homology 3 (SH3) domain and interacts with intra-cytoplasmatic proteins involved in adherens junctions and focal



adhesions of renal epithelial cells (Hildebrandt et al., 1997a). Nphp1 acts as an adaptor protein, interacting with proteins involved in these cell contacts, for example the adaptor protein p130Cas, the proline-rich tyrosine kinase 2 (Pyk2) or tensin and filamin, both actin-binding proteins (Mollet et al., 2005). It is also shown to interact with  $\beta$ -tubulin, one of the proteins forming the microtubule axoneme in the primary cilia of renal tubular epithelial cells (Donaldson et al., 2000). The role of Nphp1 in ciliary formation and function as well as cell contacts has been confirmed, by knockdown of the *nphp1* gene in MDCK cells (Delous et al., 2009). Its colocalization to primary cilia and cell adhesions, led to the discovery of physical interaction between Nphp1 and Nphp4 (Delous et al., 2009; Mollet et al., 2002). The simultaneous knockdown of *nphp1* and *nphp4* in zebrafish by two morpholino oligonucleotides (MOs), showed that the disruption of this interaction between both gene products seem to be more momentous for renal development and the formation of abnormal body curvature and heart edema, than for cloaca formation (Slanchev et al., 2011). Although juvenile nephronophthisis in humans is limited to renal phenotypes, Nphp1 was found to be expressed in photoreceptors as well. It acts in the intra-flagellar transport of molecules between the inner and outer segments and thus if defective or absent impairs the development and maturation of photoreceptors (Datta et al., 2021) and can cause retinal degeneration (Birtel et al., 2021). This backs up the observation that patients with homozygous deletions of the Nphp1 locus might show retinal degeneration, which rarely becomes symptomatic however (Caridi et al., 1998). The human *nphp1* gene localizes to the chromosome 2 and codes for a 732-amino acid (aa) protein nephrocystin (Antignac et al., 1993). The zebrafish *nphp1* orthologue, localizes to chromosome 17, has 20 coding exons and encodes for a 667 aa protein ([https://www.ensembl.org/Danio\\_rerio/Gene/Summary?db=core;g=ENSDARG00000009046;r=17:22072337-22091141](https://www.ensembl.org/Danio_rerio/Gene/Summary?db=core;g=ENSDARG00000009046;r=17:22072337-22091141)). Zebrafish Nphp1 contains the same functional domains as the human protein. The function of the SH3 is supposed to mediate the interaction between proteins to form complexes, and therefore to be involved in different cellular pathways, like cell proliferation or cell migration (Kurochkina and Guha, 2012). Coiled coils are well preserved structural motifs, which have been identified in proteins which affect the architecture of organelles, e.g. centrioles, or the activity of motor proteins (Truebestein and Leonard, 2016). Nphp1 localizes to the ciliary transition zone and to cell adhesion sites, playing a role in maintenance and formation of cell contacts and microtubule axoneme of primary cilia.

### 1.8.2 Invs/Nphp2

Inversin (Invs), the product encoded by the *nphp2* gene, was identified by Otto et al. to play an essential role in the development of nephronophthisis type II (NPH2) (Otto et al., 2003). Patients diagnosed with NPH type II, also known as infantile NPH, often show mutations in the *nphp2*

gene, often leading to enlarged kidneys on ultrasound, which is uncommon for patients with NPH, and to a rapid progression of renal dysfunction and early onset of end-stage renal disease (ESRD) at approximately 2 years of age (Tory et al., 2009). Extrarenal manifestations are a common result of *nphp2* mutations, they occur in about 80% of detected mutations and encompass hepatic involvement, frequent bronchial infections and abnormalities in cardiac development, namely valve or ventricular septal defects and situs inversus (Tory et al., 2009). The role of the Nphp2 protein in kidney organogenesis has been studied in different animal models. Consistent reversal in left-right asymmetry, a distinctive property most vertebrate internal organs share, has been observed in mutant *nphp2* mice (Yokoyama et al., 1993) and the exons 3-11 were shown to be missing in mice presenting situs inversus and renal cyst formation (Mochizuki et al., 1998). Development of severe pronephric cysts has been observed, when the *nphp2* gene was knocked-out *via* MOs (Otto et al., 2003). Its location to the primary cilium and other subcellular sites at a cell-cycle dependent manner, has been pinned down thanks to homozygote mutant mice, which showed consistent situs inversus and kidney cysts (Morgan et al., 2002). Nphp2 interacts with nephrocystin, the protein encoded by *nphp1*, and  $\beta$ -tubulin, which constitutes the microtubule axoneme of primary (non-motile) cilia of renal tubular cells (Otto et al., 2003). Studies in *C. elegans* showed that *nphp2* genetically interacts with MKS associated genes and even though it is partially redundant with *nphp1* and *nphp4* and not required for the localization of NPHP and MKS proteins to the ciliary transition zone, inversin plays an important role in ciliary formation (Warburton-Pitt et al., 2012). Studies on zebrafish and *Xenopus laevis* showed, that inversin interacts, like most Nphp gene products, in a molecular network, the *nphp2-3-9/AHI1* module (Sang et al., 2011). Knockdown of these genes resulted in pronephric cyst formation, defects in early heart looping or body edema, underlining the importance of Nphp2 for renal and cardiovascular development (Hoff et al., 2013). Inversin is found to function as a molecular switch between the canonical and non-canonical Wnt signaling pathways, which play an important role in embryonic development, encompassing regulation of cell fate, cell proliferation and migration and body axis determination (Simons et al., 2005). Inversin inhibits the canonical Wnt signaling cascade, which is important for mesenchymal-to-epithelial conversion and branching morphogenesis in kidney development (Perantoni, 2003), by mediating the degradation of cytoplasmic dishevelled (Simons et al., 2005). If inversin is defective or absent, dishevelled is not degraded and the concomitant persistent upregulation of the canonical Wnt pathway at later developmental stages, causes renal cyst formation (Simons et al., 2005). In addition, inversin plays a role the non-canonical Wnt signaling, which controls oriented cell division and apical-basolateral cell polarity, as well. It permits cytoplasmic dishevelled to accumulate at the plasma membrane

of polarized cells like tubular epithelial cells (Simons et al., 2005). The activation of the non-canonical Wnt signaling pathway in tubular epithelial cells is crucial for correct terminal differentiation and therefore formation and function of the nephron in later stages of renal development (Simons et al., 2005). The human *nphp2* gene, located on chromosome 9, is composed of 16 coding exons and encodes for a protein of 1065 amino acids (aa) (Schön et al., 2002). The *nphp2* orthologue in zebrafish is located on chromosome 16, has 17 coding exons and encodes for a 1025 aa long protein ([https://www.ensembl.org/Danio\\_rerio/Gene/Summary?db=core;g=ENSDARG00000002213;r=11:27442549-27502702](https://www.ensembl.org/Danio_rerio/Gene/Summary?db=core;g=ENSDARG00000002213;r=11:27442549-27502702)). The N-terminal half of the *nphp2* protein contains 16 ankyrin repeats, the most common structural motif in nature. The role of ankyrin has been described in protein-protein interactions (Sedgwick and Smerdon, 1999) as well as transcription initiation, cell-cycle regulation, cytoskeletal organization and many more diverse aspects (Chakrabarty and Parekh, 2022). Two IQ-domains, one highly conserved and calmodulin binding, and a second one in a poorly conserved C-terminal region, have been identified in mice, humans, chicks and zebrafish (Morgan et al., 2002). The characteristic of an IQ-domain, being calcium-independent calmodulin binding, is reported to play a role in the regulation of ion-channels, cell-cycle and cytoskeletal organization, all crucial elements of polarized cell-growth (Rhoads and Friedberg, 1997). Taken together, Nphp2 is required for regulation of cell proliferation and migration, epithelial cell polarization, ciliary formation and function, and thereby for diverse embryonal developmental processes.

### 1.8.3 Nphp4

The *nphp4* gene encodes for the protein nephrocystin 4 (Nphp4), also called nephroretinin. Mutations in the *nphp4* gene are frequently associated with juvenile nephronophthisis and Senior-Løken Syndrome (SLS), the latter being characterized by the onset of retinitis pigmentosa in addition to nephronophthisis (Mollet et al., 2002; Otto et al., 2002). Another extrarenal manifestation of NPH, caused by mutations in the *nphp4* gene, can be ocular motor apraxia (Cogan syndrome) or liver fibrosis. However no clear genotype-phenotype correlation for extrarenal manifestations could be demonstrated in a large mutational analysis of the *nphp4* gene in 250 nephronophthisis patients (Hoefele et al., 2005). The time of ESRD onset in patients with juvenile nephronophthisis is variable, ranging from 6-35 years of life (Otto et al., 2002). Nphp4 was demonstrated to interact with nephrocystin, the gene product of *nphp1*, suggesting that these two proteins act in a common signaling pathway (Mollet et al., 2002). As Nphp1 was shown to interact with  $\beta$ -tubulin and Nphp4 with  $\alpha$ -tubulin, both Nphps are crucial for correct microtubule formation

and hence ciliary function (Mollet et al., 2005). MO-mediated knockdown of *nphp1* or *nphp4* in MDCK cells (a model mammalian cell line) confirmed this role, as the results showed disturbed cilia formation and also delayed formation of tight junctions, which are essential in epithelial cell organization (Delous et al., 2009). Nphp4 localizes not only to the basal bodies of primary cilia and to the apical actin cytoskeleton in polarized epithelial tubular cells, but also to the centrosomes of dividing cells, explaining its important role to ciliary function, cell division and cell-cell and cell-matrix adhesion signaling (Mollet et al., 2005). Due to the physical and functional interactions between Nphp1, Nphp4 and Nphp8, the Nphp1-4-8 module has been defined. Nphp4 mediates the association between Nphp1 and Nphp8, an interaction shown to focalize to the ciliary transition zone and to cell-cell contacts, like basolateral or tight-junctions (Sang et al., 2011). As simultaneous knock-down of *nphp4* and *nphp2* caused an increased cyst formation, a common signaling pathway for both genes was supposed. Indeed, the proteins from both genes were shown to downregulate the canonical and upregulate the non-canonical Wnt pathway by controlling degradation and subcellular localization of dishevelled (Burcklé et al., 2011). In addition to the interaction with inversin, Nphp4 also regulates the canonical Wnt pathway, which if overactive promotes cyst formation, by stabilizing Jade-1, another inhibiting factor, and promoting its transportation to the nucleus (Borgal et al., 2012). Knock-down experiments in multi-ciliated epidermal cells of *Xenopus laevis* underlined the role of *nphp4* in the dynamic organization of the subapical layer of the cortical actin cytoskeleton, which is required for a stable connection of motile cilia to other cellular components (Yasunaga et al., 2015). Nphp4 forms a complex with the actin-modifying formin DAAM1, mediated by the polarity protein Intertuned, to assure normal ciliogenesis and correct polarization of motile cilia, creating directional fluid flow (Yasunaga et al., 2015). The human *nphp4* gene, which contains 30 exons and encodes for a protein containing 1426 amino acids was localized to chromosome 1 (Mollet et al., 2002). It contains no conserved protein domains of known function. The zebrafish orthologue is located to chromosome 8, contains 29 exons and codes for a 1417-amino acid protein ([https://www.ensembl.org/Danio\\_rerio/Gene/Summary?db=core;g=ENSDARG00000069014;r=8:21978057-22274509](https://www.ensembl.org/Danio_rerio/Gene/Summary?db=core;g=ENSDARG00000069014;r=8:21978057-22274509)). To conclude, Nphp4 is involved in the organization of the apical actin cytoskeleton, the establishment of cell-cell and cell-matrix signaling pathways and adhesions, ciliary function and planar cell polarity processes.

#### 1.8.4 Rpgrip-1L/Nphp8

Mutations in the *nphp8* gene, leading to a malfunctional Rpgrip-1L/Nphp8 protein, were described in patients with a variety of ciliopathy associated syndromes, covering a vast array of severe symptoms, for example kidney cysts, polydactyly and central nervous system malformations. The association with NPH, Joubert Syndrome type B (cerebello-oculo-renal syndrome), Meckel-Gruber Syndrome and COACH (cerebellar vermis aplasia, oligophrenia, ataxia, coloboma and hepatic fibrosis) syndrome indicates the various functions and resulting importance in early development Nphp8 has (Arts et al., 2007; Delous et al., 2007; Wolf et al., 2007). Rpgrip-1L was shown to share 31% identity with RPGR-interacting protein 1 (Rpgrip-1), which interacts with retinitis pigmentosa GTPase regulator (RPGR) in cilia of cone and rod photoreceptor cells (Delous et al., 2007). Mutations in the Rpgrip protein cause autosomal recessive congenital blindness (Leber congenital amaurosis - LCA) (Roepman et al., 2005). Since a strong interaction and colocalization to the retina between the *nphp8* and *nphp4* encoded proteins was shown, mutations in either one of the coding genes can explain retinal involvement in LCA or retinitis pigmentosa in SLS respectively (Roepman et al., 2005). This causality, mainly based of the high degree of similarity between Rpgrip and Rpgrip-1L/Nphp8, was backed up by the discovery, that Rpgrip acts as an adaptor protein, connecting RPGR to nephrocystin-6 and by this creates a connection between retinal degeneration and nephronophthisis (Gerner et al., 2010). Nphp8 localizes to the basal bodies and ciliary axonemes at the base of primary cilia together with Nphp4 and Nphp6 (Delous et al., 2007). It is a member of the Nphp1-4-8 module, a module shown to operate at cell-cell adhesion, particularly at tight-junctions (Sang et al., 2011). The different members of the MKS and the Nphp1-4-8 modules cooperate in the transition zone at the base of all cilia, to anchor the microtubules to surrounding membrane and control the access to the ciliary compartment during ciliogenesis (Williams et al., 2011). Alongside Nphp2 and Nphp4, Nphp8 was found to be essential for planar cell polarity processes, needed for example in directed cell migration or oriented cell-division. Nphp8 stabilizes Dishevelled and thereby acts in the non-canonical Wnt signaling pathway (Mahuzier et al., 2012).

The human *nphp8* gene is localized to the chromosome 16 and codes for a 1315-amino acid protein by 26 coding exons (Delous et al., 2007). The N-terminal region of *nphp8* contains five coiled-coil domains followed by two protein kinase C conserved region 2 (C2). Mutations in the N-terminal C2 domain were linked to Nphp8-Nphp4 binding deficits and the development of the severe and multiorgan cerebello-oculo-renal syndrome (Delous et al., 2007; Roepman et al., 2005). This C2 domain is necessary for the complex NPH protein interactions at the transition zone of cilia, as it provides the linkage between Nphp8 and Nphp4, which in turn localizes Nphp1 to the

transition zone (Arts et al., 2007). Coiled-coils are structural motifs found in proteins, which influence the structure of centrioles, but also in motor proteins or enzymes (Truebestein and Leonard, 2016). C2 domains are calcium-dependent membrane-targeting modules in cellular proteins involved in signal transduction and membrane trafficking. They are also assigned important assembly factor properties of the Nphp8 at the transition zone of primary cilia, as they mediate the interaction between NPH and MKS proteins (Jensen et al., 2015). The zebrafish *nphp8*-orthologue encodes for 1256-amino acid protein, which has only one C2 domain ([https://www.ensembl.org/Danio\\_rerio/Gene/Summary?db=core;g=ENSDARG00000051754;r=25:36045072-36086409](https://www.ensembl.org/Danio_rerio/Gene/Summary?db=core;g=ENSDARG00000051754;r=25:36045072-36086409)). In conclusion, Nphp8 regulates ciliary access in the transition zone, basal body positioning and planar cell polarity establishment.

## **1.9 Gene modification techniques**

In the past, researchers were reduced to simple observation of spontaneous mutations in order to deduce the function of a gene. Today several genetic tools allow for modification and intervention in the genome or genomic expression and thereby contribute to the growing insights into gene function and to a deeper understanding how they direct developmental processes, normal physiology, or disease. Loss-of-function studies in the zebrafish model rely on three major genetic approaches; ENU mutagenesis, as a reverse genetic strategy, MO-knockdown and CRISPR/Cas9-knockout, both representing forward genetic techniques (Adamson et al., 2018).

### **1.9.1 ENU mutagenesis**

Chemical N-ethyl-N-nitrosurea (ENU) mutagenesis is a widely used method to generate mutants in different vertebrate model systems. By exposing adult male zebrafish to the alkylating agent ENU, spontaneous point mutations occur in random locations alongside the entire genome (Amsterdam and Hopkins, 2006). It is *via* large-scale forward genetic screens, where offspring mutants with phenotypic effects are selected, that mutated genes can be identified using positional cloning and assigned to *in vivo* functions, hence the synonym ‘gene discovery screen’ (Acevedo-Arozena et al., 2008). Two large-scale whole-genome mutagenesis screens in zebrafish, performed in Tübingen and Boston, have identified over 1700 mutations in more than 400 newly discovered genes, which play a role in vertebrate development and organogenesis (Driever et al., 1996; Haffter et al., 1996b). Some of these mutations were bred to homozygosity in subsequent generations and mutants are now available for scientific research. Our group screened the mutational databases from the Zebrafish Mutation Project at the Wellcome Sanger Institute and ordered mutant zebrafish carrying point mutations in the genes of interest at the European Zebrafish Resource Center (EZRC), located the Karlsruher Institut für Technologie (KIT).

### 1.9.2 Morpholino oligonucleotide (MO)-induced knock-down

The use of antisense RNA as a technique to inhibit the expression of a gene of interest *in vivo*, was first introduced in the mid 80's (Izant and Weintraub, 1985). Antisense technologies helped to learn about the function of genes and the proteins they are coding for in early development by inhibiting the translation or impairing the stability of endogenous mRNA, ever since. However, the use of antisense RNA in zebrafish did not seem practicable for the investigation of zygotic gene function during early development at first, due to extensive off-target and sequence independent effects (Oates et al., 2000). It was Nasevicius et al. who first successfully made use of morpholino-modified antisense oligonucleotides (MOs) to inhibit mRNA translation in zebrafish embryos. They managed to reproduce the phenotypes of well-described gene-knockout mutants, by inducing a MO-mediated knock-down of the targeted gene (Nasevicius and Ekker, 2000). MOs are chemically modified antisense oligonucleotides, counting around 25 subunits. Their structure is similar to DNA and RNA oligonucleotides, except for the fact that the ribose rings, found in DNA or RNA, are replaced by morpholino rings, connected *via* non-ionic phosphorodiamidate links (Fig.2). MOs have a high binding affinity to complementary target nucleic acid sequences in the mRNA by Watson-Crick base-pairing and thereby interfere with protein synthesis (Moulton, 2017a). Thanks to their non-ionic backbone structure, MOs are resistant to nuclease digestion and are less likely to interact unintentionally with other components of the cell (Eisen and Smith, 2008).

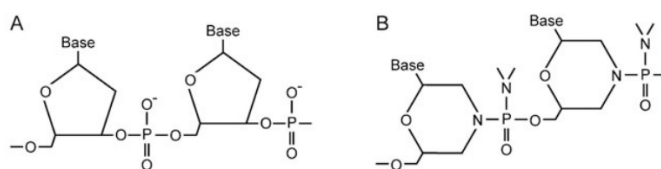


**Figure 2: Structures of conventional DNA and morpholino oligonucleotides**

(A) Conventional DNA oligonucleotide. (B) Morpholino oligonucleotide. Note the six-membered morpholino ring in B and the non-ionic phosphorodiamidate link between the two rings. (Eisen and Smith, 2008)

They are highly soluble in water, which helps to microinject them into one-cell stage embryos, where they diffuse evenly and affect all the cells of the organism. After the injection into fertilized eggs, MOs interfere either with correct splicing or inhibit the translation of the targeted gene in fundamental developmental stages during the first few days of development.

Translation blocking MOs (TBM) inhibit the initiation of the translation process by having a sequence complementary to the 5' UTR and/or the initiation codon and thereby preventing the assembly of the ribosome as the initiation complex cannot reach the start codon (Nasevicius and Ekker, 2000). The RNA transcript is not translated into a protein (Fig.3). Maternally supplied and zygotic mRNAs are not translated and the proteins they encode are therefore depleted in treated embryos (Nasevicius and Ekker, 2000).

Splice blocking MOs (SBM) interfere with the splicing process of pre-mRNA by having a sequence complementary to the exon-intron boundaries. As a result, exons are being skipped or introns remain in the mRNA after the splicing progress. SBM interfere with splicing in zygotic mRNA but not in maternal mRNA (Draper et al., 2001). The excision of exons or the inclusion of introns into the mRNA can lead to a premature stop codon downstream if the number of bases excluded or included is not evenly divisible by three, leading to a frame shift or if the intron contains an in-frame stop codon (Moulton, 2017b).

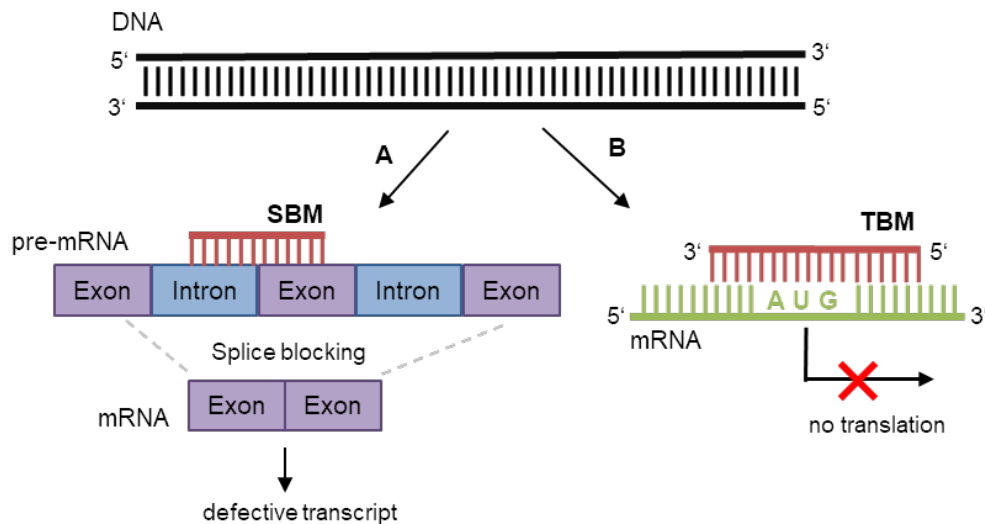


**Figure 3: Gene knock-down by MOs**

**A)** A splice blocking morpholino (SBM) pairs to an exon-intron boundary and prevents correct splicing of the pre-mRNA into mRNA (e.g. exon skipping or intron retention), which often results in a defective transcript. **B)** A translation blocking morpholino (TBM) inhibits translation by binding to a sequence in the 5' UTR of the translation start site (AUG) or including it and thereby blocking the progression of the initiation complex alongside the mRNA and thus no assembly of the ribosome at the translation start site.

Nonetheless, there are some concerns for the interpretation of experiments using MOs that were raised over the years; first there is the difficulty in the assessment of the efficiency of the gene knock-down, secondly one has to address the possibility of toxic or off-target effects, meaning the MOs might inhibit the expression of irrelevant genes instead of or in addition to the gene of interest and therefore make it difficult to judge the specificity of the MO (Kok et al., 2015).

To evaluate the existence of relevant off-target effects, a comparison of phenotypes in MO-injected embryos and existing mutants, carrying a mutation in the gene of interest, could indicate possible off-target MO effects and is therefore recommended for MO-experiments (Eisen and Smith, 2008).

The use of two different MOs targeting the same gene of interest is another approach to confirm that the observed phenotype is likely to be a genuine consequence of the MO-induced gene knockout, because the chance of off-target effects being the same for the different MOs used are considerably low (Eisen and Smith, 2008). Furthermore, it is advised to keep the concentration of MOs to a minimum in order to curtail toxicity and off-target effects.



The injection of MOs represents a powerful tool in reverse genetics, to assay for developmental abnormalities in early developmental stages, *via in vivo* gene-specific knockdown of a gene of interest. However, the knockdown is only transient, as the amount of MO per cell is gradually diluted as the number of cells increases during the development. As a rule of thumb, it has been shown that MOs can only be sufficiently effective, during the first 3 days of embryonic development (Morales and Wingert, 2017).

### **1.9.3 CRISPR/Cas9 system**

Clustered regularly interspaced short palindromic repeats (CRISPR) associated with Cas9 endonuclease, in short CRISPR/Cas9 technology has been a powerful tool in reverse genetics for targeted genome editing, emerging rapidly from a series of progressive discoveries on the procaryotic CRISPR immunity defense mechanisms over the last 35 years (Hsu et al., 2014). Nowadays, it is the preferred option over the previously used technologies in targeted genome engineering, namely zinc finger nucleases (ZFNs) (Urnov et al., 2010) and transcription activator-like effector nucleases (TALENs) (Joung and Sander, 2013). While these tools, like their names suggest, are based on the target site specific induction of double-strand breaks (DSB) in the DNA by nucleases as well, they are associated with off-target effects and a largely complicated and laborious design of target sequences and assembly of nucleases for each individual target site (Hwang et al., 2013). The CRISPR/Cas9 system on the other hand, allows universal use of the same Cas9 endonuclease for all target sites and thereby for efficient, precise, and cost-effective gene editing *via* site-specific DNA cleavage (Jinek et al., 2012). Considering these substantial advantages for scientific use, its discovery was awarded with the 2020 Nobel Prize in Chemistry (Ledford and Callaway, 2020).

The CRISPR/Cas9 system has been adapted as one of five types of CRISPR adaptive immune defense systems, which allows bacteria and archaea to recognize and degrade exogenous genetic sequences from invading phages, each by a different set of Cas endonucleases (Makarova et al., 2015). CRISPR/Cas9 is a type II CRISPR system, which was first associated with adaptive immunity in bacteria in 2007 (Barrangou et al., 2007) represents the most studied and most relevant system used for scientific applications. To understand how this mechanism can be used in scientific experiments, it is useful to look at the processes that lead to the adaptive immunity after an infection of bacteria or archaea. The acquisition of the adaptive immunity can be broken down into three stages (Fig.4).

In a first stage, the adaptive phase, when a bacteriophage invades a procaryotic cell, parts of the invasive viral or plasmid DNA (protospacers) are integrated into the so called 'CRISPR array', a

storage region for non-self nucleic acid information in the hosts DNA sequence (Barrangou et al., 2007; Mojica et al., 2005). In addition to the CRISPR array, a CRISPR/Cas type II gene locus also includes a *cas* gene operon, coding for four different Cas nucleases with various individual functions (Jansen et al., 2002). One of these Cas proteins is the Cas9 endonuclease, which is the signature endonuclease of type II CRISPR/Cas systems (Wiedenheft et al., 2012). The foreign DNA sequences are called ‘spacers’ the moment they are embedded in the host genome in between identical repeats (Barrangou et al., 2007). Protospacers, which are fitting for the integration as spacers are recognized by protospacer adjacent motifs (PAMs), a short and highly conserved sequence flanking the protospacer sequence (Mojica et al., 2009).

In a second step, the expression phase, transcription of precursor CRISPR-RNA (pre-crRNA), including transcripts of all spacers and repeats of the CRISPR array, takes place. This long pre-crRNA is then broken down by RNase III activity into individual crRNA molecules, containing a single spacer/repeat unit each (Deltcheva et al., 2011). The processing of the pre-crRNA results in mature crRNA molecules, each containing a 20 nucleotide-long target-specific guide sequence and a short fragment of transcribed repeat sequence (Brouns et al., 2008). This array of acquired crRNAs is built through experienced infections and is the key feature for sequence memory and subsequent targeted immunity against a subsequent invasion by the corresponding intruder. A trans-activating crRNA (tracrRNA), encoded by a sequence upstream of the type II CRISPR/Cas locus, binds by complementarity to the repeat sequences in the pre-crRNA transcript. This binding was shown to be important for the maturation of pre-crRNA and thus for its sequence-specific targeting abilities (Deltcheva et al., 2011).

Finally, in the interfering phase, in case of an infection a crRNA:tracrRNA duplex detects foreign DNA sequences by base pairing between the crRNA guide sequence to the target sequence, flanked by its protospacer adjacent motif (PAM). The RNA duplex then guides the CRISPR-associated DNA endonuclease Cas9 to the target, where Cas9 performs a site-specific double strand DNA break and thereby promotes the degradation and silencing of the foreign genomic information. (Garneau et al., 2010; Jinek et al., 2012) (Fig.4 and Fig.5). The PAM sequence is essential for Cas9 cleavage activity. For the Cas9 endonuclease from *Streptococcus pyogenes*, which represents the most commonly used form in eukaryotic systems, a conserved PAM with the sequence 5'-NGG-3' must follow the target sequence, to allow efficient cleavage activity (Mojica et al., 2009; Sternberg et al., 2014). Alterations in this PAM sequence can provide resistance to phages against CRISPR mediated immunity (Deveau et al., 2008). The DNA cleavage induced by Cas9 occurs 3 base pairs upstream of the PAM sequence on the strand complementary to the target sequence of

the crRNA and 3-8 base pairs upstream of the PAM sequence on the non-complementary DNA strand (Bhaya et al., 2011; Jinek et al., 2012).

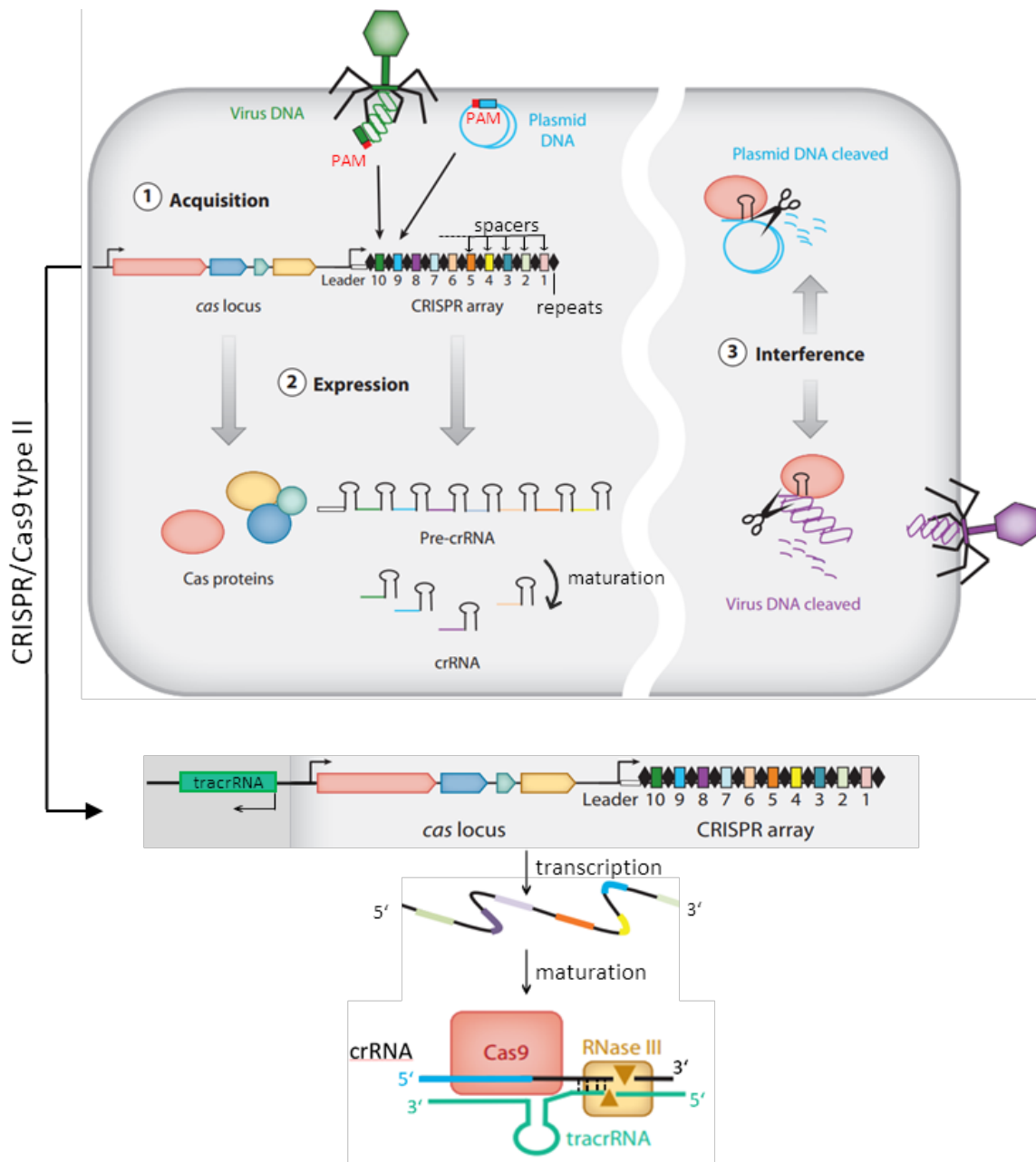


**Figure 4: The CRISPR/Cas adaptive immune system** (adapted from Bhaya, Davison and Barrangou, 2011)

**1) Acquisition:** Invading DNA is recognized by its PAM sequence and protospacers get integrated into the CRISPR array. The CRISPR array is a region in the hosts genome, containing acquired spacers (colored squares), which are separated from one another by identical repeats (black diamonds). The acquisition of new spacers requires different Cas proteins, which are encoded in the cas locus, upstream of the CRISPR array. **2) Expression:** The transcription of the whole CRISPR array, results in a long pre-crRNA, which is then broken down and processed into individual mature crRNAs. The CRISPR/Cas9 type II locus contains an additional tracrRNA encoding region (green box) upstream of the Cas locus. The tracrRNA binds to the repeat sequence of the pre-crRNA and promotes the maturation process by RNase III nuclease activity, and the association of the final active complex, consisting of Cas9 and crRNA:tracrRNA duplex. **3) Interference:** In the event of an invasion of foreign DNA, which is recognized by the crRNA:tracrRNA duplex, the Cas9 endonuclease cleaves and silences the invasive DNA, providing acquired immune-defense to bacteria or archaea.

The Cas9-induced double-strand breaks, can be repaired by either non-homologous end joining (NHEJ), resulting in small insertions and/or deletions (indels) of variable length or by homology-directed repair (HDR), allowing a knock-in of a desired template DNA sequence (Fig. 5) (Jiang and Doudna, 2017). If the indels as the result of NHEJ, occur in an early region of the sequence, they often lead to gene disruptions either through frame shift or non-sense mutations. These error-prone repair mechanisms can lead to the inactivation of genes and allow for targeted mutagenesis. The crRNA:tracrRNA duplex can be engineered as a single guide RNA (sgRNA), reuniting both structural features, responsible for target recognition and interaction with Cas9 respectively, in one chimeric structure. This can be done by linking the 3' end of the crRNA to the 5' end of the tracrRNA through a short sequence, acting as linker loop (Fig.5) (Jinek et al., 2012). By changing only the target site specific guide sequence of the sgRNA, CRISPR/Cas9 can be used for DNA-cleavage in any region of interest in a genetic sequence (Jinek et al., 2012). The CRISPR/Cas9 system, now being simplified down to two components only, can be used for targeted gene modifications by transfecting the specifically designed sgRNAs together with Cas9 mRNA or DNA into cells of various models. The use of CRISPR/Cas9 for genome editing in a whole organism, was shown to be successful in zebrafish, by targeting various gene sites in the zebrafish genome. Indels at the target sites could be observed in variable but overall relatively high frequencies (Hwang et al., 2013). In cases where the observed phenotypes do not correspond to the expected effects of the CRISPR/Cas9 induced mutation, different cellular compensation or escape mechanisms could explain the genotype-phenotype discrepancy. The knocked out gene could be compensated by redundant genes with similar functions or a different mRNA processing might prevent the expression of an expected hypomorphic or null mutant (Anderson et al., 2017). If two sgRNAs, targeting two different sites of the same gene, are co-injected together with Cas9 into zebrafish embryos, the gene sequence in between the two target sites can be cut out by the Cas9 nuclease activity and thus allows for determination of the physiological function of this gene fragment. This approach maximizes the odds that the observed phenotypes in mutant lines are indeed caused by a complete loss-of-function of the targeted gene (Kim and Zhang, 2020). Gene knockout *via* CRISPR/cas9 is complete and permanent, in contrast to MO-induced gene knockdown. It represents a useful complementary site-specific method to MOs for the observation of loss-of-function of genes in the early development but also in the adult life of model organisms.

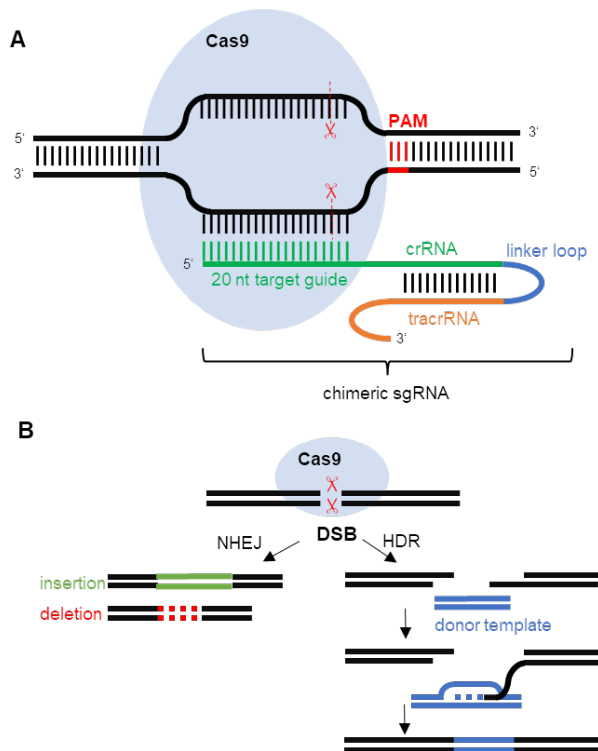


**Figure 5: CRISPR/Cas9 target binding and cleavage, followed by endogenous repair mechanisms**

**A)** Target recognition by sgRNA and Cas9 induced cleavage

The 20 nucleotide (nt) measuring target-specific guide sequence of the crRNA (green) binds to the complementary strand of the foreign genomic sequence, which is recognized by its PAM sequence (red). The chimeric sgRNA, consisting of a crRNA and tracrRNA region (orange) linked *via* a linker loop (blue), guides the Cas9 endonuclease to the target, where this cleaves both DNA strands upstream of the PAM sequence.

**B)** Genome editing by endogenous DNA repair mechanisms.

The Cas9 endonuclease induces a double strand break (DSB) at the target site, which can be repaired by either non-homologous end joining (NHEJ) or homology-directed repair (HDR). NHEJ can result in insertions and/or deletions or variable length. HDR allows to insert a genetic sequence from a donor template at the cleavage site.

## 1.10 Aims of this work

In this thesis, I wanted to make use of the zebrafish as a well-established model system in biomedical research with numerous benefits, to describe the phenotypic effects of mutations in genes of the *nphp1-4-8* complex as well as of *nphp2/inv5*. The analysis of these *nphp* mutations could help to identify functional domains within the Nphps which are important in pronephros development and cloaca formation. Furthermore, the discovery of a potential intergenerational change of phenotype frequency could indicate genetic compensation and/or define the effect of the loss of maternal wildtype gene products on maternal zygotic mutant fish. By injecting MOs into these maternal zygotic mutants, I wanted to confirm or refute the possibility of compensatory response to genetic mutations. In addition to analyzing zebrafish carrying defined *nphp* point mutations, I wanted to study *nphp* loss-of-function mutant lines generated by the targeted CRISPR/Cas9 gene editing technique and compare their phenotypic outcomes and potential compensatory mechanisms rescuing the zebrafish embryogenesis. Utilizing zebrafish to provide better understanding of kidney development will be beneficial for understanding, modelling and treating human cystic renal diseases, like nephronophthisis.

## 2. Materials and Methods

### 2.1 Materials

#### 2.1.1 Chemicals

Table 1: List of chemicals

Product	Supplier
Acetic acid (glacial)	Merck, Darmstadt, GER
Agarose for gel electrophoresis	SERVA, Heidelberg, GER
Aqua ad iniectabilia	B. Braun, Melsungen, GER
CaN <sub>2</sub> O <sub>6</sub> * 4 H <sub>2</sub> O (calcium nitrate tetrahydrate)	AppliChem, Darmstadt, GER
CaSO <sub>4</sub> (calcium sulfate)	Carl Roth, Karlsruhe, GER
CH <sub>3</sub> COONa (sodium acetate) 3M	Merck, Darmstadt, GER
ClorAm-X	AquaScience Technologies & Research, Richmond, MO, USA
Coral Pro Salt	Red Sea Fish Pharm LTD., Eilat, ISR
EDTA (ethylenediaminetetraacetic acid)	AppliChem, Darmstadt, GER
EtOH (Ethanol)	Merck, Darmstadt, GER
Ethidium bromide solution, 1%	AppliChem, Darmstadt, GER
Formamide 50%	Sigma Aldrich, Taufkirchen, GER
Gel Loading Buffer II	Thermo Fisher Scientific, Waltham, MA, USA
Gene Ruler 1kb Plus DNA Ladder	Thermo Fisher Scientific, Waltham, MA, USA
Glacial Acetic Acid	AppliChem, Darmstadt, GER
HCL (hydrochloric acid) 37%	VWR International, Radnor, USA
Heparin	Sigma Aldrich, Taufkirchen, GER
HEPES buffer	Carl Roth, Karlsruhe, GER
IPTG (isopropyl-β-D-thiogalactopyranoside)	Carl Roth, Karlsruhe, GER
KCl (potassium chloride)	Merck, Darmstadt, GER
LB-Medium	Carl Roth, Karlsruhe, GER
MeOH (methanol) 100%	VWR International, Radnor, USA
Methyl cellulose	Merck, Darmstadt, GER
Methylene blue	AppliChem, Darmstadt, GER
MgCl <sub>2</sub> (magnesium chloride)	Carl Roth, Karlsruhe, GER
MgSO <sub>4</sub> * 7H <sub>2</sub> O (magnesium sulphate7- hydrate)	Carl Roth, Karlsruhe, GER
NaCl (sodium chloride)	Carl Roth, Karlsruhe, GER
NaHCO <sub>3</sub> (sodium hydrogen carbonate)	Carl Roth, Karlsruhe, GER
NaOH (5 mol/L)	Merck, Darmstadt, GER
PFA 4% in PBS solution	Thermo Fisher Scientific, Waltham, MA, USA
Phenol Red solution	Merck, Darmstadt, GER
Phenol-Chloroform	Carl Roth, Karlsruhe, GER
PTU (1-phenyl-2-thiourea)	Merck, Darmstadt, GER
S.O.C. Medium	Thermo Fisher Scientific, Waltham, MA, USA
SCC buffer	Sigma Aldrich, Taufkirchen, GER
Tricaine (ethyl 3-aminobenzoate methanesulfonate salt)	Merck, Darmstadt, GER
TRIS HCl	Carl Roth, Karlsruhe, GER
Tween20	AppliChem, Darmstadt, GER

X-Gal (5-bromo-4-chloro-3-indolyl- $\beta$ -D-galactopyranoside)	AppliChem, Darmstadt, GER
--	---------------------------

### 2.1.2 Enzymes and biological reagents

**Table 2: List of enzymes and biological reagents**

Enzyme	Supplier
Antarctic Phosphatase	New England Biolabs, Ipswich, MA, USA
anti-Digoxigenin-AP Fab fragments	Roche Diagnostics, Mannheim, GER
BM Purple	Roche Diagnostics, Mannheim, GER
Cas9 protein with NLS	PNA BIO INC, Newbury Park, CA, USA
Exonuclease I	New England Biolabs, Ipswich, MA, USA
KOD Hot Start DNA Polymerase	Merck, Darmstadt, GER
OneTaq <sup>®</sup> Quick-Load <sup>®</sup> 2X Master Mix	New England Biolabs, Ipswich, MA, USA
Pronase from <i>Streptomyces griseus</i>	Sigma Aldrich, Taufkirchen, GER
Proteinase K	Hoffmann-La-Roche, Basel, CH
tRNA from <i>torula</i> type IV	Sigma Aldrich, Taufkirchen, GER

### 2.1.3 Bacteria

**Table 3: List of bacteria**

Bacteria	Supplier
OneShot <sup>™</sup> TOP10 chemically competent <i>E. coli</i>	Thermo Fisher Scientific, Waltham, MA, USA

### 2.1.4 Kits

**Table 4: List of kits**

Product	Supplier
GeneJET PCR Purification Kit	Thermo Fisher Scientific, Waltham, MA, USA
MEGAscript <sup>™</sup> T7 Transcription Kit	Thermo Fisher Scientific, Waltham, MA, USA
peqGOLD Plasmid Miniprep Kit I	VWR (Avantor), Radnor, PA, USA
TOPO <sup>™</sup> TA Cloning <sup>™</sup> Kit	Thermo Fisher Scientific, Waltham, MA, USA

### 2.1.5 Consumables

**Table 5: List of consumables**

Product	Supplier	Description
BlueINOX tweezers with fine tip, No. 5	Manufactures D'Outils Dumont SA, Montignez, CHE	tweezers
Borosilicate Glass Capillaries	World Precision Instruments, Sarasota, FL, USA	injection needles
Concavity Slide 2 Well	Electron Microscopy Sciences, Hatfield, UK	2-well concavity specimen slide
Gemma Micro 300	Skretting, Westbrook, ME, USA	fish food

Gemma Micro 150	Skretting, Westbrook, ME, USA	fish food
Gemma Micro 75	Skretting, Westbrook, ME, USA	fish food
Glasfirn Pi Pump 2500, size 2	Carl Roth, Karlsruhe, GER	Glass Pipette Pump
Glass beads	Carl Roth, Karlsruhe, GER	
Great Salt Lake Artemia Cysts	Sanders, South Ogden, UT, USA	Fish food
Micro Tube, 1.5 ml	Saestedt, Nürmbrecht, GER	1.5 ml Tubes
Micro Tube, 2.0 ml	Saestedt, Nürmbrecht, GER	2.0 ml Tubes
Pasteur Capillary Pipettes, long size 230mm	Brand, Wertheim, GER	glass pipettes
Pasteur pipette	Blanck Laborbedarf, Moers, GER	
PCR Soft Tubes 0.2 ml	Biozym Scientific, Oldendorf, GER	0.2 ml PCR Tube
Petri Dish, 94mmx16mm, clear with vent	Greiner Bio-One, Frickenhausen, GER	petri dish
Rotifers		

## 2.1.6 Solutions

### 2.1.6.1 Danieau's solution (30% stock)

The following ingredients are stirred until dissolved. Danieau's stock solution is stored at 4 °C.

Table 6: Ingredients for Danieau's solution (30x)

Reagent	Amount	Concentration
NaCl	101.7 g	1740 mM
KCl	1.56 g	21 mM
MgSO <sub>4</sub> • 7 H <sub>2</sub> O	2.96 g	12 mM
CaN <sub>2</sub> O <sub>6</sub> • 4 H <sub>2</sub> O	4.25 g	18 mM
HEPES buffer	35.75 g	150 mM
ddH <sub>2</sub> O	add to 1000 ml	

### 2.1.6.2 Danieau's solution (0.3% ready-to-use solution)

Ingredients are mixed in a big canister and kept at room temperature until filled in small squeeze bottles for handy use.

Table 7: Ingredients of Danieau's solution (0.3x)

Reagent	Amount	Concentration
Danieau's solution 30x stock	100 mL	
Methylene blue solution	15 mL	0.1 g/L
ddH <sub>2</sub> O	add to 10 L	



### 2.1.6.3 1-Phenyl-2-Thiourea (PTU) (100mM stock)

Table 8: Ingredients of 1-phenyl-2-thiourea (PTU) solution

Reagent	Amount
PTU	3 g
Ethanol (100%)	200 ml

PTU solution is stored at 4 °C.

### 2.1.6.4 Tricaine solution (0.4%)

Table 9: Ingredients for 0.4% Tricaine solution

Reagent	Amount
Tricaine powder	400 mg
Tris 1M (pH=9.0)	2.1 ml
ddH <sub>2</sub> O	97.9 ml

Tricaine solution is stored at 4 °C.

### 2.1.6.5 Tris-(hydroxymethyl)-aminomethane hydrochloride (Tris-HCL) 1M

Table 10: Ingredients for Tris-HCL 1M, pH=7.5

Reagent	Amount
Tris base	121.1g
HCl	Titration to pH 7.5
ddH <sub>2</sub> O	add to 1 L

Dissolve the Tris Base in ca. 800ml of ddH<sub>2</sub>O, adjust pH to 7.5 with HCl and add ddH<sub>2</sub>O to reach 1L. Store at 4 °C.

### 2.1.6.6 Ethylenediaminetetraacetate (EDTA) 0.5M

Table 11: Recipe of Ethylenediaminetetraacetate (EDTA) 0.5M

Reagent	Amount
EDTA	18.6 g
NaOH (5M)	adjust to pH 8.0
ddH <sub>2</sub> O	add to 100 ml

Dissolve the EDTA in 70ml of ddH<sub>2</sub>O, adjust pH to 8.0 with NaOH and add ddH<sub>2</sub>O to reach 100ml. Store at 4 °C.

### 2.1.6.7 Tris-acetat-EDTA-electrophoresis (TAE) Buffer (50x stock)

Ingredients are mixed and solution is adjusted to pH=8.3. Store stock solution at room temperature.

Table 12: Ingredients for 50x TAE Buffer

Reagent	Amount
TRIS base	242 mg
Glacial acetic acid	57.1 ml
EDTA (0.5M pH 8.0)	100 ml
ddH <sub>2</sub> O	1000 ml

For gel electrophoresis use mix of 60 ml 50x TAE buffer with 3 l ddH<sub>2</sub>O.

### 2.1.7 Primers for PCR and sequencing

Primers used for all PCR and sequencing, were supplied by Biomers GmbH, Ulm Germany.

Table 13: List of primers for PCR and sequencing

primer name	orientation	sequence (5' → 3')
<i>nphp1</i> -seqF2	forward	TACTGGGGAGAGAGGAGACC
<i>nphp1</i> -seqR2	reverse	ACTCTCTGATTCGCTCCAAGG
<i>invs(sa36157)</i> -gen-F1	forward	AGTCCAGCGCTAAAATGTACA
<i>invs(sa36157)</i> -gen-R1	reverse	TGTCTCTCACACACCTGTCC
<i>nphp4(sa41188)</i> -gen-F	forward	ACTAGGTTGAACAGTTGAAGGAA
<i>nphp4(sa41188)</i> -gen-R	reverse	CCCCTTCTGCACAGGAAAG
<i>nphp4(sa38686)</i> -seq-F1	forward	GTTTTCTGGTCTGCAGCTG
<i>nphp4(sa38686)</i> -seq-R1	reverse	TGGTCAATTTAAAGCATCCACAA
<i>rpgr11(sa24730)</i> -seq-F1	forward	CACACACAGCACACACAGTT
<i>rpgr11(sa24730)</i> -seq-R1	reverse	AACGTGTTTCATCAGACGCTG
<i>rpgr11(sa10096)</i> -seq-F1	forward	CAACCCAGTCCCTACATCGT
<i>rpgr11(sa10096)</i> -seq-R1	reverse	CCCGTCTGCTGTTAAACTAGA
<i>nphp2</i> -prm_Seq-F3	forward	TGACAACATTTAGCAACAGGCT
<i>nphp2</i> -ex34_Seq-R1	reverse	CAATTACAAGTGAACCTGCGAG
M13 F	forward	GTAAAACGACGGCCAGT
M13 R	reverse	GGAAACAGCTATGACCATG

### 2.1.8 Oligonucleotides for sgRNA construction

Oligonucleotides used for sgRNA construction were supplied by Biomers GmbH, Ulm Germany

**Table 14: List oligonucleotides used for sgRNA construction**

forward oligonucleotides	sequence (5' → 3')
nphp2_ex1_gRNA1	GCAGCTAATACGACTCACTATAGTGGAGTATCAGTGGCCACAGGTTTTA GAGCTAGAAATAGCAAG
nphp2_ex2_gRNA27	GCAGCTAATACGACTCACTATAGGGCCACGCCAAGCCCCAGCAGTTTTA GAGCTAGAAATAGCAAG
nphp2_ex18_gRNA9	GCAGCTAATACGACTCACTATAGTCTAACCTCTGCAATAATCGGTTTTA GAGCTAGAAATAGCAAG
nphp2_ex18_gRNA12	GCAGCTAATACGACTCACTATAGAGGTCAATACCTGTGCGTAAGTTTTA GAGCTAGAAATAGCAAG
nphp2_ex18_gRNA19	GCAGCTAATACGACTCACTATAGTACCATCTACGGCCATCCAGGTTTTA GAGCTAGAAATAGCAAG
reverse oligonucleotide	sequence (5' → 3')
sgRNArev-P04BF	AAAAGCACCGACTCGGTGCCACTTTTTCAAGTTGATAACGGACTAGCCT TATTTTAACTTGCTATTCTAGCTCTAAAAC

### 2.1.9 Morpholino oligonucleotides

Morpholino oligonucleotides (MOs) used for MO-induced gene knock-down were supplied by Gene Tools LLC, Philomath, OR, USA.

**Table 15: List of MOs**

Morpholino oligonucleotide name	sequence (5' → 3')	stock concentration
NPHP4 AUG (TBM)	GCGCTTCTCCACTCAGACATCAGAG	1mM
NPHP4Ex1_Int (SBM)	ATTTATTCCCCATCCACCTGTGTCA	1mM
Zebrafish p53 oligo	GCGCCATTGCTTTGCAAGAATTG	1mM

### 2.1.10 Hardware

**Table 16: List of hardware**

Product	Supplier	Description
AlphaImager EC System	Alpha Innotech, San Leandro, CA, USA	fluorescent-imaging of gels
Flaming/Brown Micropipette Puller P-97	Sutter instruments, Novato, CA, USA	puller for micropipettes for injections
HBO 100 W/2	Osram Licht, München, GER	fluorescent microscopy lightbulb
Heraeus B 6030	Thermo Fisher Scientific, Waltham, MA, USA	microbiological incubator
Heraeus™ Fresco™ 17 Centrifuge	Thermo Fisher Scientific, Waltham, MA, USA	microcentrifuge refrigerated
Leica DFC 450 C	Leica Microsystems, Wetzlar, GER	microscope camera for analysis and documentation
Leica MZ16 F	Leica Microsystems, Wetzlar, GER	Stereomicroscope
Mastercycler epGradient 5341	Eppendorf, Hamburg, GER	PCR thermocycler
MyFuge™12 Mini Centrifuge	Benchmark Scientific, Sayreville, NJ, USA	mini centrifuge

peqPOWER 300	Peqlab Biotechnologie, Erlangen, GER	power supply for gel electrophoresis
PerfectBlue™ horizontal minigelsystems	Peqlab Biotechnologie, Erlangen, GER	chamber for gel electrophoresis
Pneumatic Picopump PV820	World Precision Instruments, Sarasota, FL, USA	pneumatic microinjector
SpectraMax® QuickDrop Spectrophotometer	Molecular Devices, San Jose, CA USA	measurement of DNA/RNA concentrations
XENOPHOT HLX 64634	Osram Licht, München, GER	halogen lightbulb for microscopy

### 2.1.11 Software

**Table 17: List of software**

Software	Supplier	Description
A plasmid Editor (ApE) v2.0.47	ApE by M. Wayne Davis	Tool to visualize plasmid sequences
Adobe Photoshop version 13.0	Adobe, San Jose, CA, USA	Image processing
AlphaView software version 1.2.0.1.	Alpha Innotech, San Leandro, CA, USA	Gel imaging software
CHOPCHOP version 3	Labun et al. 2019	Selecting tool for CRISPR/CAS9 target sites
Ensembl Genomes	European Bioinformatics Institute	Genomic database
GraphPad QuickCalcs	GraphPad Software, San Diego, CA, USA	Statistics software
Leica Application Suite version 4.3.0	Leica Microsystems, Wetzlar, GER	Imaging of zebrafish embryos
Microsoft Excel	Microsoft, Redmond, USA	Program used for data organization and creation of graphs
Microsoft Powerpoint	Microsoft Corporation, Redmond, WA, USA	Programm used for creation of figures
Microsoft Word	Microsoft Corporation, Redmond, WA, USA	Word processing programm

### 2.2. Housing and mating conditions of adult zebrafish

All animal care and handling carried out for this thesis was conform to national regulations and animal welfare guidelines and was approved by the ethics committee for animal experiments at the Regierungspräsidium Freiburg, Germany. The housing and mating conditions of the adult zebrafish were set up according to the recommendations described by Westerfield (Westerfield, 1995).

### **2.2.1 Housing conditions**

The zebrafish were kept in tanks in an Aqua Schwarz aquarium system (Aqua Schwarz GmbH, Göttingen, Germany), with a constant change of the water in the tanks. A room temperature in the fish room of 27°C and a water temperature of 26°C -28°C was targeted. Water temperature, pH and conductivity of the water in the system were controlled on a daily basis. To best avoid fluctuations in the water composition, the 650-liter holding distribution tank of the system was filled every day with deionized water, adding 50 g of sea salt, 100 mg CaSO<sub>4</sub> and 410 ml of NaHCO<sub>3</sub> (94 g/L) solution. The water in the aquarium system is described as fish water in this thesis. A time clock ensured a steady 12-hour-light/12-hour dark cycle. Adult fish were fed three times a day with GEMMA Micro300 fish food and in the afternoon with Great Salt Lake Artemia additionally.

### **2.2.2 Mating of the zebrafish**

Zebrafish reach reproductive maturity at around three months of age and can be set up to breed all year around under laboratory conditions (Parichy, 2015). For mating, fish were set up in pairs in the afternoon in plastic mating containers, male and female being separated by a clear plastic barrier. These mating barriers were removed simultaneously in the following morning to ensure that all the embryos have the same age and share the same stage of embryonic development. To prevent the fish from eating their own spawn, removable plastic sieves were placed in the containers, separating the fish from the eggs, which accumulate on the bottom of the container. Individual fish were set up for mating for not more than once a week, to ensure recommended recovery periods (Aleström et al., 2020).

## **2.3 Embryo collection and maintenance**

Raising of the embryos was done following the guidelines described by Westerfield (Westerfield, 1995). All the experiments for this thesis were carried out on embryos no older than 48 hours post fertilization (hpf).

### **2.3.1 Embryo collection**

To harvest the eggs, the adult fish were set back into their tanks in the aquarium system, the water in the container was poured through a strainer and the collected eggs were transferred into a petri dish with fish water. Some hours after collecting, unfertilized eggs or dead embryos were sorted out under the microscope and the fertilized eggs were transferred to a petri dish containing around 25ml of 0.3x Danieau's solution, with no more than 80 embryos per dish.

### 2.3.2 Embryo maintenance

The embryos were then put in the incubator, where they could develop at 28°C for 48 hours. If the embryos were planned to be assessed under the microscope or if imaging was planned, 50µl of a 0.003% PTU (1-phenyl-2-thiourea) solution was added to the dish 24 hours post fertilization (hpf) in order to avoid skin pigmentation of the fish and preserving their natural translucency for a longer period of time (Karlsson et al., 2001). Embryos dedicated for upbringing were transferred after 5 days post fertilization (dpf) in groups of approximately 40 into small tanks filled with deionized water, 30% Danieau's solution, sea salt, ChlorAm-X, algae solution and Rotifers. After 14 dpf, the tanks were integrated into a separate aquarium system and the fish were automatically fed with GEMMA Micro75 for 14-20 dpf and then with GEMMA Micro150 for 20-40 dpf. After period of around 30 days, the fish could be integrated into the system of the adult fish.

### 2.4 Microinjection technique

The injection set-up, consisting of a pneumatic microinjector operated by a foot pedal, a micropipette holder and microscope, allowed for precise injection of solutions into fertilized zebrafish eggs. Injection needles used for injections were pulled with a Flaming/Brown Micropipette Puller, using the following settings: Heat=750, Pull=55, Velocity=80, Time=190. In order to adjust the volume of injected solution, injection time and the lumen of the micropipette were fine-tuned until a volume of ca. 4 nl was delivered per injection. The setting of the injection volume was carefully verified by measuring the drop size on a microscopic scale. Fertilized fish eggs were placed in small grooves of an agarose ramp to provide stability during the injection process. The prepared solution was injected into the yolk sack of the embryo at 1-cell stage. Injected eggs were incubated in 30% Danieau's solution at 28°C until examination at 48 hpf.

#### 2.4.1 MO injections

MO solutions containing the actual morpholino oligonucleotide (MO), p53 MO, Phenol Red and H<sub>2</sub>O were prepared just before the injection, according to the following recipe, depending on the desired MO concentration. The use of *p53* targeting MO is reported to suppress apoptotic effects induced by off-target MO-activity and therefore recommended for MO-induced gene knock-out experiments (Robu et al., 2007).

Concentration	MO	p53 MO	Phenol Red	H <sub>2</sub> O
Stock 1 mM	µl	µl	µl	µl
0,1 mM	0,5	0,5	2	2
0,2 mM	1	0,5	2	1,5
0,3 mM	1,5	0,5	2	1

## 2.5. Zebrafish lines

### 2.5.1 Transgenic lines

The use of transgenic lines, which express green-fluorescent protein (GFP) in specific tissues and organs facilitate the assessment of phenotypes by epifluorescent microscopy.

Table 18: List of transgenic zebrafish lines

Line name	Description
<i>cdh17:GFP; wt1b:GFP</i>	in-cross of wt1b:GFP and cdh17:GFP → expression of GFP regulated by cdh17 and wt1b promoters
<i>Tg(-8.0 cldnb:LY-EGFP); wt1b:GFP</i>	In-cross of wt1b:GFP and cldnb:LY-EGFP →expression of GFP regulated by the wt1b promoter and expression of EGFP and LY regulated by the cldnb promoter

wt1b:GFP expression in the glomerulus and proximal tubulus (Perner et al., 2007)

cdh17:GFP expression in the entire pronephric tubular segments (Horsfield et al., 2002)

cldnb:LY-EGFP: expression in the pronephric duct (Haas and Gilmour, 2006)

### 2.5.2 Mutant lines and their transgenic outcrosses

Table 19: List of mutant fish lines and their transgenic outcrosses

Line name (genotype)	Mutation/transcriptional consequence	affected gene (affected aa)	flanking sequence/ deleted bases
<i>nphp2_sa36157</i>	point mutation/ premature stop	invs/nphp2 (aa 314/1025)	5'- GCCTGACCTA [G/T] AGGGACGAAC -3'
<i>Tg(-8.0cldnb:LY-EGFP) T/+</i> , <i>nphp2_sa 36157 m/+</i> , <i>wt1b:GFP T/+</i>			
<i>nphp4_sa41188</i>	point mutation/ premature stop	nphp4 (aa 444/1417)	5'- TAGTGCAGAA [G/T] GAGTTTCTAG -3'
<i>Tg(-8.0cldnb:LY-EGFP) T/?</i> , <i>nphp4_sa41188 m/+</i> , <i>wt1b:GFP T/?</i>			
<i>nphp4_sa38686</i>	point mutation/ splice site variant	nphp4 (aa 764/1417)	5'- GGAGCTGAAG [G/A] TAGAACTGCC -3'

<i>Tg(-8.0cldnb:LY-EGFP) T/?</i> , <i>nphp4_sa38686 m/+</i> , <i>wt1b:GFP T/?</i>			
<i>nphp8_sa24730</i>	point mutation/ splice site variant	rpgr11/nphp8 (aa 337/1256)	5'- GTCTGTTTCC [A/T] GTTACAAGAG -3'
<i>Tg(-8.0cldnb:LY-EGFP) T/+</i> , <i>nphp8_sa24730 m/+</i> , <i>wt1b:GFP T/+</i>			
<i>nphp8_sa10096</i>	point mutation/ premature stop	rpgr11 (aa 862/1256)	5'- TGGTGGTTTA [T/A] GTTGTTTGAT -3'
<i>Tg(-8.0cldnb:LY-EGFP) T/?</i> , <i>nphp8_sa10096 m/+</i> , <i>wt1b:GFP T/?</i>			
<i>cdh17:GFP T/?</i> , <i>nphp4-ex1-del5 m/+</i> , <i>wt1b:GFP T/?</i>	deletion of 5 bp in exon1 / premature stop	nphp4 (aa 44/1417)	5'- GATTCCGCCG - CACAG - TCAGACTGCT -3'
<i>Tg(-8.0cldnb:LY-EGFP) T/?</i> , <i>nphp1-ex15-del4 m/+</i> , <i>wt1b:GFP T/?</i>	deletion of 4 bp in exon 15 / premature stop	nphp1 (aa 463/667)	5'- AGCTCACCAT - TCAT - GGTGGCACGC -3'

## 2.6 Lysis of zebrafish embryos or after fin clipping

Embryos designated for sequencing were lysed to access their genomic DNA. They were transferred into PCR tubes individually; the fish water was removed at the best and 40 µl of 50mM NaOH was added to each tube. The embryos were then incubated at 95°C for 20 minutes then cooled down to 4°C. To neutralize the pH level, 4 µl of 1 M Tris HCl was added to each tube. At this state, the embryos could be stored at -20°C or immediately used for subsequent experiments. In order to genotype adult fish, this same lysis process was carried out with small pieces cut of the tips of their tailfin.

## 2.7 Polymerase chain reaction (PCR)

Polymerase chain reaction (PCR) is a standard method in molecular biology, used to amplify DNA fragments (Analytical Methods Committee AMCTB No.59, 2014). Experiments for this thesis PCR required the use of two different PCR settings, using different DNA polymerases for each



setting. PCR was primarily used to amplify specific segments of the genomic DNA of lysed embryos for sequencing. For this application OneTaq<sup>®</sup> Quick-Load<sup>®</sup> 2X Master Mix was used. In the setting of sgRNA construction, KOD Hot Start DNA Polymerase (Merck KGaA, Darmstadt, Germany) was used.

### 2.7.1 Standard PCR

To determine the presence of mutant alleles and by this mean, categorizing fish into being wildtype, heterozygote or homozygote, PCR was used to amplify a specific segment of the affected gene.

Corresponding primer pairs for the mutations *nphp2<sup>sa36158</sup>*, *nphp4<sup>sa38686</sup>*, *nphp4<sup>sa41188</sup>*, *rpgrip1l<sup>sa24730</sup>* and *rpgrip1l<sup>sa10096</sup>* (Table 13) were used together with OneTaq<sup>®</sup> Polymerase and lysis product as DNA template, to perform the PCR according to the company's protocol.

The reaction setup for each tube was the following:

- 12.5 µl OneTaq<sup>®</sup> Quick-Load<sup>®</sup> 2X Master Mix
- 8.5 µl H<sub>2</sub>O
- 1 µl forward primer (10 pmol/µl)
- 1 µl reverse primer (10 pmol/µl)
- 2 µl DNA template

If not specified differently, based on findings of previous gradient PCR experiments, the annealing temperature was varied during the PCR according to the touchdown principle. The touchdown PCR method is a simple way to optimize primer-template interaction by applying a larger spectrum of annealing temperatures covering the estimated melting temperatures of the primers used. This approach allows for an optimized hybridization performance of the primers and therefore an increased yield, sensitivity, and specificity of the PCR (Korbie and Mattick, 2008). The annealing temperature is gradually lowered over the course of successive cycles in the touch down PCR.

The settings for PCR thermo cycler for a touchdown PCR were as listed:

**Table 20: Settings for touchdown PCR**

	<b>PCR step</b>	<b>Temperature</b>	<b>Time setting</b>
<b>1</b>	denaturation	94 °C	2 min
<b>2</b>	denaturation	94 °C	15 sec
<b>3</b>	primer annealing	62 °C	30 sec
		<b>-0,2 °C every cycle</b>	
<b>4</b>	primer extension	68 °C	1 min

5	repeat steps 2-4		32 times
6	Final extension	68 °C	7 min
7	Cool down	4 °C	forever

### 2.7.2 Gradient PCR

Gradient PCRs were performed to identify the best fitting annealing temperature of any new primers or for troubleshooting, if the PCR results were not ideal (Gerke and Hellberg, 2013).

Since the thermo cycler used in this work, has twelve rows, twelve tubes containing the reaction setup, consisting in *OneTaq*<sup>®</sup> Polymerase, H<sub>2</sub>O, forward primer, reverse primer, and DNA template, could undergo the PCR cycle with each rows presenting a different temperature for the annealing step. By covering a range of annealing temperatures and comparing the results *via* gel electrophoresis, the optimal annealing temperature for a primer pair could be pinned down. All the other steps remained unchanged from the ones in the standard PCR.

### 2.7.3 PCR in the sgRNA construction process

In the setting of sgRNA construction for gene editing *via* the CRISPR/Cas9 method, KOD Hot Start DNA Polymerase was used to amplify sgRNA templates. This method is designed to minimize the off-target primer hybridization reactions, which could lead to undesired amplifications, especially during the lower temperature conditions and thereby reduce the efficiency of the intended amplification (Chou et al., 1992).

The reaction setup for each tube was the following:

- 10 µl 10X buffer
  - 3.5 µl dNTP's
  - 4 µl MgSO<sub>4</sub>
  - 2 µl forward primer (100 pmol/ µl) (ordered for sgRNA design)
  - 2 µl reverse primer P04BF (100 pmol/µ) (not target specific)
  - 2 µl KOD Hot Start Polymerase
  - 76.5 µl H<sub>2</sub>O
- 
- Total volume 100 µl

The settings for PCR thermo cycler for a PCR were as listed:

**Table 21: Settings for PCR with KOD Hot Start DNA Polymerase**

	<b>PCR step</b>	<b>Temperature</b>	<b>Time setting</b>
1	denaturation	95 °C	2 min
2	denaturation	95 °C	20 sec
3	primer annealing	58 °C	10 sec
4	primer extension	70 °C	15 sec
5	repeat steps 2-4		31 times
6	Final extension	70 °C	5 min
7	Cool down	8 °C	forever

#### **2.7.4 PCR on PCR**

If the concentration of the PCR product from a PCR, which was performed on the genomic DNA of lysed CRISPR/Cas9 injected embryos was too low to allow clear judgment, a second PCR was performed with the PCR product of the first PCR as DNA template. This PCR on PCR was carried out with the same primers and the same settings on the thermo cycler.

#### **2.7.5 Colony PCR**

Colony PCR was performed on clones of DH10 bacteria carrying the TOPO vector, which integrated the genomic DNA of CRISPR/Cas9 injected embryos. The PCR products of this colony PCR could then be sent for sequencing in order to confirm whether or not the CRISPR/Cas9 induced gene editing worked and to determine the exact mutation of every clone individually.

The reaction setup for each tube was the following:

- 12.5 µl OneTaq<sup>®</sup> Quick-Load<sup>®</sup> 2X Master Mix
- 8.5 µl H<sub>2</sub>O
- 1 µl M13 forward primer (10 pmol/µl)
- 1 µl M13 reverse primer (10 pmol/µl)

Individual colonies, selected with the blue-white selection method (Reinard, 2021), were added in different tubes each, by being picked with a sterile pipette tip and mixed to the reaction setup.

The settings for PCR thermo cycler for a colony PCR were as listed:

**Table 22: Setting for Colony PCR**

	<b>PCR step</b>	<b>Temperature</b>	<b>Time setting</b>
<b>1</b>	denaturation	94 °C	2 min
<b>2</b>	denaturation	94 °C	15 sec
<b>3</b>	primer annealing	55 °C	30 sec
<b>4</b>	primer extension	68 °C	1 min
<b>5</b>	repeat steps 2-4		32 times
<b>6</b>	Final extension	68 °C	7 min
<b>7</b>	Cool down	4 °C	forever

## **2.8 Agarose gel electrophoresis**

To visualize the length and concentration of PCR products, agarose gel electrophoresis was used (Lee et al., 2012). Every gel was casted using a 1% agarose solution and contained 6.7 µl ethidium bromide per 100ml solution, which acts as a fluorescent tag to visualize the DNA fragments under UV-light. The gel chamber was filled with 1% TAE buffer solution, providing conductivity whilst protecting the DNA from hydrolysis and enzyme activity. On every gel, 4 µl of 1 kb Plus DNA Ladder was run alongside the samples as a gene ruler.

If the PCR was performed using *OneTaq*<sup>®</sup> Quick-Load<sup>®</sup> 2X Master Mix, 4 µl of the samples could be loaded on the agarose gel straight away. If the PCR was performed with KOD Hot Start Polymerase, the addition of a loading dye to the samples was necessary before loading them on the gel. Settings of the power supply for the electrophoresis process were set to 125V, 400mA for 20 minutes. Fluorescence images of the gels were taken for documentation purposes using the AlphaImager EC System with the Alpha View Software v.1.2.0.1.

## 2.9 Purification of PCR products

Before being sent for sequencing, PCR products of standard PCR reactions using *OneTaq*<sup>®</sup> Polymerase were prepared according to the following purification protocol:

0.5 µl Exonuclease I, 1 µl Antarctic Phosphatase and 2.5 µl H<sub>2</sub>O were added to every PCR tube containing 25 µl of PCR product. The tubes were then incubated in the PCR cycler at 37 °C for 15 minutes, then heated up to 80 °C for another 15 minutes and finally cooled down to 4 °C.

PCR products of PCRs using KOD Hot Start Polymerase, were purified using the Thermofischer Scientific GeneJET PCR Purification kit according to the following protocol:

100 µl of PCR product was mixed with 100 µl of Binding Buffer and 100 µl of isopropanol and put on the GeneJET purification column. After being centrifuged at 13.300 rpm for 1 minute, the flow-through was discarded. Then 700 µl of Wash Buffer was added to the column, before undergoing another minute in the centrifuge at 13.300 rpm. Again, the flow-through was discarded and the empty column was centrifuged one more time at 13.000 rpm for 1 minute in order remove any residual buffer. Now the purified PCR product could be harvested by putting the column on a fresh Eppendorf tube, adding 30 µl of H<sub>2</sub>O and centrifuging one more time for 1 minute at 13.300 rpm.

## 2.10 DNA sequencing (Sanger sequencing)

Sequencing of the gene products of the PCR reactions described in 2.7.1 was done using the “Sanger” method (Ableitner, 2022). This task was outsourced to two different contractors. Samples were sent either to GATC Biotech AG, Konstanz, Germany or to GENEWIZ Germany GmbH, Leipzig, Germany. The PCR samples were diluted by mixing 2 µl of PCR product with 18 µl of H<sub>2</sub>O and 1 tube containing 20 µl of the corresponding forward or reverse primer (10 pmol/µl) for every 8 sample-tubes, was added to the order. This primer is needed by the contractor to perform the second, so called “sequencing PCR” using dideoxynucleotide triphosphates (ddNTPs) in addition to the usual dNTPs and which is preliminary to the actual Sanger sequencing, which is based on capillary electrophoresis (Ableitner, 2022).

## 2.11 sgRNA construction for CRISPR/Cas9 gene editing method

The generation of large deletions in genes of the zebrafish genome, eliminating most of the open-reading frame, allows for a complete gene knockout. To generate new zebrafish mutant lines with such large deletions of the *invs/nphp2* gene, I used the CRISPR/Cas9 gene editing method. This method is based on Cas9 nuclease activity guided by two sgRNAs to the desired target sequences in the gene, causing gene knockout and therefor loss-of-function in the injected embryo. The PCR-

based strategy for the construction of the sgRNAs, described by Nakayama (Nakayama et al., 2014), is relatively simple and can be broken down to a few steps:

**Step 1: selection of target sites**

The selection of target sites was based on the ranking given by the web-based tool CHOPCHOP (Labun et al., 2019). The GeneID was taken from Ensemble.org (Howe et al., 2021) (*invs/nphp2: ENSDARG00000002213*) and target sites for knock-out using CRISPR/Cas9 were scanned for in the zebrafish genome (danRer10/GRCz10) adjusting the target specific region of gene to the option “all exons (incl. UTRs)”.

**Step 2: ordering forward primers including the chosen target sequences**

For the next step of the sgRNA template construction process, it is necessary to design and order forward (fwd) primers, which are unique to every target sequence. These primers were designed according to a common structure (Nakayama et al., 2014):

**5’-GCAGCTAATACGACTCACTATAG(N)<sub>20</sub>GTTTTAGAGCTAGAAATAGCAAG-3’**

The T7 RNA polymerase promotor sequence (violet) is followed by a Guanine base (orange), being the first base incorporated into the RNA and required for efficient transcription by the T7 RNA polymerase. Next comes the target sequence (red) not including the PAM sequence, followed again by the 5’ part of the universal scaffold. To enhance T7 polymerase efficiency an extra 5’ sequence is placed in front of the T7 promotor. The sequences of all the ordered fwd primers are listed in table 14.

**Step 3: amplification of sgRNA templates via PCR**

The PCR in this step is performed using the fwd primers, ordered in step 2 and non-specific reverse (rev) primer (sgRNArev-P04BF) shown in table 14. The PCR was carried out using KOD Hot Start DNA Polymerase, as described in 2.7.3.

**Step 4: purification of the PCR products**

Purification was done using the GeneJET PCR Purification kit as described in 2.9 to prepare the PCR products for the next step.

### **Step 5: In vitro transcription**

In the construction process of sgRNA, used for gene editing *via* CRISPR/Cas9, *in vitro* transcription is necessary to transcribe DNA into RNA. This transcription was done using the Thermo Fisher MEGAshortscript™ T7 Transcription Kit according to the company's protocol. For the reaction set-up 2 µl of each rNTP solution (ATP, CTP, GTP and UTP) were mixed and 2 µl of 10X reaction buffer, 6 µl of PCR product (0.6 µg), 2 µl of T7 Enzyme Mix and 2 µl of nuclease-free water were added. This reaction set-up was then incubated for 4 hours at 37 °C. After adding 1 µl of Turbo DNase to remove remaining DNA templates, the set-up was incubated again for 15 minutes at 37°C. The RNA product was purified by phenol-chloroform-extraction.

### **Step 6: Phenol-Chloroform-Extraction**

In order to isolate the RNA from any contamination of proteins and enzymes phenol-chloroform-extraction was used. 100 µl of the solution containing RNA to be purified were mixed with 10 µl of 3M sodium acetate and 100 µl phenol-chloroform-solution. This set-up was centrifuged for 3 minutes at 13.300 rpm, causing the sample to be separated into two phases. The upper aqueous phase contains the nucleic acids, denatured proteins are concentrated in the bottom phase composed of phenol-chloroform-solution. The upper phase was cautiously transferred to a new tube with a pipette, mixed with 250 µl of 100% Ethanol and stored for at least 20 minutes at -20°C. After this step, the tube was centrifuged for 20 minutes at 13.300 rpm and 4°C, causing the formation of a pellet at the bottom of the tube. This pellet was then washed with 70% Ethanol and centrifuged for 4 minutes at 13.300 rpm. Supernatant alcohol is discarded, and the pellet is cured for 5 minutes at room temperature. Finally, the pellet is eluted in 20 µl of ddH<sub>2</sub>O, quality was controlled *via* gel electrophoresis and the RNA concentration could be measured using spectrophotometry.

## **2.12 Crispr/Cas9 Injections**

Injections of sgRNAs for the CRISPR/Cas9 gene editing method were performed in a similar way to the injections used in the MO-induced knockdown experiments (see 2.4.1). Injection solutions, containing all five of the designed sgRNAs at the desired concentration, together with the Cas9 nuclease, Phenol Red and H<sub>2</sub>O, were prepared immediately before injection according to the recipe shown in table 23. The Cas9 nuclease, which was used is conjugated with a nuclear localization sequence (NLS) for better transport of the CRISPR/Cas9 complex into the nucleus (Hu et al., 2018). Embryos were put into Danieau's solution and stored in an incubator at 29 °C after injection.

**Table 23: Injection solutions for sgRNA microinjections.**

	<b>100 ng/μl/sgRNA</b>	<b>200 ng/μl/sgRNA</b>	<b>260 ng/μl/sgRNA</b>
sgRNAs (c=400 ng/μl)	5 x 0.5 μl	5 x 1.0 μl	5 x 1.3 μl
Cas9 nuclease (c= 2 μg/μl)	1.5 μl	1.5 μl	1.5 μl
Phenol Red	3 μl	2 μl	2 μl
H <sub>2</sub> O	3 μl	1.5 μl	/
Total volume	10 μl	10 μl	10 μl

### 2.13 TOPO Cloning

The genomic DNA of embryos injected with sgRNAs and Cas9 nuclease was amplified using PCR and served as a template for cloning, using the Thermo Fisher Scientific TOPO® TA Cloning® Dual Promoter kit with pCR 2.1-TOPO TA cloning vectors. According to the protocol provided by the company, 2 μl of PCR product, 0.5 μl Salt Solution and 0.5 μl Topo vector were mixed and incubated at room temperature for 30 minutes. After incubation the tubes, now containing recombinant TOPO vectors with integrated plasmid DNA were put on ice.

### 2.14 Transformation

Transformation of TOPO vectors containing plasmid DNA into OneShot TOP10 chemically competent *Escherichia coli*, was conducted according to the following standard protocol:

2 μl of TOPO cloning reaction product was mixed with One Shot TOP10 chemically competent *E. Coli* and incubated for 20 minutes at 0°C. The mixture was heat-shocked for 90 seconds at 42°C, allowing the penetration of plasmid DNA into the bacteria. The mixture was cooled down on ice for 2 minutes, before adding 250 μl S.O.C. medium and incubating at 37°C for 20 minutes. Bacteria were spread out evenly on ampicillin containing (100 μg/ml) agar plates for amplification using glass beads. The use of ampicillin ensures that only *E. coli* colonies with TOPO vectors, recombinant or not, carrying a specific gene in their plasmid sequence, which renders *E. coli* resistant to a ampicillin, can grow on the plate (Reinard, 2021). The agar plates have previously been treated with 40 μl IPTG (0.1M) and 40 μl X-Gal (20 mg/ml) to allow blue-white selection of the colonies later. Bacteria were then incubated at 37°C overnight.

### 2.15. Clone selection

Individual *E. coli* colonies were selected on account of the successful inclusion of the recombinant TOPO vector carrying the genomic DNA of the injected embryo, making use of the blue/white screening method. This method relies on the fact, that the genomic DNA fragments are inserted at specific sites in the plasmid sequence. If the plasmid site, which codes for components of



functional galactosidase, is disrupted by this insertion, X-Gal cannot be processed and colonies appear white (Reinard, 2021). Under microscopic control, colonies were picked with a pipette tip from the agar plate and separately inoculated in LB-medium with Ampicillin (50 µg/ml) at 37°C overnight on a shaker.

White colonies of *E. coli* contained the TOPO vector with the plasmid DNA successfully inserted, blue colonies just contained the TOPO vector, without the insert.

### **2.16 Plasmid DNA preparation – Mini preparation**

Sequencing of the plasmid DNA of individual colonies, allowed evaluating the success and dimension of the gene edit by CRISPR/Cas9. To do so, plasmid DNA was isolated from the vector using the VWR peqGold Plasmid Miniprep Kit 1 following the protocol supplied by the company. The high-copy-plasmid containing overnight-cultures were transferred to Eppendorf tubes and centrifuged for 1 minute at 13.300 rpm. Supernatant was discarded and the bacteria pellets were resuspended in 250 µl of Solution I/RNase A, lysing the bacteria. 250 µl of Solution II were added and the tubes gently inverted several times before adding 350 µl of Solution III and gently inverting them again. Next, the tubes were centrifuged for 1 minute at 13.300 rpm and the supernatants were transferred to the PerfectBind DNA columns, used to bind to the plasmid DNA and allowing for its isolation. The columns are centrifuged for 1 minute at 13.300 rpm. Two washing steps followed the first one with 500 µl of PW Plasmid Buffer and the second one with 750 µl of PE DNA Wash Buffer, with 1 minute of centrifugation at 13.300 rpm and discarding of the flow-through after each step. The sample is centrifuged for 1 minute at 13.300 rpm, the flow-through discarded and then centrifuged for 2 more minutes at 13.300 rpm to remove any residual washing solution. In order to yield the plasmid DNA, bound to the columns, the columns were transferred to new Eppendorf tubes, 30 µl of ddH<sub>2</sub>O were added and after 1 minute of waiting time, the columns are centrifuged one last time for 1 minute at 13.300 rpm. The plasmid DNA concentration can now be measured by spectrophotometry and stored at -20 °C until used for further experiments.

### **2.17 *In situ* hybridization**

*In situ* hybridization (ISH) was performed to visualize the heart loop and make it accessible for imaging of typical examples of different heart loop orientations. Embryos which have been selected for ISH at 48 hpf, were killed with tricaine and fixed in 4% PFA-PBS overnight. They were then transferred in 100% MeOH and stored at -20°C until further treatment. The *in situ* hybridization was carried out following a protocol described by Thisse et al. (Thisse and Thisse, 2014) with some minor alterations made by Annette Schmitt, a technical assistant in our lab. The staining process takes three days.

**Day1:** Before the staining process can be started, the embryos must be rehydrated by three successive incubations of 5 min each in MeOH-PBS solutions of decreasing MeOH concentration. This step was followed by four washing cycles of 5 min using 100% PBST (PBS/Tween20 0.1%). For digestion, the embryos are then transferred into tubes, containing 200  $\mu$ l of digestion solution (2 $\mu$ l Proteinase K c= 10 $\mu$ g/ml and 1ml PBST). The duration of the digestion was 11 minutes. The embryos were then refixed in 4% PFA-PBS for 20 min, washed five times in PBST for 5 min. The hybridization mix (HM+) is prepared as follows:

25 ml Formamide 50%  
12.5 ml 20x SSC  
0.5 ml Tween20 10%  
460  $\mu$ l Citric acid 1M  
50  $\mu$ l Heparin (c= 50 mg/ml)  
11.49  $\mu$ l tRNA from torula yeast type IV (c= 2.2  $\mu$ g/  $\mu$ l)

**Total: 50  $\mu$ l**

A prehybridization mix (HM-) is prepared similarly to HM+, expect for Heparin and tRNA. The embryos are prehybridized in 400 $\mu$ l HM+ for 3 hours at 70°C. The HM+ is carefully removed and discarded. Hybridization of the embryos is done by incubating them at 70°C overnight in a solution containing HM+ and 100-200 ng of the antisense RNA probe *cmlc2*, a probe which was designed in our lab.

**Day 2:** The HM+ and RNA probe-containing solution is removed. A series of successive 15min washing steps in 70°C solutions, with decreasing HM- and increasing 2xSSC percentages, follows. Subsequently the embryos are washed twice in 0.2xSSC for 30min at 70°C. In the following 10min washing steps the 0.2x SSC solution is gradually reduced, while the PBST ratio increases of the washing solution increases. To prevent the anti-DIG-antibody from binding to non-specific binding sites in the next step, the embryos are incubated for several hours in 800 $\mu$ l blocking solution, which contains 40 $\mu$ l sheep serum and 760 $\mu$ l PBST. The incubation in 200 $\mu$ l antibody solution, with contains 1 $\mu$ l anti-DIG antibody and 2ml blocking solution, takes place overnight at 4°C.

**Day 3:** The anti-DIG antibody solution is removed, and the embryos are washed six times in PBST for 15min. They are then incubated in staining buffer three times for 5 min. The staining buffer is prepared as follows:

5 ml Tris HCL 1M (pH= 9.5)  
2.5 ml MgCl<sub>2</sub> 1M  
1 ml NaCl 1M  
0.5 ml Tween20 10%  
41 ml ddH<sub>2</sub>O

**Total: 50 ml**

The embryos are transferred into well-plates and 1 ml staining solution “BM Purple” is added. The staining process, which takes place at 37°C shielded from light, is controlled regularly under the microscope, and stopped when the staining intensity is satisfying. In my case this was after a staining period of 60min. To stop the reaction, the staining solution is removed, and embryos are washed twice for 5min in stop solution (2µl EDTA (0.5mM solved in 1ml PBS). The embryos are then stored in 80% glycerol at 4°C.

## **2.18 Microscopy**

A Leica MZ16F stereo microscope was used for analysis of zebrafish embryos, as well as for microinjections or photo documentation. This microscope is equipped with UV-fluorescent lighting, enabling the analysis of transgenic lines, which express green-fluorescent protein (GFP) in specific tissues and organs, facilitating the phenotype assessment. For optimal phenotype assessment at 48 hpf, the embryos were carefully removed from their chorion using forceps and anesthetized by adding some drops of tricaine solution to the dish for easier handling and counting. Selected fish presenting well developed phenotypes were photo documented with a Leica DFC 450C camera and processed using Leica Application Suite and Adobe Photoshop. For pictures using transmitted light rather than UV-light, selected anesthetized embryos were transferred to a specimen slide into some drops of methylcellulose for better handling and to allow for the most favorable positioning.

## **2.19 Statistical analysis**

P-values for this thesis were calculated using the two-tailed Fisher’s exact test and considered statistically significant if  $p < 0.05$ . Calculations were done using the online GraphPad Software.

### 3. Results

To identify molecular functions of Nphps and their role in ciliogenesis, ciliary function and cell migration, processes which are crucial in zebrafish embryonic development, our group used a methodical approach whose different stages build upon each other. At a first stage, MO-knockdown experiments of the components of the Nphp1-4-8 module as well as Nphp2, revealed that the knockdown of all four genes resulted in glomerular cyst formation in the proximal segment of the pronephros and cloaca malformation, which is characterized by the formation of a fluid-filled cyst instead of the normal body opening. MO-induced knockdown of the *nphp4* gene resulted in the highest frequencies of both phenotypes, whereas *nphp1* knockdown was associated with a relatively low phenotype frequency. The next step was, the comparison between the phenotypes observed in zebrafish with MO-mediated depletion of the *nphp* gene (morphants), and the ciliopathy phenotypes observed in zebrafish lines carrying a defined point mutation (mutants) in these same genes. The aim was to help with the interpretation and/or validation of the MO-knockdown experiments as well as the discovery of zebrafish who might compensate their point mutation. The aim of my experiments, the results of which I will describe in the following section, was to go one step further and analyze whether the ciliopathy phenotypes in mutants might change from one generation to the next one, indicating compensatory adaptation and also determine the contribution of maternally derived products to early development.

#### 3.1 Ciliopathy phenotypes in zebrafish mutant lines with defined point mutations – an intergenerational comparison

In this multi-year project, my predecessor and fellow doctoral candidate Friedemann Zaiser, focused on the impact which point mutations in the *nphp2*, *nphp4* and *nphp8* genes, generated by chemical ENU mutagenesis, had on the cloaca formation. He described the cloaca formation, consisting in directed migration of distal pronephric tubule cells and fusion of the pronephric duct with the ectoderm in great detail. I wanted to complete his data on cloacal morphogenesis in these zebrafish mutant lines, with data on renal development, focusing especially on the incidence of glomerular cyst formation caused by defined point mutations. Furthermore, I wanted to compare the incidence of glomerular as well as cloaca cyst formation in the first generation of mutant zebrafish lines, to the following generation. This second generation is composed of maternal zygotic mutants, which means that they are devoid of any maternally derived wild-type gene products, which could influence the early developmental stages in the F1 generation and potentially mask phenotypic effects of biallelic mutations in embryos. The pairing strategy used for this intended purpose is depicted in Figure 6. First, heterozygote mutant (m/+) zebrafish were crossed, resulting in zygotic mutant zebrafish in F1. In a second step, homozygote mutant (m/m)

zebrafish from F1 were in-crossed to generate maternal zygotic mutant (m/m) fish in F2. This procedure allowed for the elimination of any contribution of maternal wildtype mRNA in the F2 generation. The wildtype (+/+) zebrafish of the F1 generation were crossed as well, to serve as control in F2.

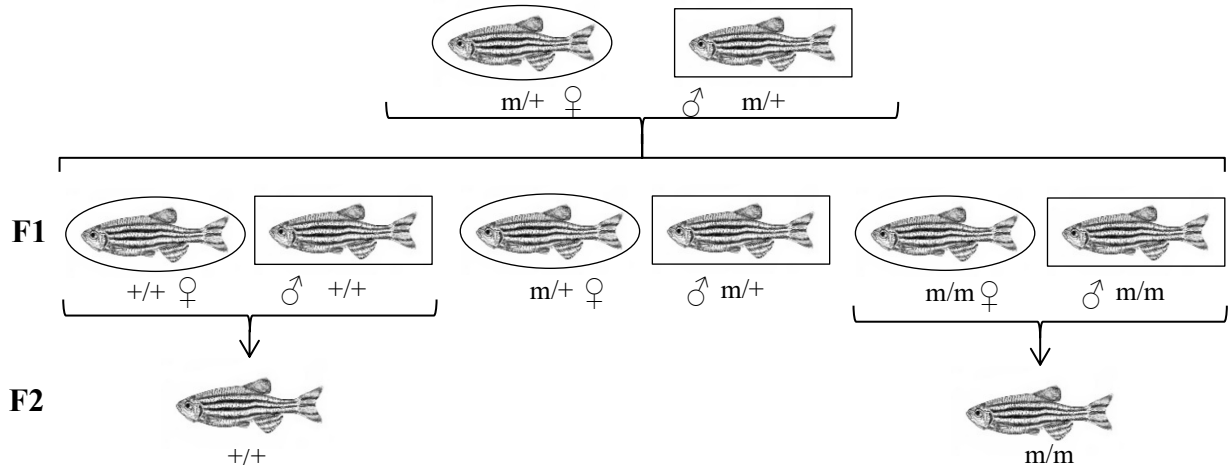


**Figure 6: Scheme of the zebrafish pairing strategy** - adapted from (Kayser et al., 2022)

The incross of heterozygote mutant fish results in zygotic mutant fish in the F1 generation. By in-crossing homozygote (m/m) male and female fish from F1, carrying either two wildtype alleles (+/+) or two mutant alleles (m/m) one can generate maternal zygotic mutants (m/m) in F2 as well as wildtype (+/+) control siblings. In maternal zygotic mutants, the influence of maternal wildtype mRNA or maternally supplied wildtype proteins is completely eliminated.

I assessed in the F2 generation, in addition to the frequency of glomerular cyst formation and cloaca malformation, four other ciliopathy-associated phenotypes, which have all been linked to ciliary dysfunction: hydrocephalus, heart edema, aberrant orientation of the heart-loop and abnormal body curvature. All these phenotypes are caused by impaired function of cilia. If cilia are defective, the cerebrospinal fluid flow is affected, which can cause the development of hydrocephalus. The formation of heart edema can also be linked to impaired fluid flow in between body compartments. Cilia in the laterality organ of the zebrafish, named Kupffer's vesicle, have been shown, to play an important role in the left-right body axis determination, which is scored for by determining the orientation of the heart loop. Abnormal body curvature is one more ciliopathy-associated phenotype, scored for in maternal zygotic mutant zebrafish lines.

### 3.1.1 Point mutations in *invs/nphp2*

The *nphp2*<sup>sa36157</sup> (G>T) (Tab. 19) line carries a nonsense mutation causing the insertion of an early stop codon after amino acid 314, terminating the protein translation process prematurely within the ankyrin repeat-containing domain (Fig. 7A). Heterozygote (m/+) fish were crossed to generate zygotic mutants in the F1 generation. The zebrafish embryos were analyzed 48 hours post fertilization and scored for glomerular cyst formation (Fig. 7B) and cloaca malformation, displaying as cysts instead of the normal body opening at the end of the pronephric duct. Data for cloaca malformation in the F1 generation were collected by Friedemann Zaiser and are shown here for reasons of comparison (Fig. 7D). In F1, homozygote mutant (m/m) zebrafish showed an increase in glomerular cyst formation and in cloaca malformation, however not being statistically significant in both cases. Heterozygote (m/+) zebrafish showed an intermediate prevalence of both ciliopathy phenotypes, an unusual observation for a recessive disease like nephronophthisis and consequently a sign of potential haplotype insufficiency. Nonetheless the difference between heterozygote (m/+) fish and their wildtype (+/+) siblings were statistically not significant (Fig. 7C-D). Breeding of maternal zygotic mutant (m/m) zebrafish in F2, eliminating any maternal contribution, was achieved following the pairing scheme depicted in Figure 6. Maternal zygotic (m/m) fish showed significantly more (2.7-fold) glomerular cysts compared to their (+/+) siblings. On the other hand, a malformation of the cloaca in (m/m) fish seemed to be only half as frequent as in the (+/+) controls (Fig. 7E). It is only by comparing the (m/m) mutant fish of the F1 and F2 generation, normalized to the frequency of glomerular cyst formation and cloaca malformation in the corresponding (+/+) controls of each generation, that a decrease in the frequency of these phenotypes becomes obvious. Glomerular cyst formation lowered to 75% and cloaca malformation even dropped to 23% in the F2 generation compared to F1 (Fig. 7F).

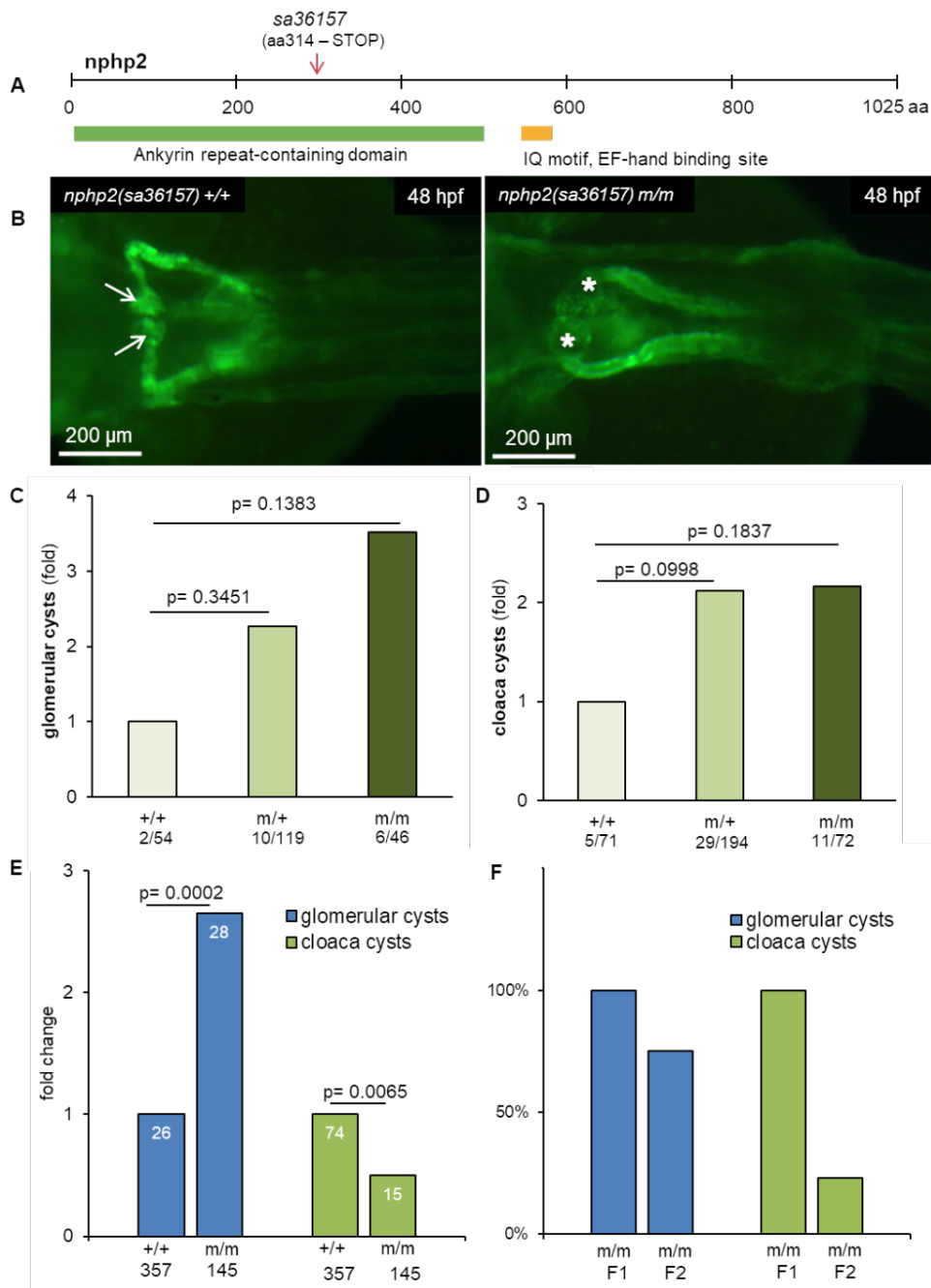


**Figure 7: Glomerular and cloaca cyst formation of F1 and F2 *nphp2*<sup>sa36157</sup> mutant fish**

(A) Graphic illustration of the *invs/nphp2* zebrafish gene. *nphp2*<sup>sa36157</sup> carries a nonsense point mutation (G>T), translating to a premature stop codon after the amino acid (aa) 314, within the ankyrin repeat-containing domain. (B) Images of the glomerular region obtained by fluorescent microscopy at 48 hours post fertilization (hpf). The image on the left shows normal glomeruli (arrows) in a wildtype (+/+) control embryo. The image on the right shows bilaterally paired glomerular cysts (stars) in a homozygote mutant (m/m) embryo. (C) and (D) Graphs showing the frequency of glomerular cyst formation and cloaca malformation (data from Friedemann Zaiser) respectively, in heterozygote (m/+) and homozygote (m/m) embryos in F1 in relation to their wildtype (+/+) siblings. The numbers underneath each column represent the number of observed embryos presenting the respective phenotype and the total number of embryos scored for each genotype. (E) Graph showing the frequency of glomerular cyst formation and cloaca malformation, in homozygote (m/m) maternal zygotic embryos in F2 in relation to their wildtype (+/+) siblings. The numbers in each column represent the number of observed embryos presenting the respective phenotype and the number underneath each column indicates the total number of embryos scored for each genotype. (F) Graph illustrating the comparison between the incidence of abnormalities in homozygote mutant (m/m) embryos in the F1 and F2 generation. For comparison, the frequency of ciliopathy phenotypes in (m/m) mutants in F1 was set to 100% and changes in maternal zygotic mutants in F2 were expressed in relation to F1. (Fisher's exact test, two-tailed)

The assessment of the four additional ciliopathy-associated phenotypes revealed that maternal zygotic mutant (m/m) embryos in the F2 generation showed significantly more hydrocephalus formation than their wildtype (+/+) siblings. Even though (m/m) embryos developed a hydrocephalus 5-times more often than the (+/+) controls, they were statistically no different considering faulty body axis determination, assessed by the orientation of the heart loop, heart edema formation or abnormal body curvature. In fact, (+/+) embryos showed slightly more abnormal heart looping and heart edema development than their mutant siblings (Fig.8).

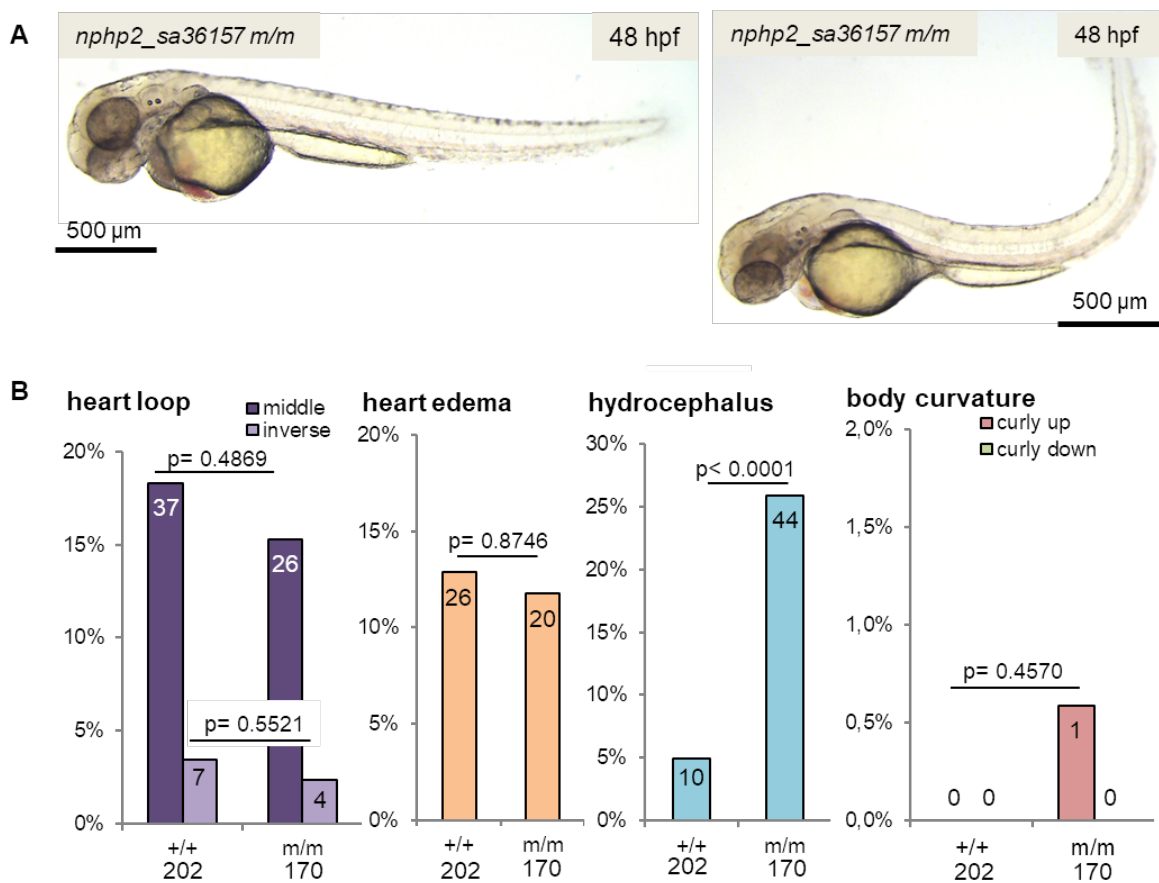


**Figure 8: Ciliopathy associated phenotypes in F2 *nphp2<sup>sa36157</sup>* mutant fish**

(A) Images of *nphp2<sup>sa36157</sup>* zebrafish embryos acquired with an optical stereo microscope at 48 hours post fertilization (hpf). The image on the left shows a homozygote mutant (m/m) embryo with a normal, straight body. The image on the right shows a typical example of abnormal body curvature, described as “curly up”, in a homozygote mutant (m/m) embryo. (B) Graphs showing the frequency of ciliopathy-associated phenotypes in *nphp2<sup>sa36157</sup>* zebrafish embryos of the F2 generation. The numbers in each column represent the number of observed embryos presenting the respective phenotype and the number underneath each column indicates the total number of embryos scored for each genotype. From left to right: Abnormal heart looping, as an indicator for faulty left-right body axis determination, is categorized into “middle” and “inverse”, comparing to the normal course of the heart loop. Heart edema, hydrocephalus, and abnormal body curvature, marked as “curly up” or “or curly down”, are additional phenotypes screened for. (Fisher’s exact test, two-tailed)



### 3.1.2 Point mutations in *nphp4*

The *nphp4*<sup>sa41188</sup> (G>T) (Tab. 19) mutation is a nonsense mutation resulting in an early stop of the translation after amino acid (aa) 444 out of 1417, truncating the protein prematurely (Fig. 9A). Heterozygote (m/+) fish were crossed to generate zygotic mutants in F1. The zebrafish embryos were analyzed 48 hours post fertilization and scored for glomerular cyst formation (Fig. 9B) and cloaca malformation. Data for cloaca malformation in the F1 generation were collected by Friedemann Zaiser and are shown here for reasons of comparison (Fig. 9D). In F1, homozygote mutant (m/m) zebrafish displayed 8.3-times more glomerular cysts than their wildtype (+/+) siblings (Kayser et al., 2022). The number of cloaca malformation in (m/m) fish was statistically no different to the (+/+) controls. Heterozygote (m/+) zebrafish showed an intermediate prevalence of glomerular cysts and even more cloaca cysts as (m/m) mutants. This could be a possible sign of haplotype insufficiency (Fig. 9C-D). The frequency of glomerular cysts in maternal zygotic (m/m) zebrafish in F2, which are exempt from any maternal contribution, dropped to 4.9-fold compared to their (+/+) siblings and was no longer statistically significant. The frequency of cloaca cyst malformation increased slightly (from 1.2-fold in F1 to 1.8-fold in F2) but did not reach significance either (Fig. 9E) (Kayser et al., 2022). The intergenerational comparison of the incidence of ciliopathy phenotypes in (m/m) mutant fish in F1 and F2 generation, normalized to the incidence in the corresponding (+/+) siblings, showed a decrease to 59% for glomerular cysts and an increase of 155% for cloaca malformation (Fig. 9F) (Kayser et al., 2022).

Regarding the four additional ciliopathy-associated phenotypes, the *nphp4*<sup>sa41188</sup> maternal zygotic mutants (m/m) of the F2 generation presented more “middle”- (14.8%) and more “inverse”-type (1.6%) heart loop configuration than their wildtype (+/+) siblings (6.8% and 0.2% respectively). The body curvature of the (m/m) mutant embryos was found at a statistically significant higher rate, being “curly down” (3.1%), compared to the (+/+) controls (0.5%). Hydrocephalus occurred more than 10-times more frequently in (m/m) embryos, whilst heart edema was not significantly more frequent in mutants than in their wildtype siblings (Fig. 10).

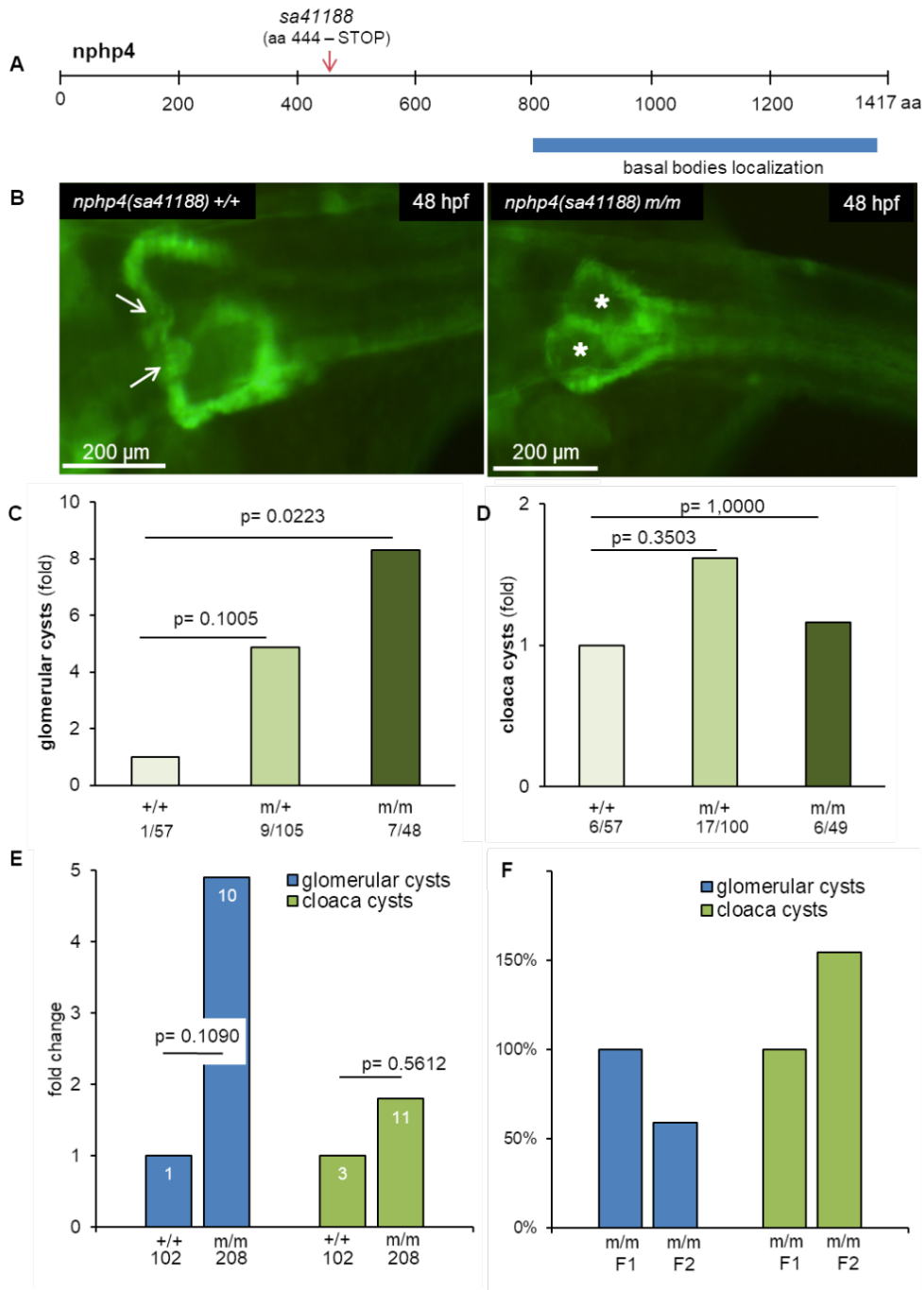


**Figure 9: Glomerular and cloaca cyst formation of F1 and F2 *nphp4<sup>sa41188</sup>* mutant fish** - adapted from (Kayser et al., 2022)

(A) Graphic illustration of the *nphp4* zebrafish gene. *nphp4<sup>sa41188</sup>* carries a nonsense point mutation (G>T), resulting in a premature stop in the translation after the amino acid (aa) 444 out of 1417. (B) Images of the glomerular region obtained by fluorescent microscopy at 48 hours post fertilization (hpf). The image on the left shows normal glomeruli (arrows) in a wildtype (+/+) control embryo. The image on the right shows bilaterally paired glomerular cysts (stars) in a homozygote mutant (m/m) embryo. (C) and (D) Graphs showing the frequency of glomerular cyst formation and cloaca malformation (data from Friedemann Zaiser) respectively, in heterozygote (m/+) and homozygote (m/m) embryos in F1 in relation to their wildtype (+/+) siblings. The numbers underneath each column represent the number of observed embryos presenting the respective phenotype and the total number of embryos scored for each genotype. (E) Graph showing the frequency of glomerular cyst formation and cloaca malformation, in homozygote (m/m) maternal zygotic embryos in F2 in relation to their wildtype (+/+) siblings. The numbers in each column represent the number of observed embryos presenting the respective phenotype and the number underneath each column indicates the total number of embryos scored for each genotype. (F) Graph illustrating the comparison between the incidence of abnormalities in homozygote mutant (m/m) embryos in the F1 and F2 generation. For comparison, the frequency of ciliopathy phenotypes in (m/m) mutants in F1 was set to 100% and changes in maternal zygotic mutants in F2 were expressed in relation to F1. (Fisher's exact test, two-tailed)

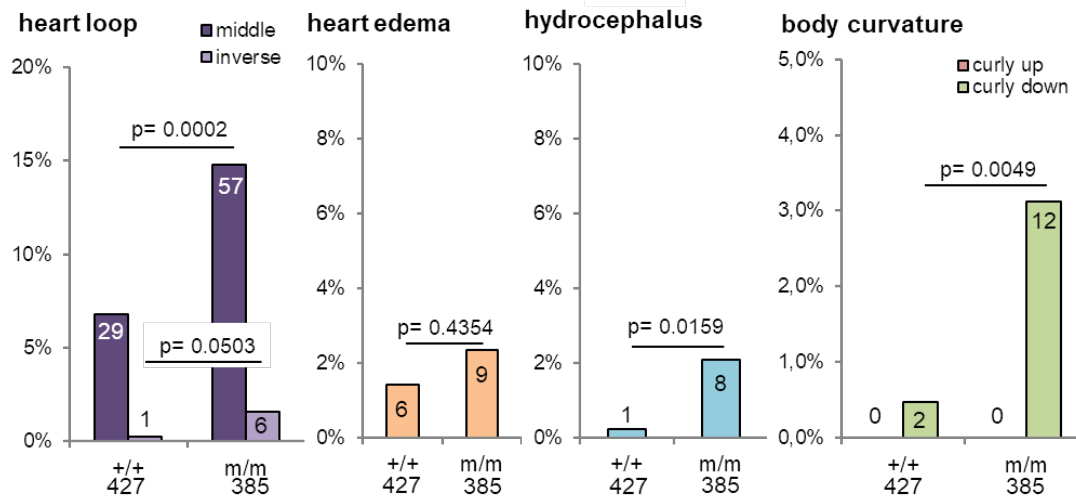


**Figure 10: Ciliopathy associated phenotypes in F2 *nphp4*<sup>sa41188</sup> mutant fish**  
 Graphs showing the frequency of ciliopathy-associated phenotypes in *nphp4*<sup>sa41188</sup> zebrafish embryos of the F2 generation. The numbers in each column represent the number of observed embryos presenting the respective phenotype and the number underneath each column indicates the total number of embryos scored for each genotype. From left to right: Abnormal heart looping, as an indicator for faulty left-right body axis determination, is categorized into “middle” and “inverse”, comparing to the normal course of the heart loop. Heart edema, hydrocephalus and abnormal body curvature, marked as “curly up” or “or curly down”, are additional phenotypes screened for. (Fisher’s exact test, two-tailed) - graphs from (Kayser et al., 2022)

The *nphp4*<sup>sa38686</sup> (G>A) (Tab. 19) mutation affects an essential splice site (ESS) at amino acid 764 (Fig. 11A). Heterozygote (m/+) fish were crossed to generate zygotic mutants in F1. The zebrafish embryos were analyzed 48 hours post fertilization and scored for glomerular cyst formation and cloaca malformation (Fig. 11B). Data for cloaca malformation in the F1 generation were collected by Friedemann Zaiser and are shown here for reasons of comparison (Fig. 11D). In F1, no statistically significant difference in the frequency of neither glomerular cysts nor cloaca malformation could be observed by comparing wild-type (+/+) zebrafish to their siblings with either one (m/+) or two (m/m) mutated alleles. (Fig. 11C-D) (Kayser et al., 2022). One generation later however, maternal zygotic (m/m) zebrafish developed 5-times more glomerular cysts and more than twice as much cloaca cysts, than their (+/+) siblings. In F2 the difference between the mutants and the wildtype zebrafish became statistically significant (Fig. 11E). When comparing F1 to F2, the staggering increase in frequency of ciliopathy phenotypes in (m/m) mutant fish in F2, becomes even more evident. The incidence of cloaca malformation in F2 increased to over 330%, compared to the (m/m) mutants in F1, the incidence being normalized to the incidence in the corresponding (+/+) controls. Regarding the glomerular cyst count, the increase by 582% between the two generations was even bigger (Fig. 11F).

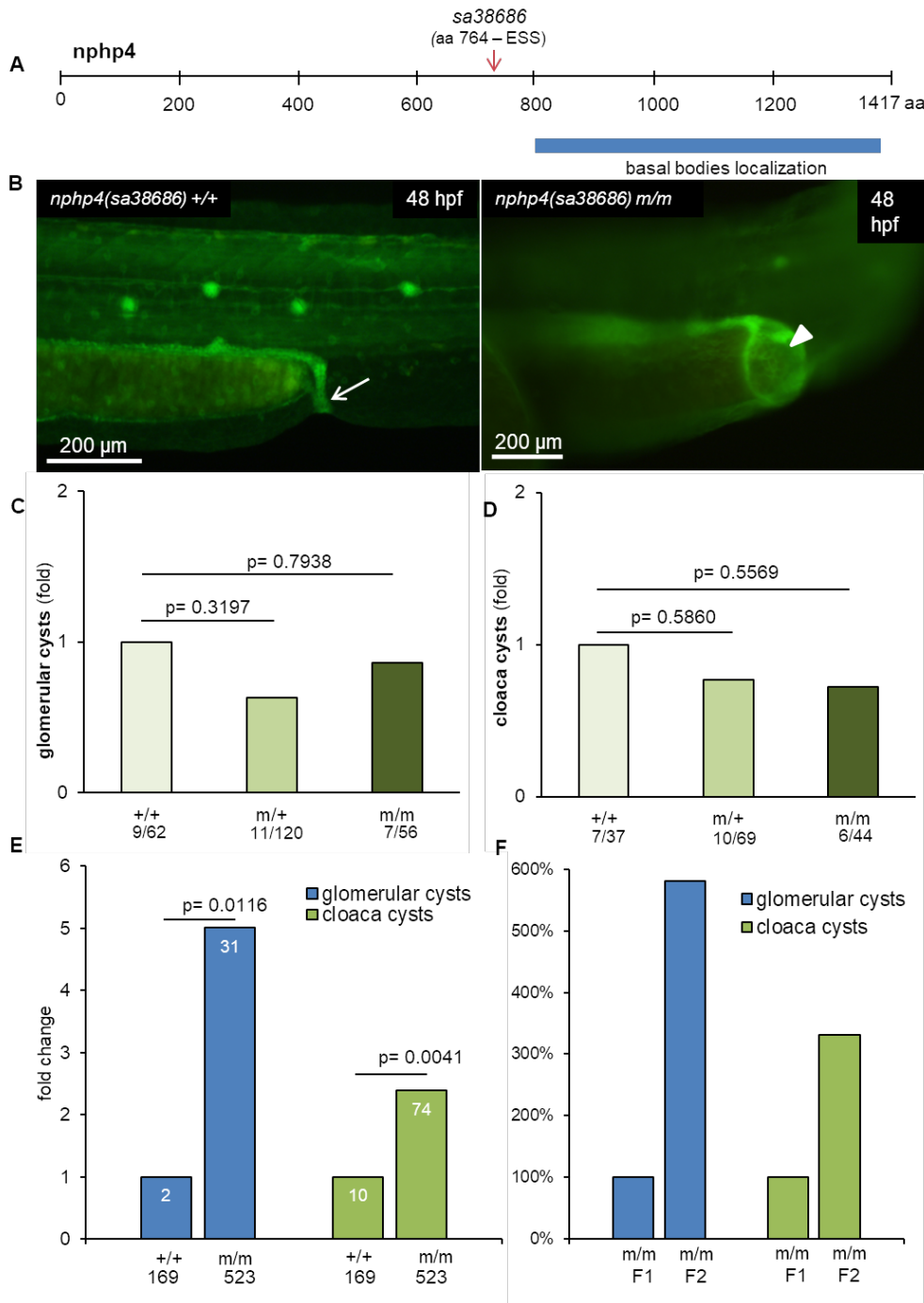


**Figure 11: Glomerular and cloaca cyst formation of F1 and F2 *nphp4*<sup>sa38686</sup> mutant fish** - adapted from (Kayser et al., 2022) (A) Graphic illustration of the *nphp4* zebrafish gene. *nphp4*<sup>sa38686</sup> (G>A) eliminates an essential splice site (ESS) at amino acid (aa) 764, causing different splicing of the pre-mRNA. (B) Images of the cloaca region obtained by fluorescent microscopy at 48 hours post fertilization (hpf). The image on the left shows a normal cloaca (arrow) in a wildtype (+/+) control embryo. The image on the right shows a typical example of cloaca malformation, characterized by the formation of a cyst instead of the normal body opening (arrowhead) in a homozygote mutant (m/m) embryo. (C) and (D) Graphs showing the frequency of glomerular cyst formation and cloaca malformation (data from Friedemann Zaiser) respectively, in heterozygote (m/+) and homozygote (m/m) embryos in F1 in relation to their wildtype (+/+) siblings. The numbers underneath each column represent the number of observed embryos presenting the respective phenotype and the total number of embryos scored for each genotype. (E) Graph showing the frequency of glomerular cyst formation and cloaca malformation, in homozygote (m/m) maternal zygotic embryos in F2 in relation to their wildtype (+/+) siblings. The numbers in each column represent the number of observed embryos presenting the respective phenotype and the number underneath each column indicates the total number of embryos scored for each genotype. (F) Graph illustrating the comparison between the incidence of abnormalities in homozygote mutant (m/m) embryos in the F1 and F2 generation. For comparison, the frequency of ciliopathy phenotypes in (m/m) mutants in F1 was set to 100% and changes in maternal zygotic mutants in F2 were expressed in relation to F1. (Fisher's exact test, two-tailed)

The occurrence of hydrocephalus formation (Fig.12A) was significantly more frequent in maternal zygotic *nphp4*<sup>sa38686</sup> mutants (m/m) of the F2 generation (6.0%), when compared to their wildtype (+/+) siblings (0.8%). Abnormal heart looping, being a correlate of faulty left-right body axis determination, was significantly more frequent in (m/m) mutants than in the wildtype (+/+) controls for both, “middle”- as well as “reverse”-type. Heart looping labelled as “middle”-type was more than 8-times more frequent in mutants compared to the (+/+) controls. Considering heart edema formation or abnormal body curvature, mutants did not differ from their (+/+) siblings (Fig. 12B).

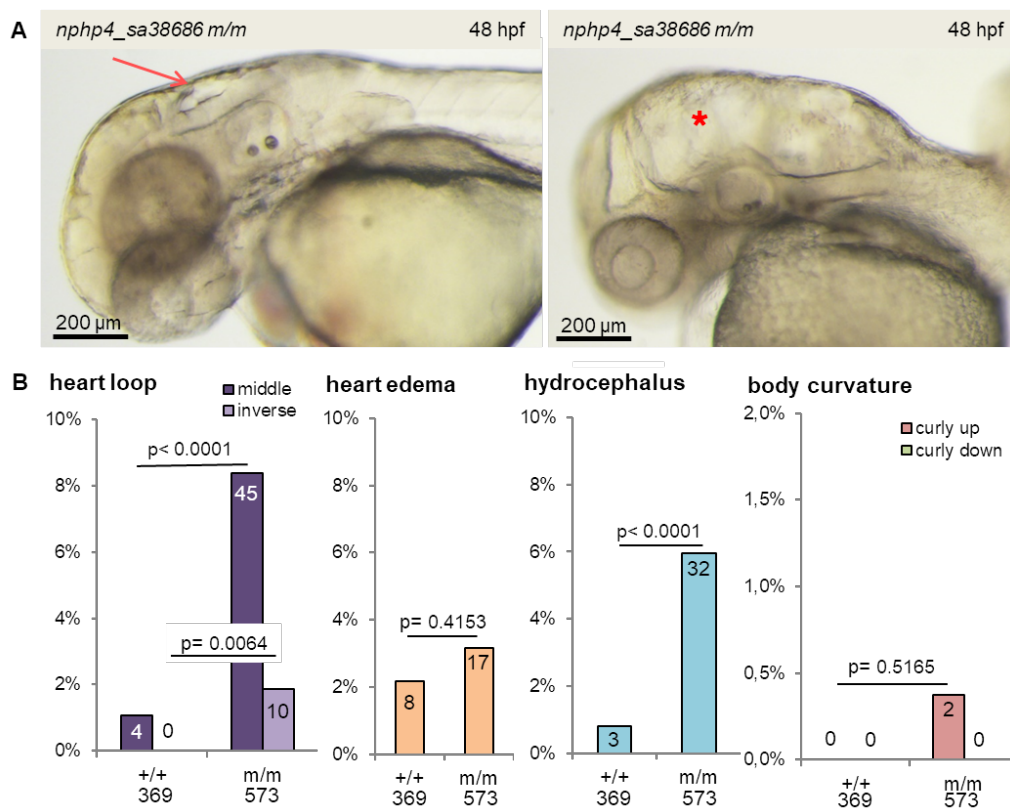


**Figure 12: Ciliopathy associated phenotypes in F2 *nphp4*<sup>sa38686</sup> mutant fish**

(A) Images of *nphp4*<sup>sa38686</sup> zebrafish embryos acquired with an optical stereo microscope at 48 hours post fertilization (hpf). The image on the left shows a homozygote mutant (m/m) embryo with a normal brain ventricular system. The image on the right shows a typical example of hydrocephalus formation, with a massively distended ventricle in a homozygote mutant (m/m) embryo. (B) Graphs showing the frequency of ciliopathy-associated phenotypes in *nphp4*<sup>sa38686</sup> zebrafish embryos of the F2 generation. The numbers in each column represent the number of observed embryos presenting the respective phenotype and the number underneath each column indicates the total number of embryos scored for each genotype. From left to right: Abnormal heart looping, as an indicator for faulty left-right body axis determination, is categorized into “middle” and “inverse”, comparing to the normal course of the heart loop. Heart edema, hydrocephalus and abnormal body curvature, marked as “curly up” or “curly down”, are additional phenotypes screened for. (Fisher’s exact test, two-tailed) – graphs from (Kayser et al., 2022)

### 3.1.3 Point mutations in *rpgrip11/nphp8*

The splicing process of the pre-mRNA is affected by the *nphp8*<sup>8sa24730</sup> (A>T) mutation (Tab. 19). This mutation eliminates an essential splice site (ESS) at amino acid 337 (Fig. 13A). Heterozygote (m/+) fish were crossed to generate zygotic mutants in F1. The zebrafish embryos were analyzed 48 hours post fertilization and scored for glomerular cyst formation (Fig. 13B) and cloaca malformation. Data for cloaca malformation in the F1 generation were collected by Friedemann Zaiser and are shown here for reasons of comparison (Fig. 13D). Homozygote (m/m) as well as heterozygote (m/+) mutant embryos in F1, showed significantly more glomerular cysts comparing to their wildtype (+/+) siblings (Fig. 13C) (Kayser et al., 2022). On the other hand, the presence of at least two mutated alleles was necessary to cause significantly more cloaca malformation in (m/m) fish (2.3-fold) compared to the wildtype (+/+) embryos (Fig. 13D). In F2, maternal zygotic (m/m) zebrafish presented more than 3-times more cloaca cysts than the wildtype controls but were no longer statistically different regarding the glomerular cyst formation (Fig. 13E) (Kayser et al., 2022). The direct intergenerational comparison between F1 and F2, confirms the increase in cloaca malformation to almost 150% and the slight decrease in glomerular cyst formation to 80%. Maternal zygotic (m/m) mutants in the F2 generation of the *nphp8*<sup>8sa24730</sup> zebrafish line, were affected more severely regarding all four of the ciliopathy-associated phenotypes observed, namely abnormal heart looping, formation of heart edema and hydrocephalus and pathologic body curvature, than the wildtype (+/+) controls. The differences reach statistical significance for all of them, except heart edema (Fig. 14).

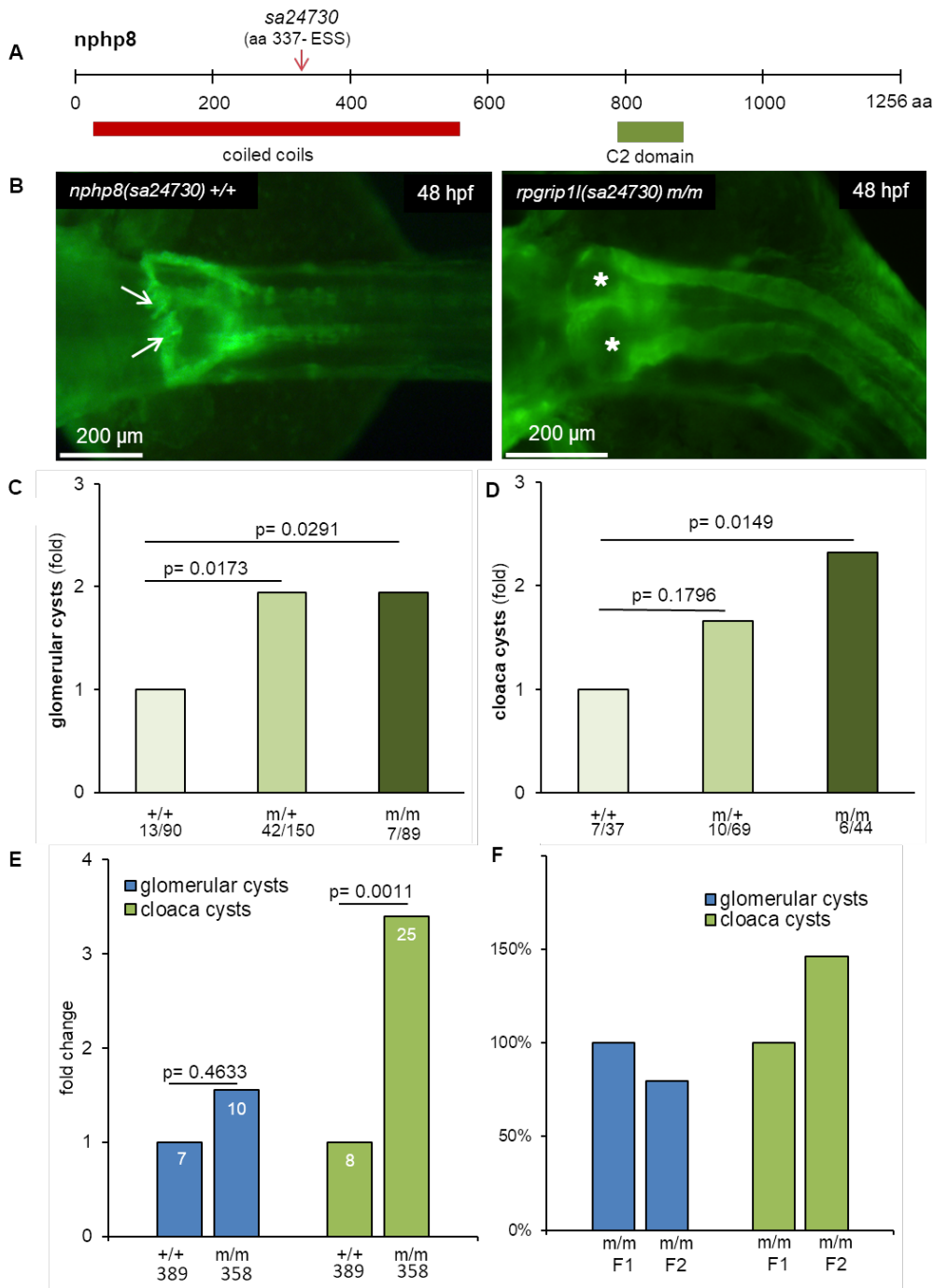


**Figure 13: Glomerular and cloaca cyst formation of F1 and F2 *nphp8*<sup>sa24730</sup> mutant fish** - adapted from (Kayser et al., 2022) (A) Graphic illustration of the *nphp8/rpgr11* zebrafish gene. The *nphp8*<sup>sa24730</sup> line carries a point mutation (A>T) eliminating an essential splice site (ESS) at amino acid (aa) 337 out of 12569. (B) Images of the glomerular region obtained by fluorescent microscopy at 48 hours post fertilization (hpf). The image on the left shows normal pronephric duct and glomerular development (arrows) in a wildtype (+/+) control embryo. The image on the right shows a typical example of glomerular cyst formation. Bilaterally paired distended glomeruli can be observed (stars) in this homozygote mutant (m/m) embryo. (C) and (D) Graphs showing the frequency of glomerular cyst formation and cloaca malformation (data from Friedemann Zaiser) respectively, in heterozygote (m/+) and homozygote (m/m) embryos in F1 in relation to their wildtype (+/+) siblings. The numbers underneath each column represent the number of observed embryos presenting the respective phenotype and the total number of embryos scored for each genotype. (E) Graph showing the frequency of glomerular cyst formation and cloaca malformation, in homozygote (m/m) maternal zygotic embryos in F2 in relation to their wildtype (+/+) siblings. The numbers in each column represent the number of observed embryos presenting the respective phenotype and the number underneath each column indicates the total number of embryos scored for each genotype. (F) Graph illustrating the comparison between the incidence of abnormalities in homozygote mutant (m/m) embryos in the F1 and F2 generation. For comparison, the frequency of ciliopathy phenotypes in (m/m) mutants in F1 was set to 100% and changes in maternal zygotic mutants in F2 were expressed in relation to F1. (Fisher's exact test, two-tailed)

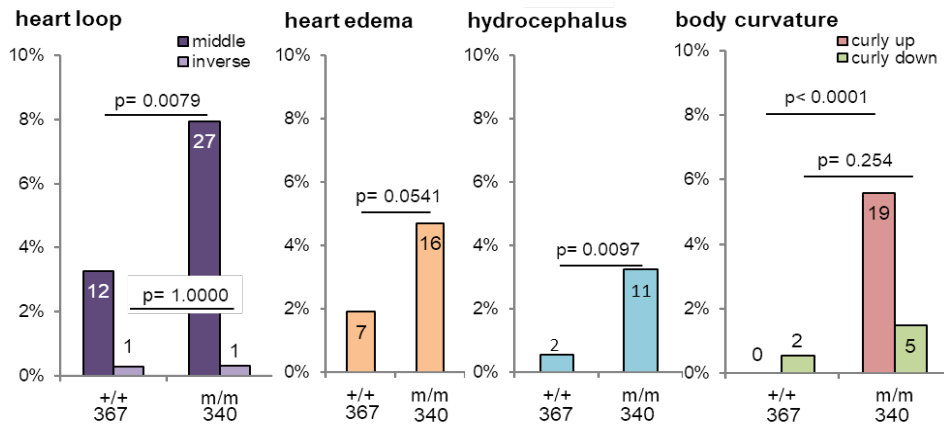


**Figure 14: Ciliopathy associated phenotypes in F2 *nphp8*<sup>8sa10096</sup> mutant fish**  
 Graphs showing the frequency of ciliopathy-associated phenotypes in *nphp8*<sup>8sa24730</sup> zebrafish embryos of the F2 generation. The numbers in each column represent the number of observed embryos presenting the respective phenotype and the number underneath each column indicates the total number of embryos scored for each genotype. From left to right: Abnormal heart looping, as an indicator for faulty left-right body axis determination, is categorized into “middle” and “inverse”, comparing to the normal course of the heart loop. Heart edema, hydrocephalus and abnormal body curvature, marked as “curly up” or “or curly down”, are additional phenotypes screened for. (Fisher’s exact test, two-tailed) - graphs from (Kayser et al., 2022)

The *nphp8*<sup>8sa10096</sup> line contains a nonsense mutation (T>A) (Tab. 19), responsible for the insertion of an early stop codon after amino acid 862, truncating the translated protein at the end of the C2 domain (Fig. 15A). Heterozygote (m/+) fish were crossed to generate zygotic mutants in F1. The zebrafish embryos were analyzed 48 hours post fertilization and scored for glomerular cysts and cloaca cysts, the letter being the result of defective cloaca formation (Fig. 15B). Data for cloaca malformation in the F1 generation were collected by Friedemann Zaiser and are shown here for reasons of comparison (Fig. 15D). Homozygote mutant (m/m) zebrafish in F1 showed a significant increase in both, glomerular and cloaca cyst formation (Kayser et al., 2022). Heterozygote (m/+) zebrafish showed an intermediate increase of both ciliopathy phenotypes, however not reaching statistical significance for either of them (Fig. 15C-D) (Kayser et al., 2022). Maternal zygotic mutant (m/m) zebrafish embryos in F2, showed remarkably more ciliopathy phenotypes compared to their wildtype (+/+) siblings (Kayser et al., 2022). In (m/m) embryos, the frequency of glomerular cysts increased by approximately 5-fold while the frequency of cloaca malformation rose to almost 12-fold (Fig. 15E). The comparison between (m/m) mutant fish of the F1 and F2 generation, underpins the observed increase in cloaca malformation, by showing a rise to 454% from one generation to the next one. The frequency of glomerular cyst formation in (m/m) mutants in F2 was comparable to their (m/m) parents in F1 (Fig. 15F).

The analysis of the ciliopathy-associated phenotypes, being abnormal heart looping (Fig. 16A), formation of heart edema (Fig. 16B), development of hydrocephalus and pathologic body curvature, revealed that the maternal zygotic *nphp8*<sup>8sa10096</sup> (m/m) embryos of the F2 generation, were no different from their wildtype (+/+) siblings, except for the body curvature phenotype. Mutants displayed an abnormal body curvature, labelled as “curly down”, at a statistically



significant higher level than the (+/+) controls. However, the frequency of 1.5% “curly down” in mutants, is not very high altogether (Fig. 16C).

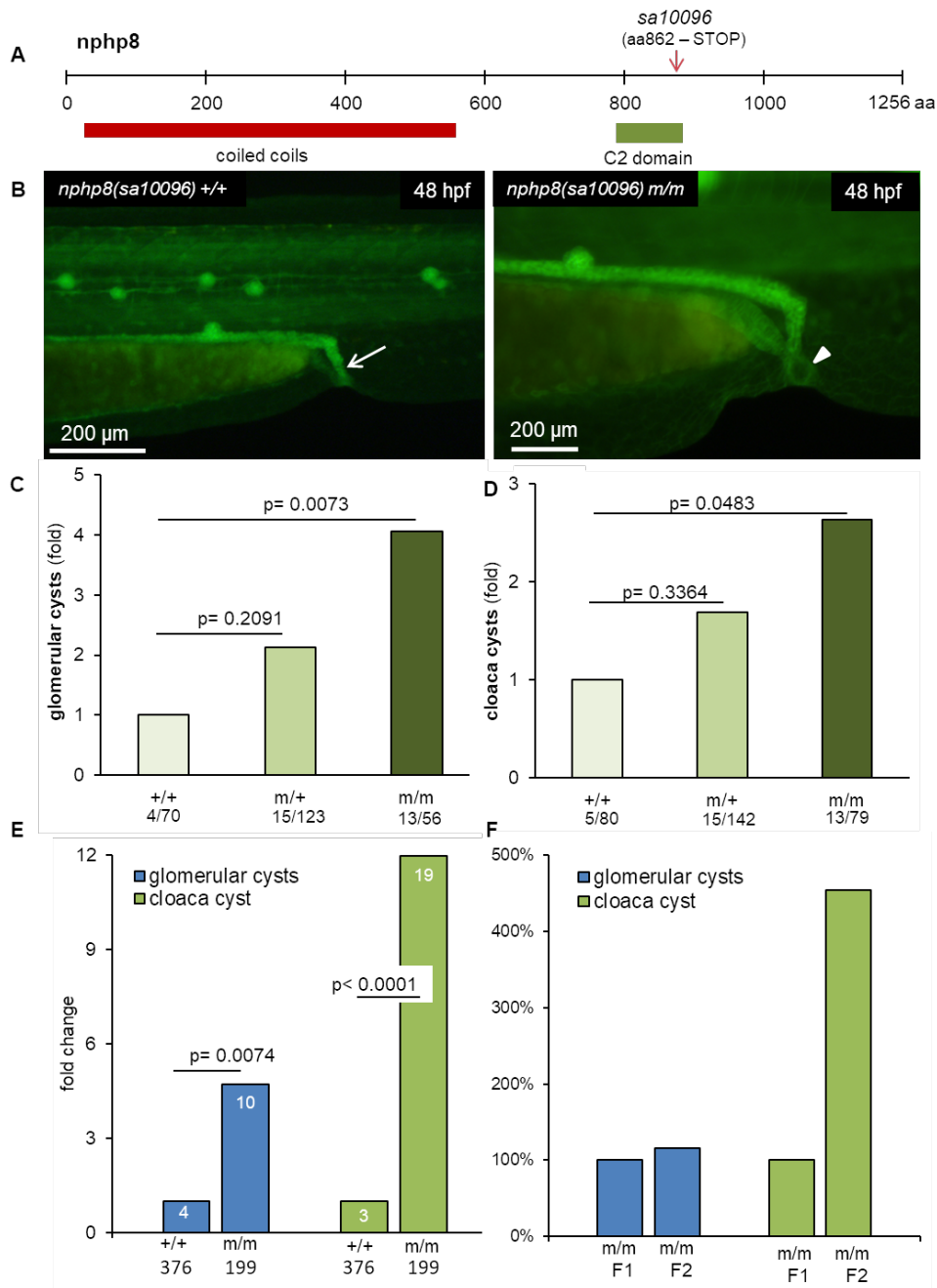


**Figure 15: Glomerular and cloaca cyst formation of F1 and F2 *nphp8*<sup>sa10096</sup> mutant fish** - adapted from (Kayser et al., 2022) (A) Graphic illustration of the *nphp8/rpgrip11* zebrafish gene. The *nphp8*<sup>sa10096</sup> mutation (T>A) is a nonsense mutation causing the insertion of a premature stop codon after amino acid (aa) 862 out of 1256 and consequently truncating the protein at the end of the C2 domain. (B) Images of the cloaca region obtained by fluorescent microscopy at 48 hours post fertilization (hpf). The image on the left shows a normal cloaca (arrow) in a wildtype (+/+) control embryo. The image on the right shows a typical example of cloaca malformation, characterized by the formation of a cyst instead of the normal body opening (arrowhead) in a homozygote mutant (m/m) embryo. (C) and (D) Graphs showing the frequency of glomerular cyst formation and cloaca malformation (data from Friedemann Zaiser) respectively, in heterozygote (m/+) and homozygote (m/m) embryos in F1 in relation to their wildtype (+/+) siblings. The numbers underneath each column represent the number of observed embryos presenting the respective phenotype and the total number of embryos scored for each genotype. (E) Graph showing the frequency of glomerular cyst formation and cloaca malformation, in homozygote (m/m) maternal zygotic embryos in F2 in relation to their wildtype (+/+) siblings. The numbers in each column represent the number of observed embryos presenting the respective phenotype and the number underneath each column indicates the total number of embryos scored for each genotype. (F) Graph illustrating the comparison between the incidence of abnormalities in homozygote mutant (m/m) embryos in the F1 and F2 generation. For comparison, the frequency of ciliopathy phenotypes in (m/m) mutants in F1 was set to 100% and changes in maternal zygotic mutants in F2 were expressed in relation to F1. (Fisher’s exact test, two-tailed)

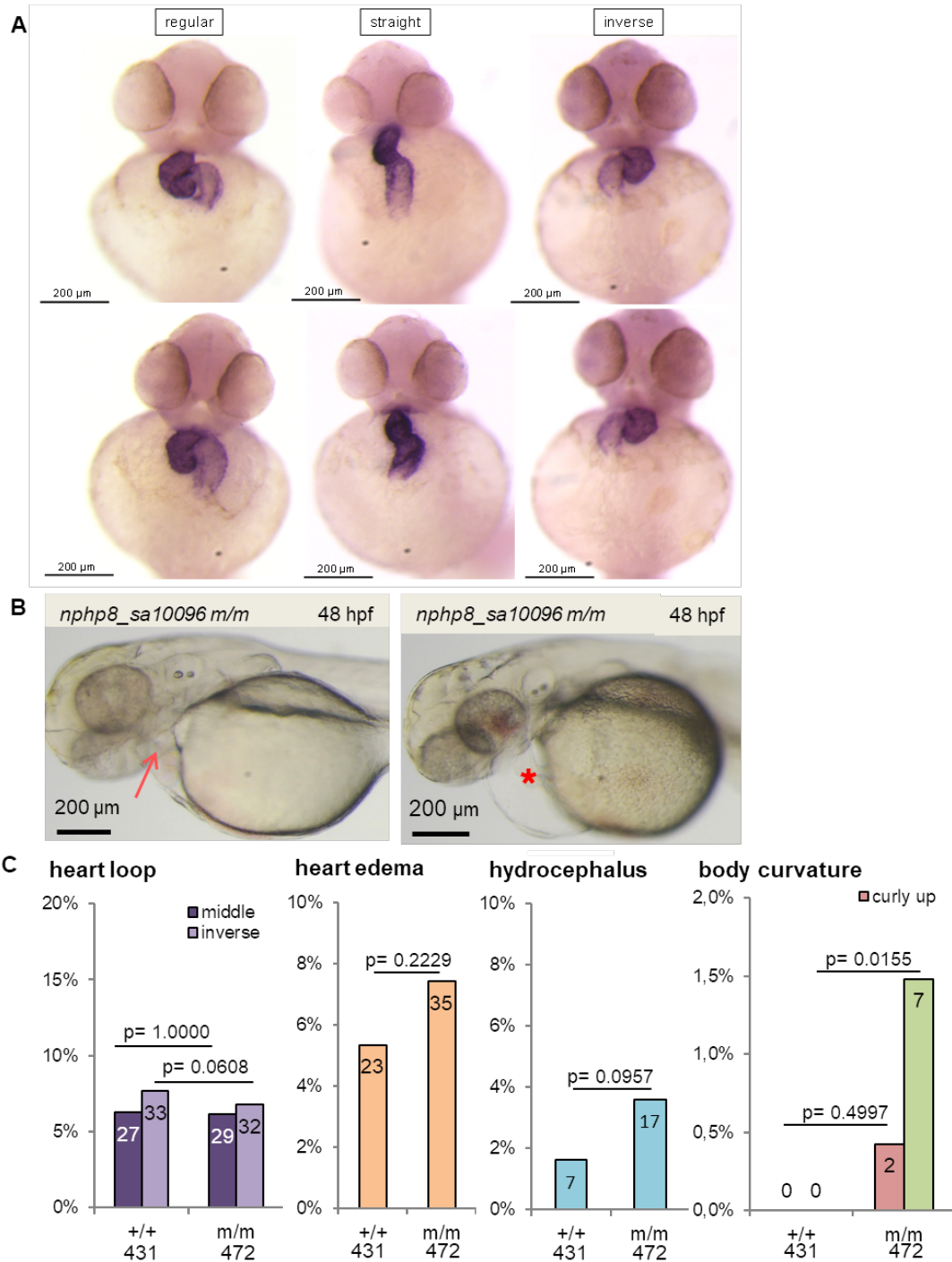


**Figure 16: Ciliopathy associated phenotypes in F2 *npbp8<sup>sa10096</sup>* mutant fish**

(A) Images of *npbp8<sup>sa10096</sup>* zebrafish embryos acquired with an optical stereo microscope at 48 hours post fertilization (hpf). The heart loop has been visualized by whole-mount in situ immuno-staining. The images on the left show regular heart loops, going from top left to bottom right. The images in the middle show typical examples heart loops, labelled as “middle”, going from top to bottom in a relatively straight line with no big looping. The images on the right show examples of “inverse” direction of the heart loop, going from bottom left to top right this time. “Inverse”-type heart loop is a correlate to situs inversus in the zebrafish embryo. (B) Images of *npbp8<sup>sa10096</sup>* zebrafish embryos acquired with an optical stereo microscope at 48 hours post fertilization (hpf). The image on the left shows a physiological cardiac compartment in a homozygote mutant (m/m) embryo. The image on the right shows a fluid-filled pericardium, characterizing the phenotype of heart edema, in this (m/m) mutant zebrafish. (C) Graphs showing the frequency of ciliopathy-associated phenotypes in *npbp8<sup>sa10096</sup>* zebrafish embryos of the F2 generation. The numbers in each column represent the number of observed embryos presenting the respective phenotype and the number underneath each column indicates the total number of embryos scored for each genotype. From left to right: Abnormal heart looping, as an indicator for faulty left-right body axis determination, is categorized into “middle” and “inverse”, comparing to the normal course of the heart loop. Heart edema, hydrocephalus and abnormal body curvature, marked as “curly up” or “or curly down”, are additional phenotypes screened for. (Fisher’s exact test, two-tailed) - graphs from (Kayser et al., 2022)

### 3.2 *nphp4* morpholino-oligonucleotide (MO)-induced knockdown

Some point mutations still allow mRNA to be transcribed. This mutated, defective mRNA can be disintegrated, and this decay might trigger compensatory mechanisms by causing transcriptional adaptation. In order to see if the observed changes in glomerular cyst formation and cloaca malformation from one generation to the next one, could be explained by mutation-induced genetic compensation I conducted MO knockout experiments on maternal zygotic embryos of the F2 generation of both *nphp4* zebrafish lines with point mutations. I used one translation-blocking (TBM) and one splice-blocking MO (SBM), targeting the ATG translation initiation codon and the splice donor site of exon 1 in the *nphp4* mRNA respectively. The efficiency and specific targeting of these MOs have been proved in earlier works (Slanchev et al., 2011).

#### 3.2.1 *nphp4*<sup>sa41188</sup> MO knockdown

Splice-blocking (SBM) and translation-blocking (TBM) MOs, targeting the *nphp4* gene, have been injected into one-cell staged embryos of the zebrafish *nphp4*<sup>sa41188</sup> F2 generation. The injection of SBM (0.1mM) and TBM (0.2mM) in wildtype (+/+) embryos caused glomerular cyst formation at significantly higher rates (39.4-fold and 67.8-fold respectively), compared to untreated wildtype embryos. Homozygote mutant (m/m) embryos also remained partly sensitive to both MOs and developed significantly more glomerular cysts when injected with SBM or TBM than their untreated siblings. However, this increase caused by the MO-knock down was less important in the (m/m) embryos (10.5-fold for SBM 0.1mM and 9.8-fold for TBM 0.2mM) by contrast to frequency observed in MO-treated (+/+) fish (Fig. 17A). The injection of TBM (0.2mM) in wildtype (+/+) embryos could cause cloaca cyst formation at a higher rate (5.1-fold), whilst SBM (0.1mM) injection had no significant effect. When injected into (m/m) mutant embryos both MOs, SBM as well as TBM, induced significantly more cloaca malformation (2.6-fold and 2.9-fold respectively) than in their untreated siblings. Again, this increase in phenotypes in treated versus untreated embryos, is less important in maternal zygotic mutants than in wildtype controls (Fig. 17B).

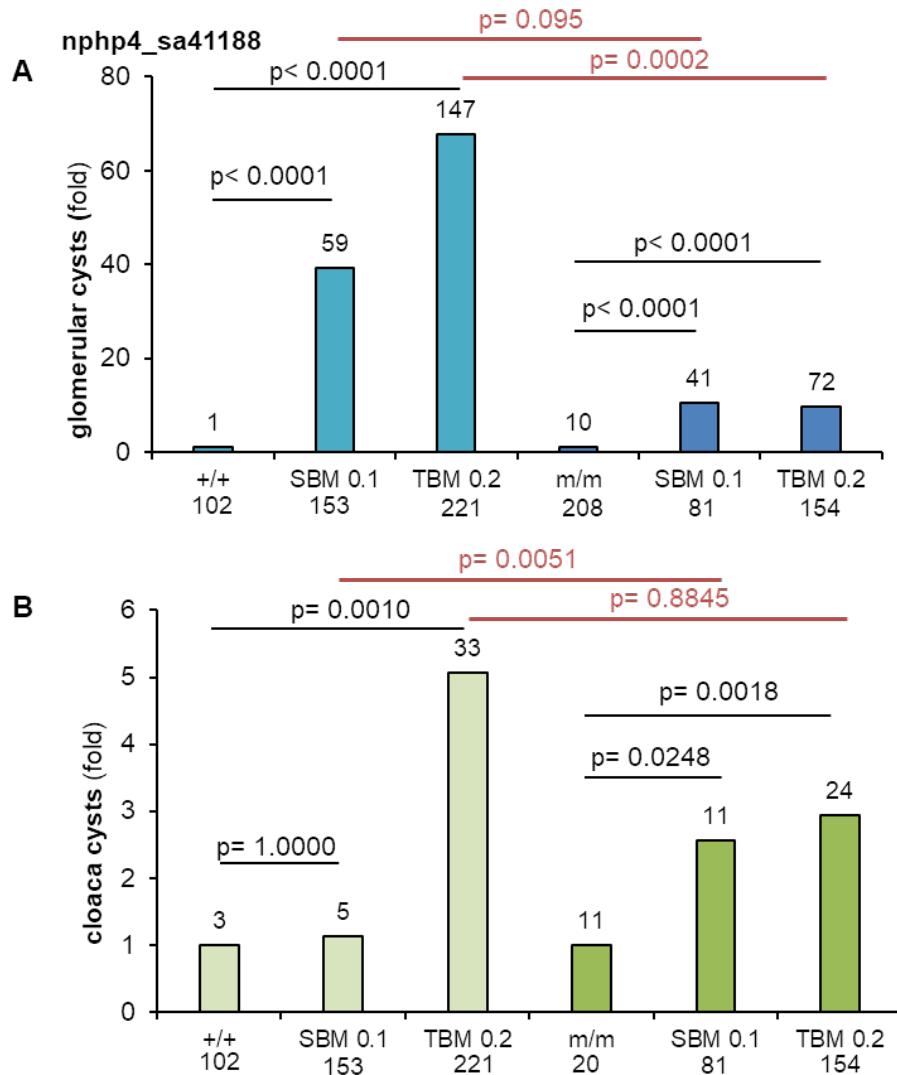


**Figure 17: MO induced knockdown of *nphp4<sup>sa41188</sup>* in maternal zygotic mutants** (adapted from Kayser et al., 2022).

(A) Graph showing the increase of glomerular cyst formation in *nphp4<sup>sa41188</sup>* zebrafish embryos of the F2 generation, when injected with splice-blocking (SBM) (0.1mM) or translation-blocking (TBM) (0.2mM) MO, normalized to the frequency to their untreated wildtype (+/+) or homozygote mutant (m/m) siblings. SBM and TBM have been injected into one-cell staged (+/+) (light blue columns) and (m/m) (dark blue columns) embryos. The numbers above each column represent the number of observed embryos presenting glomerular cysts and the number underneath each column indicates the total number of embryos scored for each subgroup. (B) Graph showing the increase of cloaca cyst formation in *nphp4<sup>sa41188</sup>* zebrafish embryos of the F2 generation, when injected with splice-blocking (SBM) (0.1mM) or translation-blocking (TBM) (0.2mM) MO, normalized to the frequency to their untreated (+/+) or (m/m) siblings. SBM and TBM have been injected into one-cell staged (+/+) (light green columns) and (m/m) (dark green columns) embryos. The numbers above each column represent the number of observed embryos presenting cloaca cysts and the number underneath each column indicates the total number of embryos scored for each subgroup. (Fisher's exact test, two-tailed)

### 3.2.2 *nphp4*<sup>sa38686</sup> MO knockdown

To analyze the impact the MO-induced knockdown has in the F2 generation of the *nphp4*<sup>sa38686</sup> zebrafish line, I injected splice-blocking (SBM) and translation-blocking (TBM) MOs, in two different concentrations each, into one-cell staged embryos. The injection of SBM (0.1mM) and SBM (0.2mM) as well as the injection of TBM (0.2mM) and TBM (0.3mM) in wildtype (+/+) embryos caused significantly more glomerular cyst formation (from 39.3-fold up to 58.8-fold) compared to untreated wildtype embryos. The increase in glomerular cyst formation in MO-injected (m/m) mutants (about 7-fold), although still being statistically significant for both MOs at the two different concentrations each, is significantly lower in comparison to the effect the MO-induced knockdown has in wildtype embryos (Fig. 18A) (Kayser et al., 2022).

Regarding cloaca cyst formation, only the (+/+) embryos injected with SBM (0.1mM) and TBM (0.2mM) differed statistically speaking from the untreated embryos. In mutant (m/m) embryos, the injection of TBM caused significantly more cloaca cysts compared to their untreated siblings. The increase between treated and untreated embryos, being 2.3-fold for mutants injected with TBM (0.3mM) is less than half as big as the increase, which TBM in this same concentration has on wildtype embryos (5.0-fold). Interestingly the splice-blocking (SBM) MO causes less cloaca malformation in embryos injected with SBM (0.1mM) and SBM (0.2mM) (0.3-fold and 0.9-fold respectively), than in the untreated mutants (Fig. 18B).

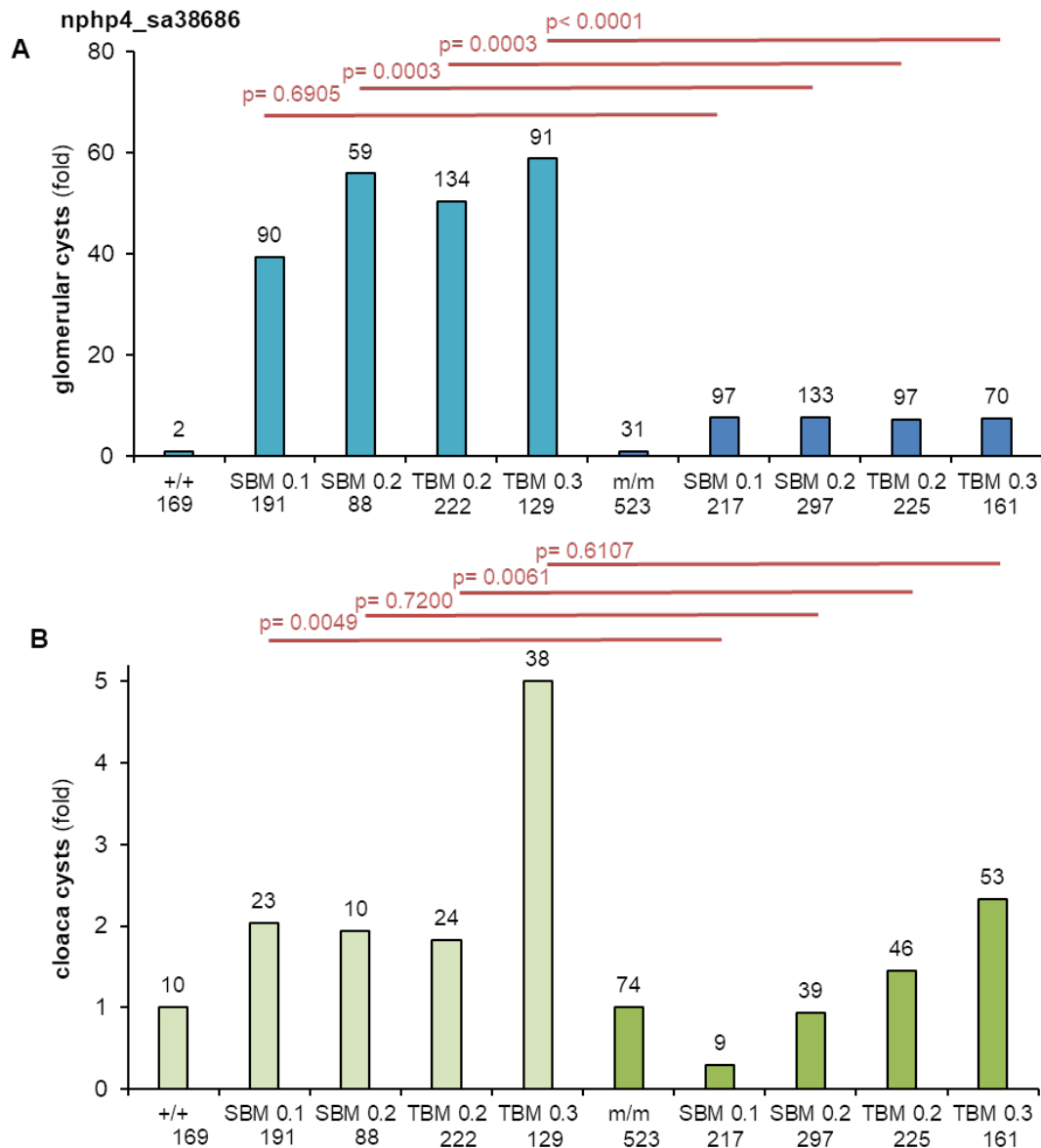


**Figure 18: MO-induced knockdown of *nphp4<sup>sa38686</sup>* in maternal zygotic mutants** (adapted from Kayser et al., 2022).

(A) Graph showing the increase of glomerular cyst formation in *nphp4<sup>sa38686</sup>* zebrafish embryos of the F2 generation, when injected with splice-blocking (SBM) or translation-blocking (TBM) MO, normalized to the frequency to their untreated wildtype (+/+) or homozygote mutant (m/m) siblings. SBM and TBM have been injected in two different concentrations each (0.1mM & 0.2mM and 0.2mM & 0.3mM respectively) into one-cell staged (+/+) (light blue columns) and (m/m) (dark blue columns) embryos. The numbers above each column represent the number of observed embryos presenting glomerular cysts and the number underneath each column indicates the total number of embryos scored for each subgroup. (B) Graph showing the increase of cloaca cyst formation in *nphp4<sup>sa38686</sup>* zebrafish embryos of the F2 generation, when injected with splice-blocking (SBM) or translation-blocking (TBM) MO, normalized to the frequency to their untreated (+/+) or (m/m) siblings. SBM and TBM have been injected in two different concentrations each (0.1mM & 0.2mM and 0.2mM & 0.3mM respectively) into one-cell staged (+/+) (light green columns) and (m/m) (dark green columns) embryos. The numbers above each column represent the number of observed embryos presenting cloaca malformation and the number underneath each column indicates the total number of embryos scored for each subgroup. (Fisher's exact test, two-tailed)

### 3.3 Ciliopathy phenotypes in zebrafish mutant lines with large deletions

In addition to the zebrafish lines, carrying point mutations, which are characterized by changes of individual nucleotides and cause either the insertion of a premature stop codon or the deletion of an essential splice site, I wanted to analyze lines with extensive deletions generated by the CRISPR/Cas9 gene modification method. In these zebrafish lines, most of the open-reading frame was eliminated, leaving basically no protein translation left. This approach for gene knockout could help to define the MO-induced knockdown of *nphps* more closely and provide complementary information. The questions for these zebrafish mutant lines with large deletions were the same as for the lines carrying point mutations, asking whether these mutations might lead to an increase in cystic glomerular and cloaca malformation and if they did so, whether there might be compensation taking place in a subsequent generation.

#### 3.3.1 *nphp4-ex1-del5*

The *nphp4-ex1-del5* mutational zebrafish line was generated by a single gRNA targeting the first exon of twenty-nine in the *nphp4* gene and causing a deletion of 5 base pairs (bp) (Tab. 19). This deletion gives rise to a frame shift after amino acid (aa) 16 and finally leads to an early stop codon, ending the translation of the *nphp4* protein after the first 44 out of 1417 aa already (Fig. 19A). I faced serious technical difficulties in the sequencing of embryos in F1, as most sequencing results were of poor quality or sequencing was not possible at all. All my attempts on troubleshooting were unsuccessful as neither different primers nor different PCR or Sanger sequencing set-ups allowed for reliable results. As it seemed, two secondary structures formed in the PCR product, one of which includes the deletion of interest. Thus, the polymerase could not read the PCR products and sequencing was not possible. It is for this reason, that I was only able to gather data on maternal zygotic mutant (m/m) zebrafish embryos in F2, as some already genotyped wildtype (+/+) and (m/m) fish were raised and at fertile age.

The (m/m) embryos in F2 showed 2.6-times more glomerular cyst formation (Fig. 19C-D) and 7.4-times more defective cloaca formation compared to their wildtype (+/+) siblings (Fig. 19B/D). Maternal zygotic (m/m) mutants in the F2 generation of the *nphp4-ex1-del5* zebrafish line, were apparently no different from the (+/+) controls in regard of the prevalence of ciliopathy-associated phenotypes screened for, namely abnormal heart looping, formation of heart edema and hydrocephalus and pathologic body curvature (Kayser et al., 2022). Abnormal body curvature, especially the phenotype scored as “curly up”, was actually 5-times more frequent in wildtype embryos than in mutants (Fig. 20).

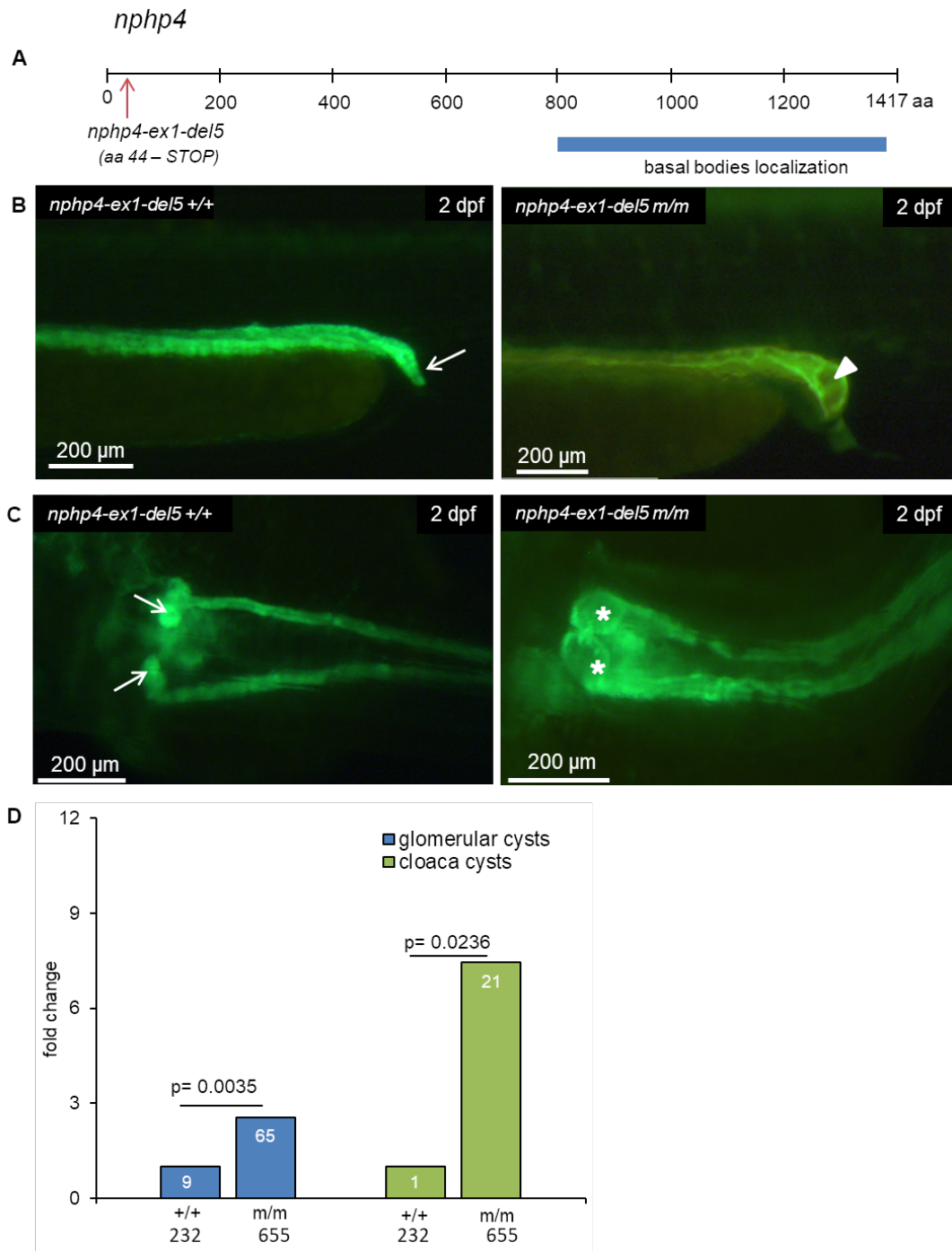


**Figure 19: Glomerular and cloaca cyst formation in F2 *nphp4-ex1-del5* mutant fish**

(A) Graphic illustration of the *nphp4* zebrafish gene. The *nphp4-ex1-del5* is generated by the CRISPR/Cas9 gene modification method, using a single gRNA targeted against the first exon of *nphp4*, causing the deletion of 5 base pairs (bp) and the insertion of a premature stop codon at the amino acid (aa) 44 out of 1417. (B) Images of the cloaca region obtained by fluorescent microscopy at 48 hours post fertilization (hpf). The image on the left shows a normal cloaca (arrow) in a wildtype (+/+) control embryo. The image on the right shows a typical example of an obstructed cloaca, leading to a cystic formation at the end of the pronephric duct instead of the normal body opening (arrowhead) in a homozygote mutant (m/m) embryo. (C) Images of the glomerular region obtained by fluorescent microscopy at 48 hours post fertilization (hpf). The image on the left shows normal pronephric duct and glomerular development (arrows) in a wildtype (+/+) control embryo. The image on the right shows an example of glomerular cyst formation, easily recognized as fluid-filled, distended glomeruli (stars) in this homozygote mutant (m/m) embryo. (D) Graph showing the frequency of glomerular cyst formation and cloaca malformation, in homozygote (m/m) maternal zygotic embryos in F2 in relation to their wildtype (+/+) siblings. The numbers in each column represent the number of observed embryos presenting the respective phenotype and the number underneath each column indicates the total number of embryos scored for each genotype. (Fisher's exact test, two-tailed)



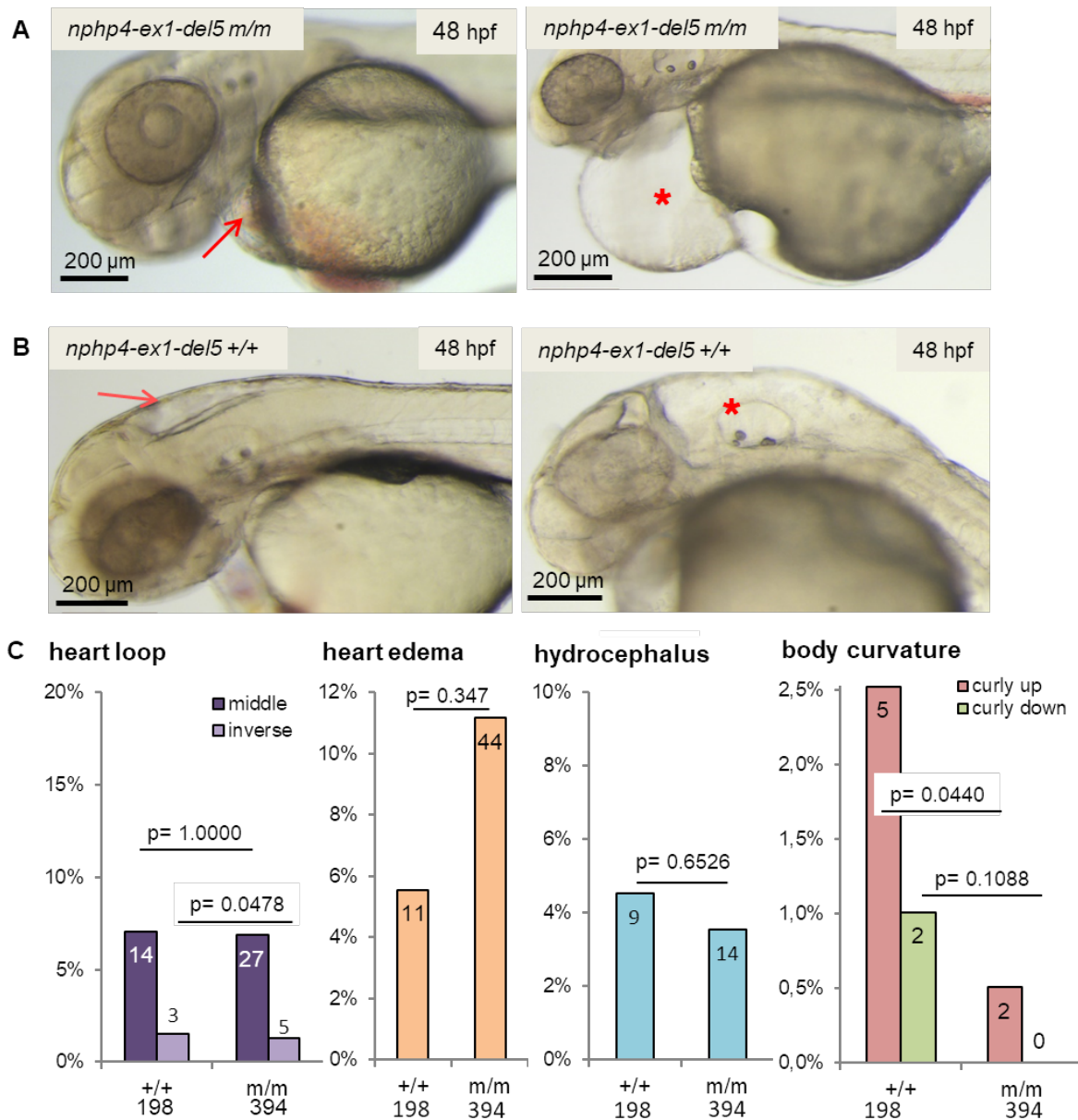


**Figure 20: Ciliopathy associated phenotypes in F2 *nphp4-ex1-del5* mutant fish**

(A) Images of *nphp4-ex1-del5* zebrafish embryos acquired with an optical stereo microscope at 48 hours post fertilization (hpf). The image on the left shows a physiological cardiac compartment in a homozygote mutant (m/m) embryo (arrow). The image on the right shows an impressive example of heart edema, characterized by a fluid-filled pericardium, in this (m/m) mutant zebrafish (star). (B) Images of *nphp4-ex1-del5* zebrafish embryos acquired with an optical stereo microscope at 48 hours post fertilization (hpf). The image on the left shows a wildtype (+/+) embryo with a regular sized brain ventricular system (arrow). In contrast, the image on the right shows a typical example of hydrocephalus formation, with a massively distended ventricle in a wildtype embryo (star). (D) Graphs showing the frequency of ciliopathy-associated phenotypes in *nphp4-ex1-del5* zebrafish embryos of the F2 generation. The numbers in each column represent the number of observed embryos presenting the respective phenotype and the number underneath each column indicates the total number of embryos scored for each genotype. From left to right: Abnormal heart looping, as an indicator for faulty left-right body axis determination, is categorized into “middle” and “inverse”, comparing to the normal orientation of the heart loop. Heart edema, hydrocephalus and abnormal body curvature, marked as “curly up” or “or curly down”, are additional phenotypes screened for. (Fisher’s exact test, two-tailed)

### **MO-mediated gene knockdown of *nphp4-ex1-del5***

To evaluate potential compensation in the F2 generation, I injected translation-blocking MO (TBM) in two different concentrations (0.1mM and 0.2mM) in wildtype (+/+) and homozygote mutants (m/m) of this second generation. Generally speaking, the second-generation mutants were largely resistant to the TBM in both concentrations and developed significantly less glomerular cysts (Fig. 21B) than their wildtype counterparts, when comparing wildtype and mutant embryos injected with the same concentration of TBM (Fig. 21C). The same observation could be made in the assessment of cloaca malformation (Fig. 21A) in TBM-treated wildtype and mutant embryos. Mutants developed less cloaca cysts when treated with TBM than their wildtype counterparts with the same treatment, this time the difference being statistically significant only for the higher concentration (TBM 0.2mM). This overall resistance to TBM-mediated gene depletion being noticed, the embryos who underwent TBM treatment still developed significantly more of both cystic phenotypes than their untreated siblings (Fig. 21D).

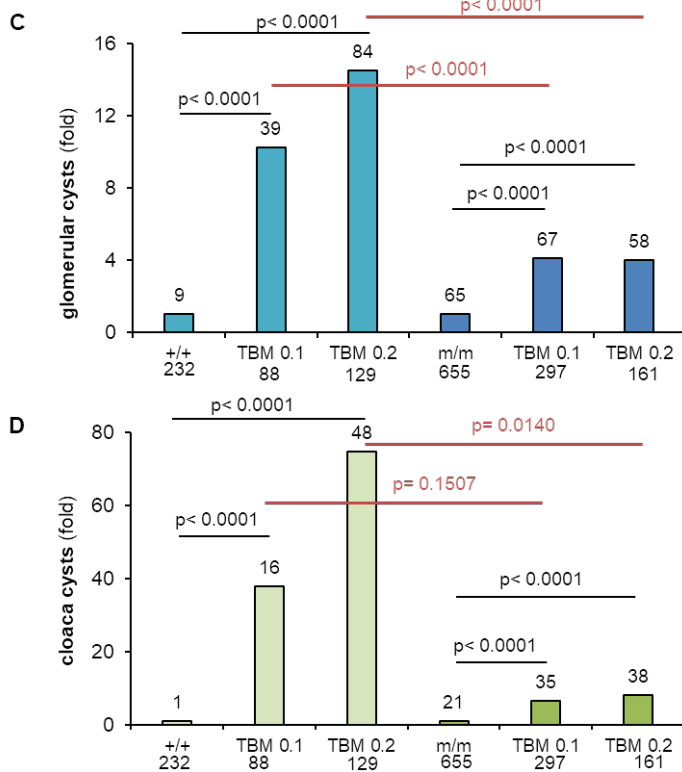
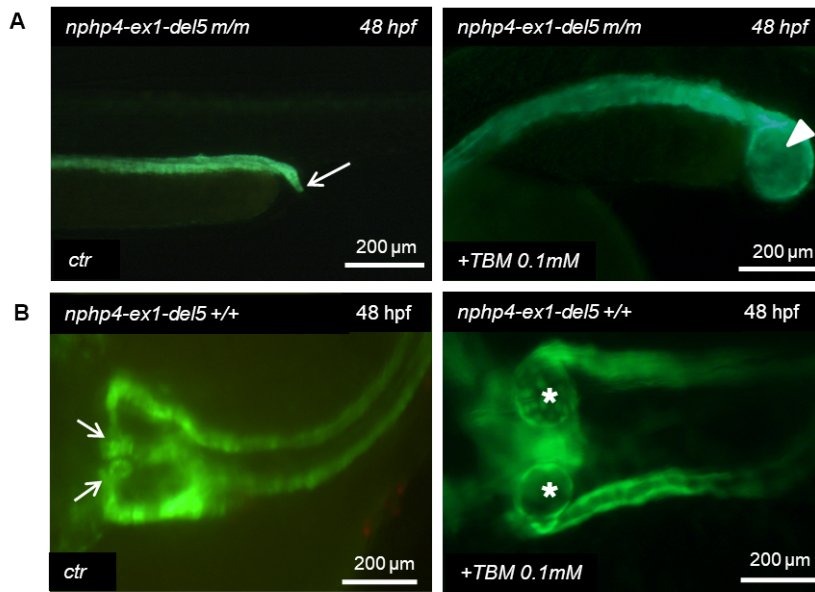


**Figure 21: MO-induced knockdown of *nphp4-ex1-del5* in maternal zygotic mutants**

(A) Images showing the cloaca region of *nphp4-ex1-del5* homozygote mutant (m/m) zebrafish embryos under fluorescent light at 48hpf. The image on the left shows a regularly developed cloaca (arrow) of an untreated (m/m) embryo. The image on the right is exemplary for cloaca malformation, causing cystic enlargement of the distal pronephric duct (arrowhead) in this (m/m) embryo treated with translation-blocking (TBM) MO (0.1mM). (B) Images showing the proximal pronephric ducts and glomeruli of *nphp4-ex1-del5* wildtype (+/+) zebrafish embryos under fluorescent light at 48hpf. The image on the right illustrating regular glomerular development (arrows) in this untreated (+/+) embryo. On the left one can see two bilaterally paired glomerular cysts (stars) in a (+/+) embryo treated with TBM (0.1mM). (C) Graph showing the increase of glomerular cyst formation in *nphp4-ex1-del5* zebrafish embryos of the F2 generation, when injected with translation-blocking MO (TBM), normalized to the frequency to their untreated (+/+) or (m/m) siblings. TBM has been injected in two different concentrations (0.1mM and 0.2mM) into one-cell staged (+/+) (light blue columns) and (m/m) (dark blue columns) embryos. The numbers above each column represent the number of observed embryos presenting glomerular cysts and the number underneath each column indicates the total number of embryos scored for each subgroup. (D) Graph showing the increase of cloaca cyst formation in *nphp4-ex1-del5* zebrafish embryos of the F2 generation, when injected with TBM, normalized to the frequency to their untreated (+/+) or (m/m) siblings. TBM has been injected in two different concentrations (0.1mM and 0.2mM) into one-cell staged (+/+) (light green columns) and (m/m) (dark green columns) embryos. The numbers above each column represent the number of observed embryos presenting cloaca malformation and the number underneath each column indicates the total number of embryos scored for each subgroup. (Fisher's exact test, two-tailed)

### 3.3.2 *nphp1-ex15-del4*

Unfortunately, no zebrafish lines carrying point mutations in the *nphp1* gene, generated by chemical ENU mutagenesis, have been identified in mutagenesis screens so far. To study the role of *nphp1* in zebrafish embryogenesis, a new mutant line had to be generated. Our group created the *nphp1-ex15-del4* mutational zebrafish line using the CRISPR/Cas9 gene editing method. A single gRNA targeted the exon15 of *nphp1* and caused a deletion of 4 base pairs (bp) (Tab. 19). This deletion gave rise to a frame shift after amino acid (aa) 454, which finally leads to the insertion of a stop codon after the first 463 out of 667 aa, excluding exons 16-20 (Fig. 22A) (Kayser et al., 2022). Since only 6 heterozygote (m/+) fish (1 male, 5 females) were available to me, incross of (m/+) fish seemed not to be efficient nor representative enough to generate an F1, which could be assessed for phenotypes and sent for sequencing. That is why I decided to cross the female (m/+) fish with the 3 male (m/m) fish, which I had at my disposal, to generate zygotic mutants in the F1 generation. Since this cross could only yield (m/+) and (m/m) embryos, I in-crossed (+/+) fish, of which I had 14, to generate a wildtype control to F1. The zebrafish embryos were analyzed 48 hours post fertilization and scored for glomerular cyst formation and cloaca malformation. Considering this rather special pairing constellation out of necessity, the Mendelian ratio could not be evaluated in F1. Homozygote mutant (m/m) zebrafish showed a significant increase in glomerular cysts, occurring at a 6.3-times higher rate than in the wildtype (+/+) embryos. A noticeable but non-significant increase in cloaca malformation could be observed in homozygote mutant zebrafish (Fig. 22B). However, the overall low percentage of both phenotypes in homozygote mutant embryos should be mentioned. Glomerular cysts occurred in 2.7%, cloaca cysts in 6.7% of the observed (m/m) zebrafish. Due to the lack of female (m/m) fish, no F2 generation could be generated and hereinafter compared to F1.

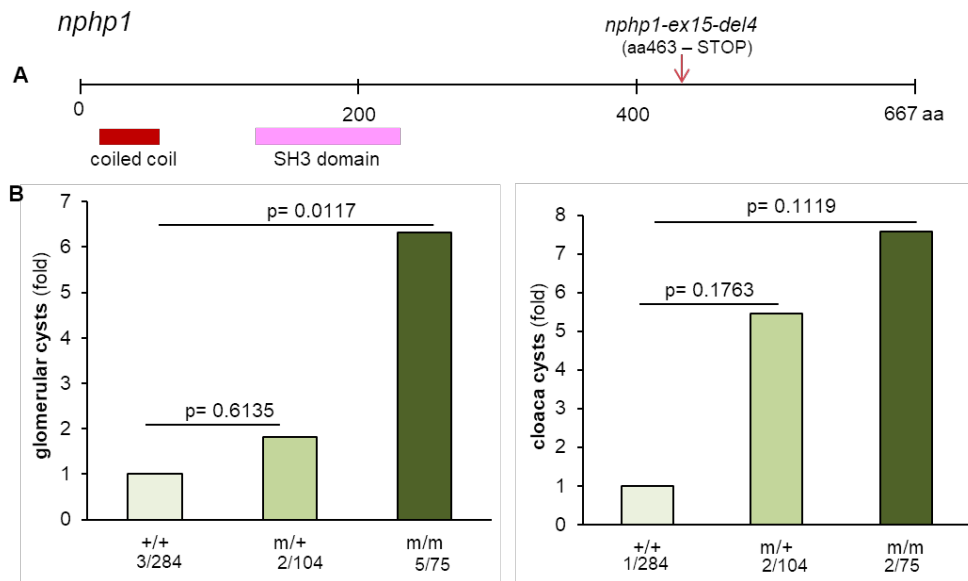


**Figure 22: Glomerular and cloaca cyst formation in F1 *nphp1-ex15-del4* mutant fish**

(A) Graphic illustration of the *nphp1* zebrafish gene. The *nphp1-ex15-del4* is generated by the CRISPR/Cas9 gene modification method, using a single gRNA targeted against the exon 15 of *nphp1*, causing the deletion of 4 base pairs (bp) and the insertion of a premature stop codon at the amino acid (aa) 463 out of 667. (B) Graphs showing the frequency of glomerular cyst formation and cloaca malformation respectively, in heterozygote (m/+) and homozygote (m/m) embryos in F1 in relation to their wildtype (+/+) siblings. The numbers underneath each column represent the number of observed embryos presenting the respective phenotype and the total number of embryos scored for each genotype. (Fisher's exact test, two-tailed)

### 3.4 Generation of a new *invs/nphp2* mutant line by CRISPR/Cas9

Zebrafish mutant lines carrying extensive deletions play a fundamentally important role in the study of gene functions as they deliver complementary insights to zebrafish with point mutations. Since I collected data for the *invs\_sa36157* mutant fish line and in order to enlarge our already comprehensive repertoire of lines with large deletions, the generation of a new mutant *invs/nphp2* fish line with most of the gene being deleted, seemed interesting for use in future studies. I used the CRISPR/Cas9 system, a powerful genomic engineering method, to generate a line with most of the open-reading frame being deleted, which will be available for subsequent assessment of the consequences *in vivo*.

To achieve this, target sites were selected as close as possible to the beginning and the end of the *nphp2* gene. The *nphp2* gene of the zebrafish contains 18 exons, hence it appeared best to select target sites aiming for the promotor region or the first exons to induce a double-strand break at the very beginning and target sites in exon 18 to induce double-strand breaks at the end of the gene. I conditioned the selection of potentially fitting target sites on the ranking made by CHOPCHOP, a web-based tool for CRISPR/Cas9 single guide RNA (sgRNA) target site selection. This tool optimizes the selection of sgRNA target sites, which is crucial for efficient guidance of the CRISPR effector protein Cas9. Cas9 is ultimately responsible for cutting the genome at the intended location. For this selection process, CHOPCHOPs algorithm includes factors influencing

efficiency additionally to complementarity between sgRNA and target location. Factors being the location of the target sequence within the gene, with its accessibility and flanking regions, possible mismatches, the GC-content, self-complementary regions and the number of off-targets, CHOPCHOP provided a ranking list of possible target sites in the end (Labun et al., 2019).

Because target sites in the promotor region of the *nphp2* gene were all poorly ranked, I chose sgRNA target sites in the first exon (*nphp2\_ex1\_sgRNA1*) and in the exon 2 with the highest ranking available (*nphp2\_ex2\_sgRNA27*). I selected three target sites in the exon 18 with the highest possible ranking to generate three sgRNAs (*nphp2\_ex18\_sgRNA9*, *nphp2\_ex18\_sgRNA12* and *nphp2\_ex18\_sgRNA19*) cutting the gene at its very end (Fig 23A-B).

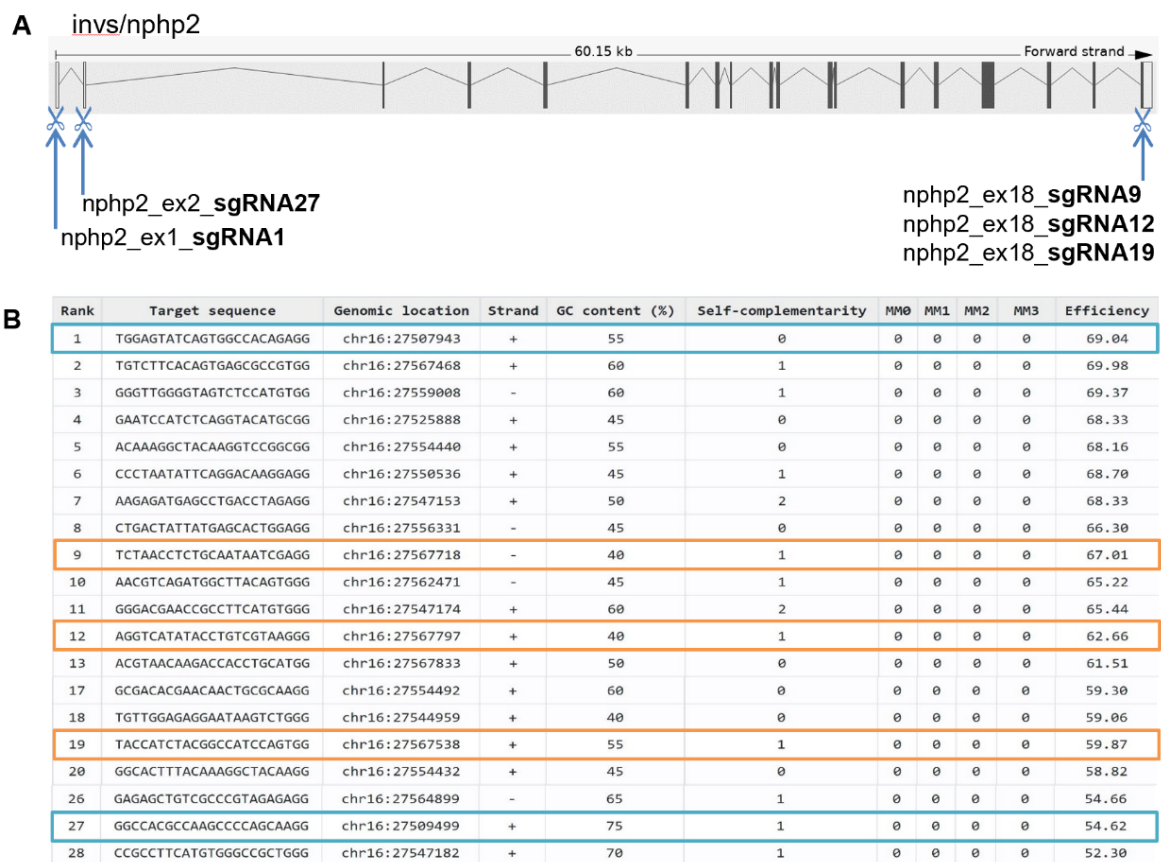


**Figure 23: sgRNA target selection for CRISPR/Cas9 mutation of *nphp2***

(A) Illustration of the *invs/nphp2* gene. Target sites of the designed sgRNAs are indicated by the blue arrows. Two sgRNAs guiding the Cas9 nuclease to cut the gene at the beginning and three sgRNAs targeting sequences in the exon 18 to cut the gene at the end were designed. (B) Target sites for the sgRNA design were chosen in consideration of their ranking given by CHOPCHOP. The target sequences chosen at the beginning of the gene are framed in blue, the ones at the end are framed in orange.

All five of the constructed sgRNAs were injected collectively into fertilized one-cell staged transgenic *cdh17:GFP;wt1b:GFP* zebrafish eggs in three different concentrations (100 ng/μl, 200 ng/μl, 260 ng/μl) (Table 23) to find the highest tolerable concentration. The embryos were checked one day after the injection to assess lethality and induction of obvious phenotypes linked to the injection itself. For all three sgRNA concentrations, neither lethality nor abnormal phenotypes were significantly more frequent in injected fish compared to their untreated siblings.

The limitation of OneTaq polymerase only being able to amplify targets up to 6 kilobases (kb) according to the supplier (New England Biolabs), was made use of to confirm successful dual-sgRNA directed gene deletion. If the sgRNAs failed to guide the Cas9 protein to the target sites and consequently preventing efficient cutting of the gene, the product would be too big for amplification *via* PCR and no PCR product, allowing subsequent Sanger sequencing, would be obtained. A forward primer upstream of the sgRNA target sites aiming for exon1 and exon2 (*nphp2*-prmSeq-F3) as well as a reverse primer complementary to a sequence downstream of the sgRNA targeting exon 18 (*nphp2*-ex18Seq-R1) were ordered (Table 13). Some injected embryos were chosen randomly after 24 hpf and were lysed to gain access to their genomic DNA. PCR was performed on this genomic DNA using the ordered primers and the PCR products were checked *via* gel electrophoresis. As already explained, the PCR could only work, if the CRISPR/Cas mediated gene deletion had been taken place, deleting the base pairs between one of the sgRNAs targeting the beginning of the gene and one of the sgRNAs targeting its end. This would consequently approach the gene regions complementary to the forward and the reverse primer sufficiently, so that the Taq polymerase could synthesize a DNA product. If this was the case, bands would become visible in gel electrophoresis, showing the presence of DNA products, and indicating their length. In my experiments, the PCRs on 1 out of 6 genomic DNAs of fish injected with sgRNA 100 ng/μl and on all 6 out of 6 genomic DNAs of fish injected with sgRNA 260 ng/μl worked, as PCR products ranging from around 500 to 1400 base pairs (pb) became visible as bands in gel electrophoresis (Fig. 24). Since the injection with the highest concentration seemed to be more effective while not being toxic at the same time, I continued my experiment with the highest concentration of 260 ng/μl.

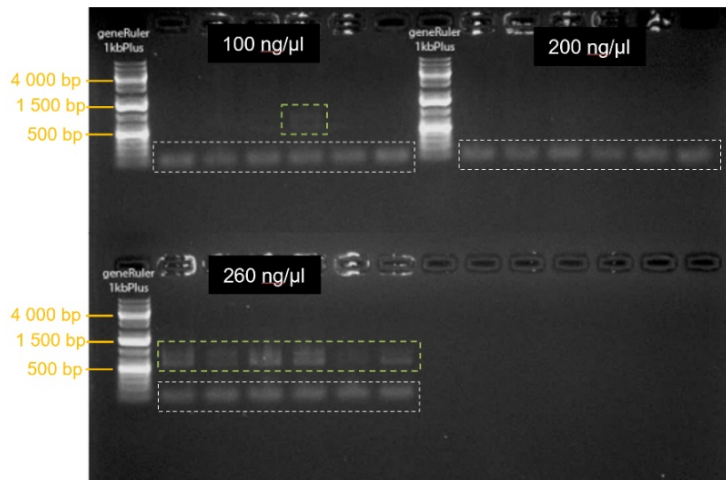


**Figure 24: Electrophoresis gel showing PCR products of genomic DNA from sgRNA-injected embryos**

Six embryos were lysed for every sgRNA-concentration of injection solution used and PCRs were performed on their genomic DNA. A marker labelled “geneRuler 1kbPlus” was run together with the PCR products, allowing estimation of the length of the products in base pairs (bp). The bands framed in green represent the PCR products of genomic DNA of embryos where the CRISPR/Cas9 mediated knockout worked. The bands framed in white represent the primers only.

Since five sgRNAs were injected simultaneously, it was not possible to determine which combination of sgRNAs was responsible for the deletion in every genomic DNA analyzed with gel electrophoresis only. The PCR products of genomic DNA, which became visible on gel electrophoresis, were therefore cloned into TOPO vectors and transformed into OneShot TOP10 chemically competent *Escherichia Coli*. With the blue-white selection method, colonies which integrated the vector containing the PCR product, were identified and a colony PCR was performed on them. The products of this colony PCR were checked on gel electrophoresis again and sent for Sanger sequencing together with the standard primer M13R (Table 13). The sequencing of the colony PCR of 6 out of 28 colonies transformed with the vector containing the genomic PCR products revealed successful deletion of the gene. In these six clones, complementarity with the *invs/nphp2* gene was found and deletions ranging from 59 851 to 59 861 base pairs (bp) could be confirmed. In all six clones, parts of the *nphp2\_prm\_sgRNA1* and *nphp2\_ex18\_sgRNA12* were found as border regions at the beginning or at the end of the deletion respectively, indicating that it is this pair of sgRNAs that was responsible for the Cas9 mediated deletion (Fig. 25).



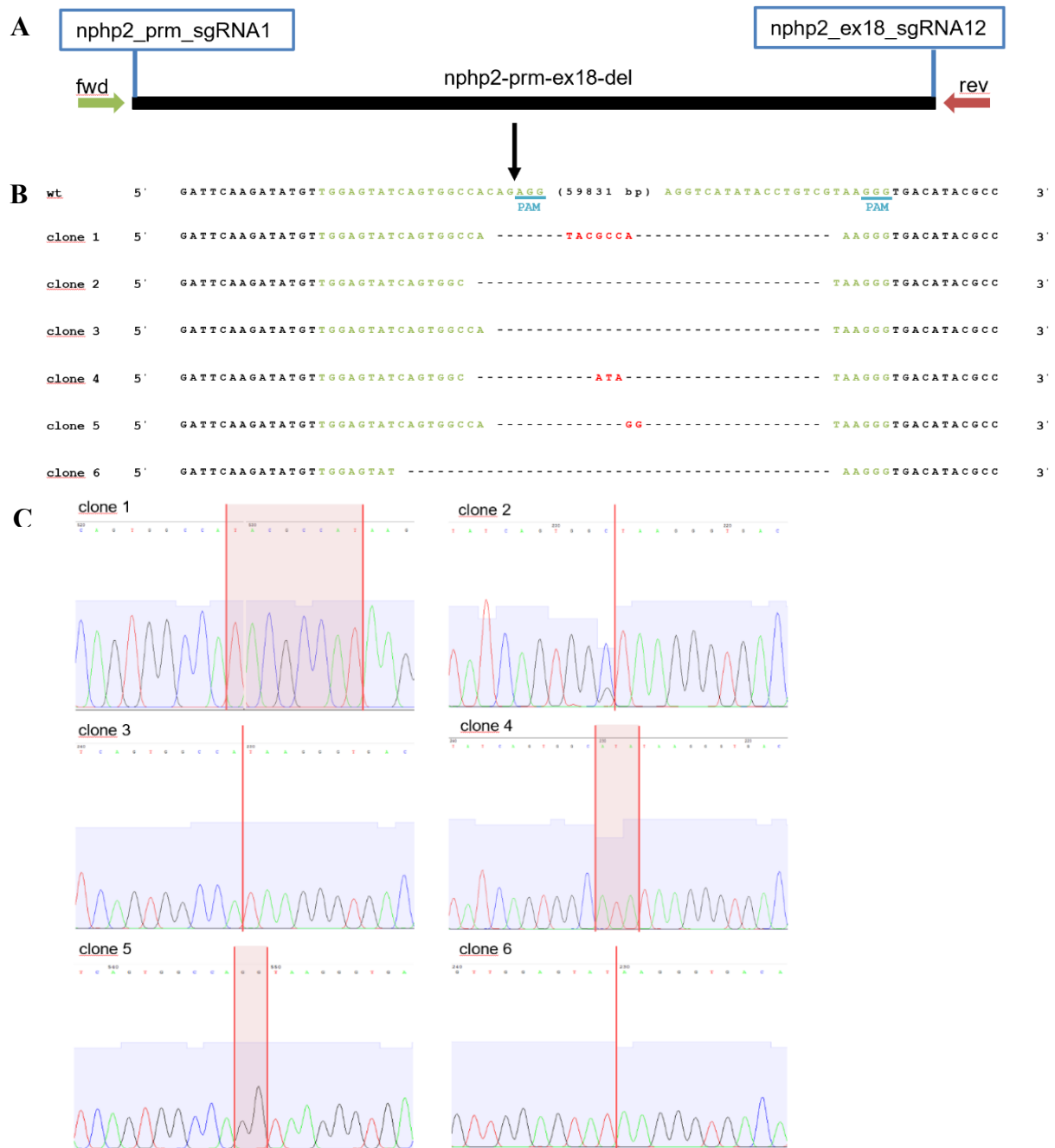


**Figure 25: Successful sgRNA directed deletion of *npbp2/invs* via CRISPR/Cas9**

(A) Graphic illustration of the *npbp2/invs* gene with the two sgRNAs targeting a sequence in the promoter region (*npbp2\_prm\_sgRNA1*) and in the exon 18 (*npbp2\_ex18\_sgRNA12*) respectively. A forward (fwd) primer was selected to bind upstream of *npbp2\_prm\_sgRNA1* and a reverse primer (rev) to bind downstream of *npbp2\_ex18\_sgRNA12*, enabling PCR and sequencing if the CRISPR/Cas9 gene knockout had worked. (B) Gene sequence of *npbp2* wildtype and clones containing the successfully mutated *npbp2* gene. The sgRNA target sites are marked in green, the PAM sequences are marked in blue, in the wildtype sequence 59831 base pairs (bp) are not shown. The bp marked in red represent potentially added bp in between the two cutting points in the corresponding clone. (C) Sequencing results of the six clones, illustrating the reassembly of the upstream and downstream end (red line) and the potentially added bp in between the two cutting points (highlighted in red).

## 4. Discussion

The variable penetrance and expressivity of different mutations causing ciliopathy-associated phenotypes, have been described in multiple experiments and were assumed to be the phenomena, underlying the sometimes-missing genotype-phenotype correlation. Differences between phenotypes caused by mutations in different genes and phenotypes observed in MO-treated embryos deficient of those same genes, have caused disbelief in the ability of the different genetic approaches when it comes to characterization of gene functions (Kok et al., 2015; Stainier et al., 2015). Friedemann Zaiser described in his thesis, the discrepancy between cloaca cyst formation in morphant zebrafish in comparison to mutant zebrafish. Zebrafish who had their *nphp2*, *nphp4* or *nphp8* genes knocked down by morpholino oligonucleotide injections (morphants), showed more cloaca malformation than mutant embryos, who carried chemically induced point mutations in the same *nphp* genes. This difference being most manifest for the *nphp4* gene, he suggested genetic compensation in *nphp4* mutants.

### 4.1 Zebrafish lines with defined *nphp* point mutations show no consistent genotype-phenotype correlation in F1

In the original description of infantile NPH (NPH type II), seven patients presenting early onset of severe renal failure, hypertension, renal enlargement and hepatic involvement, all culminating in ESRD and death within the first two years of life, were described (Gagnadoux et al., 1989). In one of these children, a T>C missense mutation affecting the nucleotide 1478 of the *nphp2* gene and replacing the leucine amino acid at position 493 by a serine amino acid, was detected. Other individuals with early onset of NPH type II and ESRD were detected to carry nonsense mutations, truncating the Nphp2 protein for example at the amino acid (aa) 603 or 907 out of 1065 aa (Otto et al., 2003). Homozygote *nphp2*<sup>sa36157/sa3615</sup> zebrafish embryos, carrying this particular mutation, which truncates the Nphp2 protein already at aa314 after the 9<sup>th</sup> ankyrin-repeat containing domain, only showed a mild increase in glomerular cyst formation and cloaca malformation, compared to their wildtype siblings. Furthermore, the *nphp2*<sup>sa36157</sup> mutation did not seem to cause situs inversus at a higher rate in zebrafish, like it was described in mutant mice (Yokoyama et al., 1993). The results of *nphp2* MO-mediated knockdown experiments on zebrafish, stating severe pronephric cysts, ventral body curvature and randomization of the heart looping (Otto et al., 2003) could not be confirmed as clearly in *nphp2*<sup>sa36157</sup> mutant fish.

By positional cloning, mutations in the *nphp4* gene could be identified in different consanguineous families with individuals diagnosed with juvenile nephronophthisis and retinitis pigmentosa (Otto et al., 2002). One mutation, a C>T nonsense mutation truncating the *nphp4* protein after aa658, was described to lead to ESRD onset relatively early (6-22 years), comparing to the onset observed

being caused by another C>T nonsense mutation, leading to a premature stop codon only after aa779 (28-35 years) (Otto et al., 2002). A similar trend could be observed in the zebrafish lines carrying *nphp4* point mutations. While homozygote *nphp4*<sup>sa41188/sa41188</sup>, harboring this mutation, which truncates the protein after aa444, showed more than 8-times more glomerular cysts than their wildtype siblings, homozygote *nphp4*<sup>sa38686/sa38686</sup> fish, the mutation affecting the splicing process only after aa764, did not develop more glomerular cysts than the wildtype controls.

In humans as well as in mice, complete loss of Nphp8 function due to truncating mutations, leads to Meckel-Gruber syndrome (MKS), characterized by severe developmental defects, ultimately resulting in embryonal lethality (Delous et al., 2007). Both analyzed zebrafish lines carrying point mutations, were viable and fertile. The *nphp8*<sup>sa10096</sup> mutation, truncating the protein after aa862 at the end of the C2 domain, as well as the *nphp8*<sup>24730</sup> mutation, which eliminates an essential splice site after aa337, caused a significant increase of glomerular and cloaca cyst formation in homozygote embryos comparing to their wildtype siblings. The severity of phenotypes in NPH patients with *nphp8* mutations, who develop diverse and severe phenotypes like MKS, JBTS or COACH syndrome, seemed to be reflected in the zebrafish model as well. The presence of only one mutated allele of both mutations in heterozygote zebrafish embryos, showed to be sufficient to cause an intermediate frequency in phenotypes. Heterozygote *nphp8*<sup>sa24730/+</sup> fish even presented statistically significantly more glomerular cysts than the wildtype controls, underlining the serious consequences this mutation, which interferes with the Nphp8 protein translation already after 9 out of 27 exons. The *nphp8*<sup>sa24730</sup> mutation affects the coiled coils containing structural protein motif. This motif was assigned to contribute to the role of Nphp8 as an assembly factor at the transition zone of primary cilia, linking proteins from both NPH and MKS complexes (Jensen et al., 2015). This crucial role of the coiled coils domain of Nphp8, which Friedemann Zaiser stated for normal cloaca development in his thesis, seemed to apply to pronephros development as well, as one mutant allele was sufficient to cause glomerular cysts. In the human *nphp8* gene, two C2 domains were described. The N-terminal one was linked to play an important role in the interaction between Nphp8 and Nphp4, which if disrupted by a mutation in this C2 domain, leads to severe symptoms characterizing the multiorgan cerebello-oculo-renal syndrome (Joubert syndrome Type II) (Delous et al., 2007). Even though the zebrafish Nphp8 protein only shows one C2 domain in a position corresponding to the C-terminal C2 domain in human Nphp8 (the ‘less important one’), the *nphp8*<sup>sa10096</sup> mutation leads to a clear increase in glomerular and cloaca cyst formation, demonstrating the importance of this C2 domain.

Even tough mutations are an important element in evolution, organisms have developed several buffering mechanisms, which provide a so called ‘genetic robustness’. This genetic robustness

ensures similar outcomes up to a certain degree, despite genetic perturbations, environmental changes, or different genetic background. The missing clear genotype-phenotype correlation in the analyzed point-mutation-carrying zebrafish mutants, could be explained by several theories (El-Brolosy and Stainier, 2017). The complete lack or variable severity of phenotypes in mutants could be attributed for example to gene redundancy, the presence of two genes, who act in similar processes and therefore prevent that the inactivation of either of them becomes disruptive (Nowak et al., 1997). Secondly, a point mutation could result in a so called hypomorphic allele, which still retains some wild-type function and subsequently fails to produce the expected pathologic phenotype. The concept of intracellular networks, regulating signaling, metabolic or transcriptional processes, could explain compensatory mechanisms following a genetic mutation as well. If the function of one gene, which is part of such a network, is perturbed by a mutation, other genes acting in that same network might upregulate their expression and thereby compensate for the missing gene (Levine and Davidson, 2005). The lack of ciliopathy-typic phenotypes in zebrafish, even though mutations in homologues genes have been associated to severe phenotypes in other model systems or to human disease, could also be due simply to evolutionary differences between these organisms. Another interesting hypothesis, which recently gained attention in scientific research, would be that mutants could compensate for the deleterious gene mutation in their genome, by transcriptional adaptation processes. This adaptation leads to an increased expression of adapting genes, which have a similar sequence to the mutated gene and can therefore compensate for the gene loss (El-Brolosy and Stainier, 2017). Experiments in zebrafish, injecting wildtype mRNA into mutant embryos, showed no effect on adapting gene expression and hence provided evidence, that transcriptional adaptation is not triggered by the loss-of-function of the protein itself, but by a trigger upstream of protein function (El-Brolosy et al., 2019). A potential trigger for such a compensatory process could be the mutant mRNA, which is targeted and degraded by cellular mRNA surveillance systems. One of these surveillance systems is the nonsense-mediated decay (NMD) pathway, which targets mRNA containing a premature termination codon (PTC). Insertion of a PTC can be caused obviously by non-sense mutations but also by mutations affecting the splicing process as well. PTC containing mRNA is recognized and degraded by an intricate complex of interacting proteins and factors. This pathway protects the cells against the effect of mutated alleles, which encode for proteins with no or undesired functions (Rossi et al., 2015). After NMD activation, different decay pathways degrade the deleterious mRNA (Lykke-Andersen and Jensen, 2015). The mutant mRNA decay is thought to contribute to compensation in different ways; the resulting mRNA fragments could guide transcription factors or chromatin remodelers to the regulatory regions of potentially compensating genes. The

increasing availability of RNA binding proteins (RBPs), which regulate gene expression by stabilizing mRNAs of functionally related genes, could stabilize mRNA from compensatory genes all the more since the defective mRNA is degraded by NMD (El-Brolosy and Stainier, 2017). Since the injection of MOs causes disruption of mRNA processing, no mRNA can be degraded by NMD and no translational adaptation can occur, which could explain the discrepancies in phenotypes between mutants and morphants. Nevertheless, the exact activation processes of the transcription of adapting genes are still not well understood to date and even dissenting between different model systems. While some works claimed that the generation and subsequent degradation of mRNA by NMD is crucial for compensation, others said differently. Experiments on transcriptional adaptation in *C. elegans* showed that a particular mutation in the actin gene *act-5* gene was followed by upregulation of an adapting gene *act-3*. While *act-3* mRNA levels were elevated in mutants, *act-5* mRNA levels were reduced, indicating decay mechanisms of the mutated mRNA. When SMG-6, an important endonuclease known to act in NMD, was eliminated in mutant nematodes showing transcriptional adaptation, by MO-derived *smg-6* gene knockdown, the levels of the mutant mRNA rose again, while the compensating mRNA levels sunk. However, no transcriptional adaptation could be shown by measuring transcript levels of mutant and adapting mRNAs for a different mutation in the *act-5* gene. These results raised the question, whether endonucleolytic degradation of mutant mRNA is necessary for transcriptional adaptation and which factors have an impact on whether mRNA is degraded and induces compensatory processes or not (Seroby et al., 2020). It is not clear to which extent one can compare and generalize adaptation processes between different model systems and even between genes in the same model system. The study of mRNA levels in zebrafish carrying these point mutations, could provide further insights into their adaptation process in future studies.

In addition to its role in the adaptation processes, NMD of the defective protein from an altered allele, which has a dominant negative effect, can save heterozygote mutation carriers, as long as the healthy allele expresses sufficient functional protein. If the expression level of the functional allele is not sufficient for normal physiological function of the encoded protein, it is called 'haplotype insufficiency' (Fig. 26) (Lykke-Andersen and Jensen, 2015). Haplotype insufficiency could be observed in heterozygote (*m/+*) zebrafish in all mutant lines analyzed in this work. Heterozygote mutants with a more severely truncating mutation (*nphp4<sup>sa41188</sup>* and *nphp8<sup>sa24730</sup>*) however, showed haplotype insufficiency to a greater extent than mutants carrying a mutation which allows a bigger portion of the protein being translated (*nphp4<sup>sa38686</sup>* and *nphp8<sup>sa10096</sup>*). The more severely truncated proteins seem to have more deleterious phenotypic effects as even the

presence of one mutated allele is sufficient to cause phenotypes and NMD not being able to prevent these effects sufficiently.

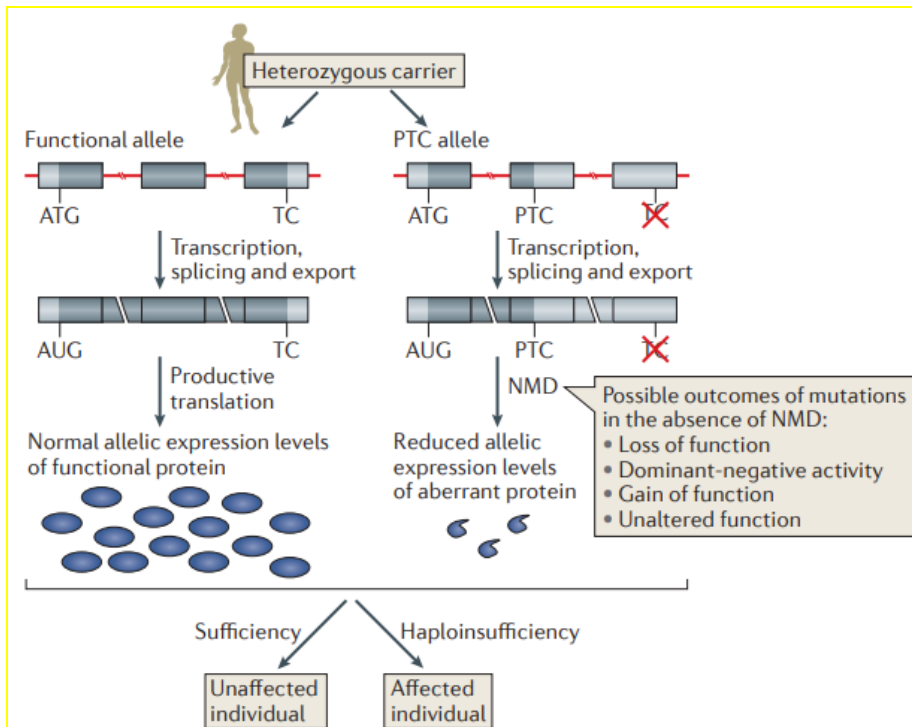


**Figure 26: Non-sense mediated decay (NMD) in heterozygous carriers of premature termination codons (PTCs).**

NMD can prevent several possible phenotypic outcomes of PTC-generating mutations. In heterozygous carriers (illustrated by a functional allele (left) and an allele with a PTC-introducing mutation (right)), total levels of functional protein are halved, which may be either sufficient or insufficient to retain normal physiological function (Lykke-Andersen and Jensen, 2015).

## 4.2 Intergenerational compensation of phenotypes in zebrafish lines with defined point mutations

Numerous studies have shown, that zebrafish are able to compensate for the loss of gene functions up to a certain degree (El-Brolosy et al., 2019; El-Brolosy and Stainier, 2017; Rossi et al., 2015). In consideration of these findings, a next logical step was to investigate whether zebrafish carrying one of these point mutations would pass this acquired compensation down to their progeny or if the phenotypes would become worse from one generation to the next one, like it is typically known for human genetic diseases with recessive inheritance. The generation of maternal zygotic mutants (F2 generation) by pairing male and female heterozygote fish from F1 (in-cross), was possible because fish of all mutant lines analyzed, were viable and fertile. The analysis of this F2 generation permitted not only the observation of potential compensation, but also the assessment of the loss of any contribution by maternal wildtype mRNA on the development of ciliopathy phenotypes. Embryos from heterozygote parents carry maternally inherited wildtype mRNA or proteins, which maintain normal gene function in early developmental stages, as the zygotic genome is only activated at a slightly later stage of development. In animals, maternal gene products are essential

in the earliest stages of embryogenesis as they regulate manifold processes, such as cell division, early patterning and axis formation until the activation of the zygotic genome takes over (Abrams and Mullins, 2009). This maternal to zygotic transition stage occurs at different stages among animals. Zebrafish rely on this maternal information for several more cleavage cycles as for example humans or mice (Marlow, 2010). Even after the activation of the zygotic genome, maternal products continue to influence different processes (Pelegri, 2003). Thus, they could mask the effect of the mutant allele in F1, even in homozygote mutant fish.

Homozygote *nphp2*<sup>sa36157/sa36157</sup> in the F2 generation showed a decline in glomerular and cloaca cysts compared to F1 mutants, normalized to their respective wildtype siblings. A similar amelioration in F2 was observed in homozygote *nphp4*<sup>sa41188/sa41188</sup> mutants, who developed roughly half as much glomerular cysts than their F1 homologues and were no longer different from their wildtype siblings. The opposite was the case for homozygote *nphp4*<sup>sa38686/sa38686</sup> mutants; while mutants in F1 were no different from their wildtype siblings, the *nphp4*<sup>sa38686</sup> mutation caused a massive increase in both manifestations one generation later in F2. Consistent with this worsening in glomerular and cloaca cyst formation, homozygote *nphp4*<sup>sa38686/sa38686</sup> mutants in F2 presented abnormal heart looping and hydrocephalus formation at a significant higher level (7.6-fold and 7.5-fold respectively) than the wildtype controls. Though the assessment of the additional four ciliopathy associated phenotypes also showed a significant difference between homozygote *nphp4*<sup>sa41188/sa41188</sup> mutants and their wildtype siblings, the increase of abnormal heart-looping in mutants compared to the wildtype fish was smaller (2.2-fold) and the overall percentage for hydrocephalus formation in mutants was considerably low (2.1%), compared to the *nphp4*<sup>sa38686</sup> mutation (6.0%).

It seems that compensation from one generation to the next one is mainly observed in mutant lines, carrying more severely truncating mutations. Both mutations, *nphp2*<sup>sa36157</sup> and *nphp4*<sup>sa41188</sup>, induce the insertion of a premature stop codon and the subsequent elimination of the C-terminal 711 and 973 amino acids respectively. The shortened protein is causing significantly more cloaca malformation and glomerular cyst formation in homozygote mutants in F1, a phenomenon that is partially compensated one generation later in F2. The mutations that permit a bigger portion of the protein being correctly translated, like the *nphp4*<sup>sa38686</sup> mutation, which is interfering with the splicing process only at aa 764 out of 1417, seem to cause no obvious increase of phenotypes in F1, which this time changes drastically one generation later in F2, where the manifestation of both phenotypes is shockingly higher. Several theories could explain this constellation: The mutant mRNA in *nphp2*<sup>sa36157</sup> and *nphp4*<sup>sa41188</sup> could be more eligible for mRNA mediated decay and therefore might trigger translational adaptation more. The evolutionary pressure for genetic

compensation in these more severe mutations could also be higher and therefore promote the upregulation of related genes more. The F2 generation of these two mutations seems better adapted for the loss of maternally derived wildtype RNA, than the *nphp4*<sup>sa38686</sup> mutants, for whom the loss of maternal information worsens the phenotypic outcome.

This inverse relationship between phenotype severity in F1 and F2 due to intergenerational compensation, as observed in both *nphp4* mutant lines, could only be partially confirmed for the screened *nphp8* mutants. While both mutations caused significantly more glomerular cysts and cloaca malformation in homozygote mutants in F1 already, only the glomerular cyst formation could be slightly ameliorated by 20% thanks to compensation in the *nphp8*<sup>sa24730</sup> F2 generation. The observation that mutations, which leave most of the protein intact, worsen in phenotype severity from one generation to the next one with the concomitant loss of maternally derived RNA, could also be affirmed for the *nphp8*<sup>sa10096</sup> mutation. The insertion of an early stop codon after aa 862 still permits over two thirds of the *nphp8* protein being translated but causes an increase in cloaca cyst formation to 454% when comparing mutants from F2 and F1 to their wildtype siblings. However, when considering the incidence of the additional four ciliopathy-associated phenotypes in the F2 generation of *nphp8*<sup>sa10096/sa10096</sup> mutants, it was not higher than in *nphp8*<sup>sa24730/sa24730</sup> mutants, carrying a mutation in the first quarter of the gene, but the opposite was the case. The formation of hydrocephalus, a read-out for deficient neural development and resulting severe neurological phenotypes, which were linked to *nphp8* mutations in mice and humans (Delous et al., 2007), could only be observed in mutants homozygote for the more severely truncating mutation (*nphp8*<sup>sa24730</sup>). One can conclude that both *nphp8* mutations caused more phenotypes in mutants than in wildtype controls in the F1 as well as in the F2 generation and that intergenerational compensation occurred on a smaller scale in comparison to the *nphp4* mutations. Mutations in the *nphp8* gene seem to be more severe and less available for compensation, which is consistent with the severity of the of the mammalian phenotype.

### **4.3 Resistance to MO-induced knockdown in *nphp4* mutants**

MO-knockdown experiments showed the consequences of *nphp4* gene depletion, being abnormal body curvature, glomerular cyst formation and cloaca malformation (Slanchev et al., 2011). Friedemann Zaiser's results were consistent with this, as the *nphp4* knockdown showed the highest frequency of glomerular and cloaca cyst formation in his knockdown experiments of *nphp2*, *nphp4* and *nphp8*. As he could not find a clear genotype-phenotype correlation in zebrafish carrying point mutations in the *nphp4* gene considering cloaca malformation, he suggested a possible compensation in these mutants. Studies have claimed that phenotypes observed in MO-mediated



knockdown experiments may be linked to toxic and off-target effects and therefore limit their significance in terms of identification of the gene function in question (Kok et al., 2015). A possible explanation for the discrepancies in phenotype expression between morphants (knockdown) and mutants (knockout), was put forward by Rossi et al., being genetic compensation triggered by deleterious mutations but not by gene knockdown. They detected a lack of phenotypes in zebrafish and mice with mutations in epidermal growth factor like 7 (*efl7*) gene, which is coding for Eglf7, an extracellular matrix protein in endothelial cells, important for vascular tube development. The injection of antisense MOs targeting the *efl7* gene, on the other hand led to severe vascular defects when injected into wildtype embryos. The analysis of the transcriptome and proteome revealed that the expression of Emilins (proteins with the same main functional domain as Eglf7), was upregulated in mutants but not in morphants. No upregulation of these compensating genes could be detected in embryos, who had their *efl7* transcript elongation disrupted by CRISPR/Cas9 gene editing either. Together these findings suggested that protein translation, even if the protein is truncated or non-functional, is important for genetic compensation processes and represented the first identification of transcriptional adaptation processes (Rossi et al., 2015). These findings are consistent with the compensatory pathway triggered by mRNA mediated decay suggested by Lykke-Andersen (Lykke-Andersen and Jensen, 2015). The awareness of such compensating mechanisms encourages the quest for modifier genes by comparing mutants and morphants ever since.

The MO-induced knockdown of the *nphp4* gene in maternal zygotic mutant zebrafish, showed that both mutant lines (*nphp4*<sup>sa41188</sup> and *nphp4*<sup>sa38686</sup>) became largely resistant to the additional gene knockout, as the MO had less effect in mutants than in the wildtype controls. This rules out that the observed effects are caused by off-target and non-specific effects of the MO injections. It also indicates that mutant embryos in F2 compensate the loss of *nphp4* by some means. Nevertheless, all treated mutants still showed more phenotypes than untreated siblings. Different theories for compensation are conceivable and MO-knockdown experiments might help to confirm or reject them. If the fragment of the Nphp4 protein, which is still translated despite of the mutation, would be sufficient to prevent or to attenuate the phenotypic consequences of the mutation in F2 mutants, then the knockdown of the *nphp4* gene, eliminating this residual protein function altogether, would cause phenotypes in these embryos at a similar level to MO-treated wildtype fish. The same would be the case if the defective and truncated mRNA, with no residual function, which is still transcribed in untreated mutant embryos and which triggers compensatory mechanisms *via* mRNA-decay, will no longer be transcribed due to MO-induced gene knockout. If, on the other hand, the maternal zygotic mutant fish would compensate their deleterious mutation by

upregulation of related genes *via* alternative compensatory processes, which are not mRNA-decay induced, then the additional MO-knockdown specifically aimed for *nphp4* would show no effect in the treated mutants in comparison to their untreated siblings. However, the difference in phenotype frequency between treated wildtype fish and mutant fish, is undeniable as well as MO-treated mutants develop more glomerular and cloaca cysts than untreated mutant embryos. Considering this constellation, neither of the compensation scenarios can be fully observed, but compensation seems reasonably certain.

The compensation over two subsequent generations observed in *nphp4<sup>sa41188</sup>* mutants could be explained (as already suggested in 4.2) by the severely truncated mRNA, which is prone to mRNA-mediated decay-induced translational adaptation and which translates into a non-functional rather short protein fragment, raising the adaptational pressure. Both effects could promote the upregulation of compensating genes, which ameliorates the phenotypes in F2 and additionally protects the mutants in F2 from the impact, the absence of maternal wildtype RNA could have. The *nphp4* MO-knockdown has hardly any effect in *nphp4<sup>sa41188</sup>* mutants, as it does not interfere with the protein translation of compensatory genes. On the other side, the lack of MO-induced effects in *nphp4<sup>sa38686</sup>* mutants of the F2 generation, next to the staggering increase in glomerular and cloaca cyst formation in F2 compared to F1, cannot be explained by this theory. The worsening in F2 could be explained by the loss of maternally derived wildtype information, which could be damped less effectively this time, as the *nphp4<sup>sa38686</sup>* mutation is not as severely truncating and therefore less stimulation for compensatory processes. The reduced translational adaptation from F1 to F2 could again be related to less mRNA decay or less evolutionary pressure. As *nphp4* was knocked out using MOs in the *nphp4<sup>sa38686</sup>* mutation, the observed lack of MO-response, which is interpreted as sign of compensation, seems to be in contradiction with this actual observation being a lack of compensation. It could however be justified assuming the compensatory processes occurred in the F2 embryo itself only after the MO injection. The additional gene knockout could elevate the adaptational pressure in the F2 generation only and not in the F1 generation already, as it seems to be the case for the *nphp<sup>sa41188</sup>* mutation.

The effect of splice-blocking MO (SBM) and translation-blocking MO (TBM) on *nphp4* were comparable in my experiments. Even tough effects of SBM were shown to be less severe compared to TBM (Burcklé *et al.*, 2011, thesis of Friedemann Zaiser), my results are consistent with literature, since SBM do not interact with maternal mRNA (Draper *et al.*, 2001). In F2 maternal wildtype RNA is eliminated altogether, thereby cannot mask the effect of SBM and since both MOs perturb the expression of zygotic mRNA, the effects are equally pronounced.

#### 4.4 Ciliopathy phenotypes in zebrafish mutant lines with large deletions

Nephronophthisis is characterized by its phenotypic and genotypic heterogeneity. Some mutations in different *nphp* genes lead to severe phenotypes, while no clear genotype-phenotype correlation can be observed for some other mutant lines. These discrepancies are supposed to be attributed to genetic compensation to certain degree. Embryos with point mutations in *nphp* genes, causing a premature stop or the elimination of an essential splice site, keep up the translation of the mutated gene, resulting in fragments of the Nphp protein still being assembled. These defective mRNA fragments can trigger genetic compensation processes, as they are degraded by mRNA surveillance systems, setting off mRNA-decay induced transcriptional adaptation (TA) mechanism, being a recently described and highly investigated compensatory process (El-Brolosy et al., 2019; Rossi et al., 2015). A lot of questions around the exact mechanisms in this process, which modulate the expression of adapting genes and thereby compensate for some genetic mutations, remain open to this day. For example, what are the requirements for mutant mRNA degradation products to fulfill to trigger transcriptional adaptation? Why do some loss-of-function mutations induce translational adaptation, while others do not? The comparison of the transcriptional adaptation, which follows different mutations with different effects on the mRNA transcription, could help to gain greater insights into this process. The design of loss-of-function alleles using the CRISPR/Cas9 method, allows the study of transcriptional adaptation response to different kinds of mutations (Fig. 27) (Sztal and Stainier, 2020).

Our group set off to the task of using the CRISPR/Cas9 gene editing method to generate *nphp* mutations in zebrafish causing an early disruption of the open-reading frame (ORF). Selecting sgRNA target sequences in the first exons of *nphp1* and *nphp4*, successfully created zebrafish

lines, which are supposed to be prone to mRNA-decay induced genetic compensation as they still transcribe short mRNA fragments.

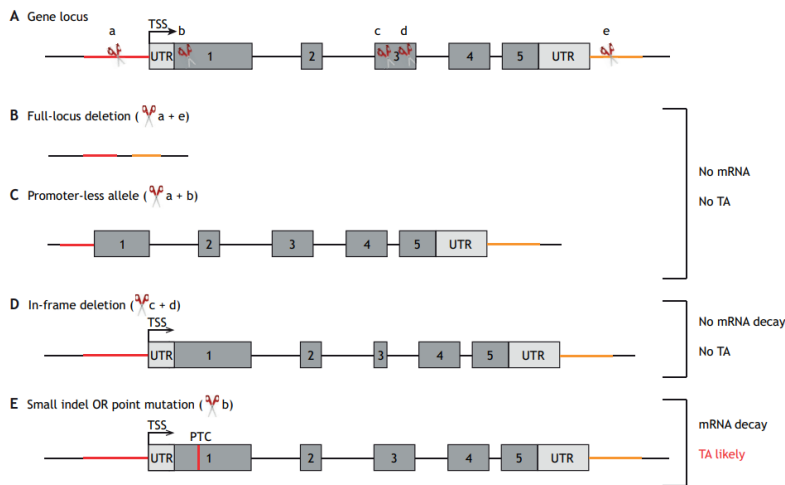


**Figure 27: How to avoid transcriptional adaptation (TA) when designing loss-of-function alleles.**

(A-D) When designing loss-of-function alleles for a given locus (A), several approaches can be used to avoid TA, including full-locus deletion (B), RNA-less alleles through deletion of promoter and/or regulatory elements (C), and in-frame deletions of important functional domains (D). (E) By contrast, small indels (insertions or deletions) or PTC-causing point mutations introduced early in the coding sequence often cause mutant mRNA decay (Lindeboom, Supek and Lehner, 2016; Hoek *et al.*, 2019), and thus are more likely to induce TA. Note that in-frame deletions (D) can cause No-Go decay. (Sztal and Stainier, 2020)

### 4.3.1 *nphp4-ex1-del5*

Unfortunately, since no data for the F1 generation could be collected due to difficulties in sequencing, no direct comparison between F1 and F2 can be made. However, the observations of the ciliopathy associated phenotypes in maternal zygotic mutant embryos in F2 allows for some hypotheses being put forward. Firstly, as the homozygote mutants (m/m) still present significantly more cloaca and glomerular cysts than their wildtype (+/+) siblings, no complete compensation seems to have occurred in F2. If compensation had occurred to a lesser degree from one generation to the next one, it could only be evaluated in a direct intergenerational comparison. Secondly, the observation made for *nphp4<sup>sa38686</sup>* and *nphp4<sup>sa41188</sup>*, that the more severely truncating mutation tends to be better compensated in F2, proves to be true for *nphp4-ex1-del5* as well. Glomerular cysts occurred in mutants of *nphp4<sup>sa38686</sup>* in 5.9%, *nphp4<sup>sa41188</sup>* in 4.8% and in *nphp4-ex1-del5* in 3.2%. In this respect, one can suggest, that even a mutated protein, truncated after 44 aa already, is likely to be degraded and that the resulting decay fragments might trigger a translational adaptation response. This compensation would also be consistent with the fact that *nphp4-ex1-del5* mutants in F2, are no different from their wildtype siblings in regard of abnormal heat-looping, abnormal body curvature, heart edema or hydrocephalus formation. *Nphp4<sup>sa38686</sup>* and

*nphp4*<sup>sa41188</sup> mutants on the other hand showed significantly more abnormal heart-looping and hydrocephalus formation compared to their wildtype siblings.

The additional knockdown of the *nphp4* gene by translation blocking MO (TBM) in *nphp4-ex1-del5* embryos of the F2 generation, led to a constellation which supports the hypothesis of compensation even further. Mutants revealed to be largely resistant to the injection of TBM, developing only a fraction of glomerular and cloaca cysts observed in treated wildtype fish. However, like it was already the case for *nphp4*<sup>sa38686</sup> and *nphp4*<sup>sa41188</sup> as well, treated mutants still developed significantly more cystic malformations than their untreated mutant siblings. So, on the one hand a compensation in mutants is reasonably certain, on the other hand this compensation cannot be fully explained by upregulation of unrelated genes, which are not affected by the *nphp4* TBM, because the TBM still has visible effects.

#### 4.3.2 *nphp1-ex15-del4*

As several studies showed that *nphp1* and *nphp4* gene products colocalize to the primary cilium and physically interact (Delous et al., 2009; Mollet et al., 2002). Mutations in *nphp4* were shown to play a role in nephronophthisis and cloaca development (Slanchev et al., 2011), therefore the study of the consequences, which mutations in *nphp1* might have, seemed interesting as well. Besides mutations in *nphp1* were described as to be the most prevalent in humans, making up to 21% of the cases (Hildebrandt et al., 2009). Unfortunately, no point mutations in *nphp1* have been identified in in mutagenesis screens so far and thus no zebrafish carrying point mutations in this gene were available. The generation of a new mutant line with the CRISPR/Cas9 gene editing method was done by our group, yielding the *nphp1-ex15-del4* mutant line. Even though, Slanchev et al. showed that the MO-induced knockdown of *nphp1* did not cause cloaca malformation at a significant level, in my experiments, homozygote mutant fish developed more cloaca cysts (7.6-fold) compared to their wildtype siblings, but the difference was not significant either. Even one mutant allele was enough to cause cloaca cysts in heterozygote fish at an intermediate frequency, although the difference to the wildtype controls not being significant.

Homozygote mutant (m/m) fish showed significantly more glomerular cysts (6.3-fold) than wildtype controls, but an overall frequency of 2.7% seems rather low, considering the frequency of glomerular cysts in F1 (m/m) mutants of the *nphp2*, *nphp4* and *nphp8* mutant lines ranged from 12.5% to 28.1%. The observed renal-limited effect of *nphp1* disruption, is consistent with the purely renal manifestations of nephronophthisis caused by *nphp1* mutations in human patients (Hildebrandt et al., 1997b). The MO-mediated knockdown of *nphp1* however caused around 20% dilated pronephric ducts (Slanchev et al., 2011). This phenotypic discrepancy between morphants

and mutants is consistent with current literature, where researchers noticed that the MO induced knockdown of genes in zebrafish (morphants) caused more phenotypes than could be observed in fish carrying mutations of these genes (mutants) (El-Brolosy et al., 2019; Rossi et al., 2015). As the *nphp1-ex15-del4* mutation causes the insertion of a premature stop codon only after amino acid 463 out of 667, leaving almost 70% of the protein intact, this low impact on glomerular and cloaca development, could be assigned to either the residual function of the mutant transcript or to the mRNA decay induced transcriptional adaptation, or even to a combination of both. According to the theory set up earlier, this mutation leaving most of the protein intact and lacking phenotypes in F1, could have more severe consequences in the F2 generation, like it was observed for *nphp4<sup>sa38686</sup>*. For this to prove to be true, more homozygote (m/m) fish would have to be raised and in-crossed to generate an F2 generation in future studies.

#### **4.4 The CRISPR/Cas9 method can be used to generate new loss-of-function mutants**

The CRISPR/Cas9 technology allows for site-specific modifications by taking advantage of the RNA-dependent recognition of specific DNA sequences and the thereby guided Cas9 endonuclease activity. The Cas9 induced double strand breaks (DSB) are repaired, in the absence of a repair template, by the endogenous repair mechanism of non-homologous end joining (NHEJ), which is prone to cause small insertions and/or deletions (indels) into the DNA strand. If these indels are introduced into exons, they could lead to a frame shift of the open-reading frame and install a premature termination codon. If these alterations however are avoided in transcription by alternative splicing, alternative initiation- or termination sites or if they do not cause any frame shift or premature stop codon insertion, the function of the protein might be conserved through an isoform. Subsequently no conclusions could be drawn on the gene's loss of function in this case. CRISPR/Cas9 mutations, which are expected to disrupt gene function, can also fail to do produce null alleles, if the mutant mRNA is prone to non-sense mediated decay, which can induce genetic compensation (Anderson et al., 2017; Tuladhar et al., 2019).

The odds of generating loss-of-function mutants become higher, when two target sites at opposite sides of the DNA strand are targeted simultaneously by injecting two different sgRNAs at the same time. This could be causing the elimination of a sequence, spanning over several exons or even a whole gene (Kim and Zhang, 2020). The sequence in between these two target sites gets cut out and as I have targeted the first and the last exon of the *nphp2* gene, most of the reading frame is eliminated and the gene's function gets severely disrupted. The creation of zebrafish lines with elimination an entire *nphp* gene, including the respective promotor region, could even be assumed

to be unavailable for compensatory mechanisms linked to the decay of residual mRNA fragments altogether (Fig. 27) (El-Brolosy et al., 2019).

In my attempt to create a loss-of-function mutation of the *nphp2* gene, I observed the successful deletion in 6 out of 28 colonies (21.4%) of *E. coli*, transformed with the vector containing the genomic PCR products of cumulated F0 injected fish. The length of the deletions ranged from 59 851 to 59 861 base pairs (bp) and were all mediated by the same two sgRNAs targeting the first and the last exon of the *nphp2* gene (*nphp2\_prm\_sgRNA1* and *nphp2\_ex18\_sgRNA12*). For future analysis of this newly created mutation, these two sgRNAs should be injected together with Cas9 into wildtype fish. Possible F0 founder fish should be identified by fin clipping and sequencing their genomic DNA. If the mutation is heritable and found in founder fish, they should be raised and outcrossed with wildtype fish, as soon as they reach a reproductive age. If the mutation has successfully entered the germline, the resulting F1 would be heterozygote carriers of the mutation. Homozygote F2 fish, could then finally be screened for phenotypic abnormalities. This efficient germline transmission of such large deletions can be expected to be found in around 5% of the F1 fish (Kim and Zhang, 2020). As the elimination of the promotor region was not possible due to the lack of suitable target sites, the mutated allele is neither a promotor-less allele nor a full-locus deletion and the residual protein translation could possibly lead to mRNA decay and subsequently to transcriptional adaptation (Fig. 27).

The interpretation of such mutations with extensive deletions, should in any case be done with consideration of the fact, that the eliminated sequence does not only include exons, which are coding for the protein in the end, but also intron sequences, which hold information for important factors for transcriptional regulation of the targeted gene but also potentially unrelated genes (Anderson et al., 2017). Anderson et al. therefore pleaded to preferably generate non-sense or indel-mutations in strategically chosen loci, instead of large deletions, to be able to make reliable conclusions about the function of a gene or a genetic region of interest (Zhang et al., 2020).

It is not possible to make predictions on the effect of the mutation generated in this work, simply by analyzing deletions caused by CRISPR/Cas9 editing on mRNA level. Whether this large deletion, providing that it would enter the germline, will reveal itself to trigger transcriptional adaptation or whether it impairs the translational adaptation of unrelated genes, which are all limiting factors to the generation and interpretation of large *nphp2* knockout mutants by the applied approach, will have to be addressed in future studies.

## 4.5 Conclusion

To summarize my findings made by the analysis of ciliopathy-associated phenotypes in zebrafish lines carrying one of these *nphp* mutations, one can say, three things; Firstly, no consistent genotype-phenotype correlation could be observed in F1 mutants, when comparing phenotypes to reports of other model systems or MO-derived knockdown experiments. This was especially true for *nphp2* mutants. Secondly, mutations leaving most of the Nphp protein intact tend to result in a low frequency of glomerular cysts and cloaca malformation in the first generation but are prone to cause more severe phenotypes in the second generation, in which maternal wildtype products are missing altogether. On the other hand, mutations truncating the Nphp protein more severely or affecting the splicing process of the pre-mRNA at an earlier stage, leaving very little functional protein behind, seem to cause a great deal of phenotypes in the first generation, which become rarer one generation later. This inverse relationship of mutational severity and phenotypic expression over two subsequent generations could be explained by several theories, the most promising one seeming to be transcriptional adaptation. The decay of altered Nphp proteins by non-sense mediated decay seems to trigger the upregulation of related genes to a certain degree. This compensation, and thereby thirdly, could be corroborated by MO-derived gene knockdown experiments. However, as the additional gene knockdown experiments showed, the upregulation of related genes cannot be responsible for the compensatory effect on its own, as the *nphp* knockdown still had an effect on mutant fish. These auxiliary compensatory processes will have to be further investigated in the future, as well as the identification of factors involved in this transcriptional adaptation. The presence of potential gene modifiers could help to explain the varying penetrance and expressivity of different mutations and thereby conceivably lead the way to novel therapeutic approaches. By manipulating the protein structure or expression levels of these modifiers one could amplify transcriptional adaptation by promoting the upregulation of compensating genes and by that lessen the phenotypic effects of mutations and the concomitant disease burden in patients.

Even though the use of zebrafish as a model for a human disease, like nephronophthisis, requires a greater degree of abstraction than the use of other mammalian and therefore evolutionary more closely related models, the insights made in my experiments might contribute to a greater understanding of the pathogenicity of different mutations in *nphp* genes and the associated compensatory processes. My hope is that my findings might one day be proven beneficial for treatment of nephronophthisis in human patients.



## 5. German summary / Zusammenfassung

Die Nephronophthise (NPH) ist eine seltene genetische Nierenerkrankung mit einem autosomal-rezessivem Vererbungsmuster. Sie stellt die häufigste genetische Ursache für ein terminales Nierenversagen im Kindes- und frühen Erwachsenenalter dar. Bisher hat man Mutationen in mehr als 25 verschiedenen NPHP Genen mit der NPH in Verbindung bringen können.

In dieser Doktorarbeit wurde anhand des Zebrafisches, verschiedene chemisch-induzierte Punktmutationen in den *nphp1*, *nphp2*, *nphp4* und *nphp8* Genen untersucht. Mutierte Zebrafische wurden auf das Auftreten von glomerulären Zysten und zystischen Fehlbildungen der Kloaka hin untersucht. Die in Studien beschriebene Diskrepanz im Auftreten von pathologischen Phänotypen bei Fischen, welche mit einem Morpholino Oligonukleotid (MO) zur gezielten Depletion von einem spezifischen *nphp* Gen behandelt wurden, verglichen mit solchen, die eine Punktmutation im gleichen Gen aufwiesen und weniger stark betroffen schienen, sorgte für das Aufkommen der Hypothese einer sogenannten „genetischen Robustheit“. Diese Kompensationsmechanismen in mutierten Fischen scheinen durch Degradationsprozesse von mRNA ausgelöst zu werden, ein Prozess, der bei den MO-behandelten Fischen fehlt. Die Annahme, dass diese Fähigkeit zur Kompensation von einer Generation auf die nächste weitervererbt werden könne, konnte in dieser Arbeit bestätigt werden. Der direkte Vergleich zweier Generationen (F1 vs. F2) zeigte eine Reduktion im Auftreten von Phänotypen in F2, woraufhin auf eine gewisse Kompensation geschlossen werden kann. Träger von schwerwiegenderen Mutationen zeigten tendenziell mehr pathologische Phänotypen in F1, jedoch aufgrund von effektiveren Kompensationsprozessen weniger Phänotypen in F2 als Träger von leichteren Mutationen, welche die Proteine weniger stark verkürzen. Mutationen im *nphp8* Gen, welche auch beim Menschen mit einer besonders schweren Symptomatik einhergehen, zeigten eine geringere Fähigkeit zur Kompensation als Mutationen im *nphp4* Gen. Durch MO-Depletion von *nphp4* konnte ein Hochregulieren der Transkription von verwandten Genen, als möglicher Kompensationsmechanismus bestätigt werden, da mutierte Fische in F2 gegen die Gen-Depletion resistent schienen.

Zusätzlich zu den Punktmutationen, wurden auch Fischlinien mit weitreichenden Mutationen in den *nphp1* und *nphp4* Genen, welche mit Hilfe der CRISPR/Cas9 Methode generiert wurden, auf deren phänotypisches Auftreten und Fähigkeit zur Kompensation hin untersucht. Die Arbeitshypothese von zumindest teilweise kompensierenden, durch den Abbau mutierter Genprodukte ausgelösten Mechanismen, konnte auch hier untermauert werden. Die CRISPR/Cas9 Methode wurde zudem in dieser Arbeit eingesetzt, um eine neue “loss-of-function” Mutation im *nphp2* Gen zu schaffen. Diese Mutation steht somit zukünftigen Forschungsvorhaben zur Verfügung.

## **6. Acknowledgments**

I want to express my special gratitude to Prof. Gerd Walz for providing me with the great opportunity to be part of one of his research projects in the department of nephrology. Without his expert advice and supervision this work would not have been possible.

I am also particularly grateful to Dr. Toma Yakulov for his experienced guidance and kind support during my time in the lab, as well as during the process of writing this thesis.

Furthermore, I want to thank Prof. Martin Moser for taking on the position of the second reviewer.

My sincere thanks also go to the whole AG Walz, especially to Annette Schmitt and Carina Kramer, for their unfailing assistance and friendliness, as well as to my fellow labmates Friedemann, Hannah, Clara, Konstantin and Luna for the good-humored atmosphere and helpful discussions in the lab.

Finally, I would like to thank my parents, Annette and Pit, my sister, Lis, and my girlfriend, Julie, for their unconditional support and encouragement. I remain gratefully in their debt.

## 7. References

- Ableitner, O., 2022. Introduction to Molecular Biology, 1st ed. Springer.
- Abrams, E.W., Mullins, M.C., 2009. Early zebrafish development: It's in the maternal genes. *Curr. Opin. Genet. Dev.*, Pattern formation and developmental mechanisms 19, 396–403. <https://doi.org/10.1016/j.gde.2009.06.002>
- Acevedo-Arozena, A., Wells, S., Potter, P., Kelly, M., Cox, R.D., Brown, S.D.M., 2008. ENU mutagenesis, a way forward to understand gene function. *Annu. Rev. Genomics Hum. Genet.* 9, 49–69. <https://doi.org/10.1146/annurev.genom.9.081307.164224>
- Adamson, K.I., Sheridan, E., Grierson, A.J., 2018. Use of zebrafish models to investigate rare human disease. *J. Med. Genet.* 55, 641–649. <https://doi.org/10.1136/jmedgenet-2018-105358>
- Ahmadi, A., Rad, N.K., Ezzatizadeh, V., Moghadasali, R., 2020. Kidney Regeneration: Stem Cells as a New Trend. *Curr. Stem Cell Res. Ther.* 15, 263–283. <https://doi.org/10.2174/1574888X15666191218094513>
- Airik, R., Kispert, A., 2007. Down the tube of obstructive nephropathies: The importance of tissue interactions during ureter development. *Kidney Int.* 72, 1459–1467. <https://doi.org/10.1038/sj.ki.5002589>
- Al-Awqati, Q., Oliver, J.A., 2002. Stem cells in the kidney. *Kidney Int.* 61, 387–395. <https://doi.org/10.1046/j.1523-1755.2002.00164.x>
- Aleström, P., D'Angelo, L., Midtlyng, P.J., Schorderet, D.F., Schulte-Merker, S., Sohm, F., Warner, S., 2020. Zebrafish: Housing and husbandry recommendations. *Lab. Anim.* 54, 213–224. <https://doi.org/10.1177/0023677219869037>
- Amsterdam, A., Hopkins, N., 2006. Mutagenesis strategies in zebrafish for identifying genes involved in development and disease. *Trends Genet.* 22, 473–478. <https://doi.org/10.1016/j.tig.2006.06.011>
- Analytical Methods Committee AMCTB No.59, 2014. PCR – the polymerase chain reaction. *Anal Methods* 6, 333–336. <https://doi.org/10.1039/C3AY90101G>
- Anderson, J.L., Mulligan, T.S., Shen, M.-C., Wang, H., Scahill, C.M., Tan, F.J., Du, S.J., Busch-Nentwich, E.M., Farber, S.A., 2017. mRNA processing in mutant zebrafish lines generated by chemical and CRISPR-mediated mutagenesis produces unexpected transcripts that escape nonsense-mediated decay. *PLOS Genet.* 13, e1007105. <https://doi.org/10.1371/journal.pgen.1007105>
- Antignac, C., Arduy, C.H., Beckmann, J.S., Benessy, F., Gros, F., Medhioub, M., Hildebrandt, F., Dufier, J.-L., Kleinknecht, C., Broyer, M., Weissenbach, J., Habib, R., Cohen, D., 1993. A gene for familial juvenile nephronophthisis (recessive medullary cystic kidney disease) maps to chromosome 2p. *Nat. Genet.* 3, 342–345. <https://doi.org/10.1038/ng0493-342>
- Arts, H.H., Doherty, D., Beersum, S.E.C. van, Parisi, M.A., Letteboer, S.J.F., Gorden, N.T., Peters, T.A., Märker, T., Voesenek, K., Kartono, A., Ozyurek, H., Farin, F.M., Kroes, H.Y., Wolfrum, U., Brunner, H.G., Cremers, F.P.M., Glass, I.A., Knoers, N.V.A.M., Roepman, R., 2007. Mutations in the gene encoding the basal body protein RPGRIP1L, a nephrocystin-4 interactor, cause Joubert syndrome. *Nat. Genet.* 39, 882–888. <https://doi.org/10.1038/ng2069>
- Barrangou, R., Fremaux, C., Deveau, H., Richards, M., Boyaval, P., Moineau, S., Romero, D.A., Horvath, P., 2007. CRISPR Provides Acquired Resistance Against Viruses in Prokaryotes. *Science* 315, 1709–1712. <https://doi.org/10.1126/science.1138140>
- Baumgaertel, M.W., Kraemer, M., Berlitz, P., 2014. Chapter 24 - Neurologic complications of acute and chronic renal disease, in: Biller, J., Ferro, J.M. (Eds.), *Handbook of Clinical Neurology, Neurologic Aspects of Systemic Disease Part I*. Elsevier, pp. 383–393. <https://doi.org/10.1016/B978-0-7020-4086-3.00024-2>

- Bertram, J.F., Douglas-Denton, R.N., Diouf, B., Hughson, M.D., Hoy, W.E., 2011. Human nephron number: implications for health and disease. *Pediatr. Nephrol.* 26, 1529–1533. <https://doi.org/10.1007/s00467-011-1843-8>
- Bhaya, D., Davison, M., Barrangou, R., 2011. CRISPR-Cas systems in bacteria and archaea: versatile small RNAs for adaptive defense and regulation. *Annu. Rev. Genet.* 45, 273–297. <https://doi.org/10.1146/annurev-genet-110410-132430>
- Birtel, J., Spital, G., Book, M., Habbig, S., Bäumner, S., Riehmer, V., Beck, B.B., Rosenkranz, D., Bolz, H.J., Dahmer-Heath, M., Herrmann, P., König, J., Issa, P.C., 2021. NPHP1 gene-associated nephronophthisis is associated with an occult retinopathy. *Kidney Int.* 100, 1092–1100. <https://doi.org/10.1016/j.kint.2021.06.012>
- Borgal, L., Habbig, S., Hatzold, J., Liebau, M.C., Dafinger, C., Sacarea, I., Hammerschmidt, M., Benzing, T., Schermer, B., 2012. The ciliary protein nephrocystin-4 translocates the canonical Wnt regulator Jade-1 to the nucleus to negatively regulate  $\beta$ -catenin signaling. *J. Biol. Chem.* 287, 25370–25380. <https://doi.org/10.1074/jbc.M112.385658>
- Brouns, S.J.J., Jore, M.M., Lundgren, M., Westra, E.R., Slijkhuys, R.J.H., Snijders, A.P.L., Dickman, M.J., Makarova, K.S., Koonin, E.V., van der Oost, J., 2008. Small CRISPR RNAs Guide Antiviral Defense in Prokaryotes. *Science* 321, 960–964. <https://doi.org/10.1126/science.1159689>
- Burcklé, C., Gaudé, H.-M., Vesque, C., Silbermann, F., Salomon, R., Jeanpierre, C., Antignac, C., Saunier, S., Schneider-Maunoury, S., 2011. Control of the Wnt pathways by nephrocystin-4 is required for morphogenesis of the zebrafish pronephros. *Hum. Mol. Genet.* 20, 2611–2627. <https://doi.org/10.1093/hmg/ddr164>
- Cardenas-Rodriguez, M., Badano, J.L., 2009. Ciliary biology: Understanding the cellular and genetic basis of human ciliopathies. *Am. J. Med. Genet. C Semin. Med. Genet.* 151C, 263–280. <https://doi.org/10.1002/ajmg.c.30227>
- Caridi, G., Murer, L., Bellantuono, R., Sorino, P., Caringella, D.A., Gusmano, R., Ghiggeri, G.M., 1998. Renal-retinal syndromes: association of retinal anomalies and recessive nephronophthisis in patients with homozygous deletion of the NPH1 locus. *Am. J. Kidney Dis. Off. J. Natl. Kidney Found.* 32, 1059–1062. [https://doi.org/10.1016/s0272-6386\(98\)70083-6](https://doi.org/10.1016/s0272-6386(98)70083-6)
- Chakrabarty, B., Parekh, N., 2022. Sequence and Structure-Based Analyses of Human Ankyrin Repeats. *Molecules* 27, 423. <https://doi.org/10.3390/molecules27020423>
- Chou, Q., Russell, M., Birch, D.E., Raymond, J., Bloch, W., 1992. Prevention of pre-PCR mispriming and primer dimerization improves low-copy-number amplifications. *Nucleic Acids Res.* 20, 1717–1723. <https://doi.org/10.1093/nar/20.7.1717>
- Costantini, F., 2006. Renal branching morphogenesis: concepts, questions, and recent advances. *Differentiation* 74, 402–421. <https://doi.org/10.1111/j.1432-0436.2006.00106.x>
- Costantini, F., Kopan, R., 2010. Patterning a Complex Organ: Branching Morphogenesis and Nephron Segmentation in Kidney Development. *Dev. Cell* 18, 698–712. <https://doi.org/10.1016/j.devcel.2010.04.008>
- Datta, P., Cribbs, J.T., Seo, S., 2021. Differential requirement of NPHP1 for compartmentalized protein localization during photoreceptor outer segment development and maintenance. *PLOS ONE* 16, e0246358. <https://doi.org/10.1371/journal.pone.0246358>
- Delous, M., Baala, L., Salomon, R., Laclef, C., Vierkotten, J., Tory, K., Golzio, C., Lacoste, T., Besse, L., Ozilou, C., Moutkine, I., Hellman, N.E., Anselme, I., Silbermann, F., Vesque, C., Gerhardt, C., Rattenberry, E., Wolf, M.T.F., Gubler, M.C., Martinovic, J., Encha-Razavi, F., Boddaert, N., Gonzales, M., Macher, M.A., Nivet, H., Champion, G., Berthéléme, J.P., Niaudet, P., McDonald, F., Hildebrandt, F., Johnson, C.A., Vekemans, M., Antignac, C., Rütther, U., Schneider-Maunoury, S., Attié-Bitach, T., Saunier, S., 2007. The ciliary gene RPGRIP1L is mutated in cerebello-oculo-renal syndrome (Joubert

- syndrome type B) and Meckel syndrome. *Nat. Genet.* 39, 875–881.  
<https://doi.org/10.1038/ng2039>
- Delous, M., Hellman, N.E., Gaudé, H.-M., Silbermann, F., Le Bivic, A., Salomon, R., Antignac, C., Saunier, S., 2009. Nephrocystin-1 and nephrocystin-4 are required for epithelial morphogenesis and associate with PALS1/PATJ and Par6. *Hum. Mol. Genet.* 18, 4711–4723. <https://doi.org/10.1093/hmg/ddp434>
- Deltcheva, E., Chylinski, K., Sharma, C.M., Gonzales, K., Chao, Y., Pirzada, Z.A., Eckert, M.R., Vogel, J., Charpentier, E., 2011. CRISPR RNA maturation by trans-encoded small RNA and host factor RNase III. *Nature* 471, 602–607. <https://doi.org/10.1038/nature09886>
- Deveau, H., Barrangou, R., Garneau, J.E., Labonté, J., Fremaux, C., Boyaval, P., Romero, D.A., Horvath, P., Moineau, S., 2008. Phage Response to CRISPR-Encoded Resistance in *Streptococcus thermophilus*. *J. Bacteriol.* <https://doi.org/10.1128/JB.01412-07>
- Diep, C.Q., Peng, Z., Ukah, T.K., Kelly, P.M., Daigle, R.V., Davidson, A.J., 2015. Development of the zebrafish mesonephros. *genesis* 53, 257–269. <https://doi.org/10.1002/dvg.22846>
- Donaldson, J.C., Dempsey, P.J., Reddy, S., Bouton, A.H., Coffey, R.J., Hanks, S.K., 2000. Crk-Associated Substrate p130Cas Interacts with Nephrocystin and Both Proteins Localize to Cell–Cell Contacts of Polarized Epithelial Cells. *Exp. Cell Res.* 256, 168–178. <https://doi.org/10.1006/excr.2000.4822>
- Draper, B.W., Morcos, P.A., Kimmel, C.B., 2001. Inhibition of zebrafish fgf8 pre-mRNA splicing with morpholino oligos: A quantifiable method for gene knockdown. *genesis* 30, 154–156. <https://doi.org/10.1002/gene.1053>
- Dressler, G.R., 2006. The Cellular Basis of Kidney Development. *Annu. Rev. Cell Dev. Biol.* 22, 509–529. <https://doi.org/10.1146/annurev.cellbio.22.010305.104340>
- Driever, W., Solnica-Krezel, L., Schier, A.F., Neuhauss, S.C.F., Malicki, J., Stemple, D.L., Stainier, D.Y., Zwartkruis, F.J.T., Abdelilah, S., Rangini, Z., Belak, J., Boggs, C., 1996. A genetic screen for mutations affecting embryogenesis in zebrafish. *Development* 123, 47–46. <https://doi.org/10.5167/uzh-215>
- Drummond, I., 2003. Making a zebrafish kidney: a tale of two tubes. *Trends Cell Biol.* 13, 357–365. [https://doi.org/10.1016/S0962-8924\(03\)00124-7](https://doi.org/10.1016/S0962-8924(03)00124-7)
- Drummond, I.A., 2000. The zebrafish pronephros: a genetic system for studies of kidney development. *Pediatr. Nephrol.* 14, 428–435. <https://doi.org/10.1007/s004670050788>
- Drummond, I.A., Majumdar, A., Hentschel, H., Elger, M., Solnica-Krezel, L., Schier, A.F., Neuhauss, S.C., Stemple, D.L., Zwartkruis, F., Rangini, Z., Driever, W., Fishman, M.C., 1998. Early development of the zebrafish pronephros and analysis of mutations affecting pronephric function. *Development* 125, 4655–4667. <https://doi.org/10.1242/dev.125.23.4655>
- Eisen, J.S., Smith, J.C., 2008. Controlling morpholino experiments: don't stop making antisense. *Development* 135, 1735–1743. <https://doi.org/10.1242/dev.001115>
- El-Brolosy, M.A., Kontarakis, Z., Rossi, A., Kuenne, C., Günther, S., Fukuda, N., Kikhi, K., Boezio, G.L.M., Takacs, C.M., Lai, S.-L., Fukuda, R., Gerri, C., Giraldez, A.J., Stainier, D.Y.R., 2019. Genetic compensation triggered by mutant mRNA degradation. *Nature* 568, 193–197. <https://doi.org/10.1038/s41586-019-1064-z>
- El-Brolosy, M.A., Stainier, D.Y.R., 2017. Genetic compensation: A phenomenon in search of mechanisms. *PLOS Genet.* 13, e1006780. <https://doi.org/10.1371/journal.pgen.1006780>
- Fliegauf, M., Benzing, T., Omran, H., 2007. When cilia go bad: cilia defects and ciliopathies. *Nat. Rev. Mol. Cell Biol.* 8, 880–893. <https://doi.org/10.1038/nrm2278>
- Gagnadoux, M.F., Bacri, J.L., Broyer, M., Habib, R., 1989. Infantile chronic tubulo-interstitial nephritis with cortical microcysts: variant of nephronophthisis or new disease entity? *Pediatr. Nephrol.* 3, 50–55. <https://doi.org/10.1007/BF00859626>
- Garneau, J.E., Dupuis, M.-È., Villion, M., Romero, D.A., Barrangou, R., Boyaval, P., Fremaux, C., Horvath, P., Magadán, A.H., Moineau, S., 2010. The CRISPR/Cas bacterial immune

- system cleaves bacteriophage and plasmid DNA. *Nature* 468, 67–71.  
<https://doi.org/10.1038/nature09523>
- Gerke, N., Hellberg, A., 2013. Eppendorf Application Note 289 6.
- Gerlach, G.F., Wingert, R.A., 2013. Kidney organogenesis in the zebrafish: insights into vertebrate nephrogenesis and regeneration. *WIREs Dev. Biol.* 2, 559–585.  
<https://doi.org/10.1002/wdev.92>
- Gerner, M., Haribaskar, R., Pütz, M., Czerwitzki, J., Walz, G., Schäfer, T., 2010. The retinitis pigmentosa GTPase regulator interacting protein 1 (RPGRIP1) links RPGR to the nephronophthisis protein network. *Kidney Int.* 77, 891–896.  
<https://doi.org/10.1038/ki.2010.27>
- Goetz, S.C., Anderson, K.V., 2010. The primary cilium: a signalling centre during vertebrate development. *Nat. Rev. Genet.* 11, 331–344. <https://doi.org/10.1038/nrg2774>
- Gupta, S., Ozimek-Kulik, J.E., Phillips, J.K., 2021. Nephronophthisis-Pathobiology and Molecular Pathogenesis of a Rare Kidney Genetic Disease. *Genes* 12, 1762.  
<https://doi.org/10.3390/genes12111762>
- Haas, P., Gilmour, D., 2006. Chemokine Signaling Mediates Self-Organizing Tissue Migration in the Zebrafish Lateral Line. *Dev. Cell* 10, 673–680.  
<https://doi.org/10.1016/j.devcel.2006.02.019>
- Haffter, P., Granato, M., Brand, M., Mullins, M.C., Hammerschmidt, M., Kane, D.A., Odenthal, J., van Eeden, F.J., Jiang, Y.J., Heisenberg, C.P., Kelsh, R.N., Furutani-Seiki, M., Vogelsang, E., Beuchle, D., Schach, U., Fabian, C., Nusslein-Volhard, C., 1996a. The identification of genes with unique and essential functions in the development of the zebrafish, *Danio rerio*. *Development* 123, 1–36. <https://doi.org/10.1242/dev.123.1.1>
- Haffter, P., Granato, M., Brand, M., Mullins, M.C., Hammerschmidt, M., Kane, D.A., Odenthal, J., van Eeden, F.J., Jiang, Y.J., Heisenberg, C.P., Kelsh, R.N., Furutani-Seiki, M., Vogelsang, E., Beuchle, D., Schach, U., Fabian, C., Nüsslein-Volhard, C., 1996b. The identification of genes with unique and essential functions in the development of the zebrafish, *Danio rerio*. *Dev. Camb. Engl.* 123, 1–36.
- Hannema, S.E., Hughes, I.A., 2007. Regulation of Wolffian Duct Development. *Horm. Res. Paediatr.* 67, 142–151. <https://doi.org/10.1159/000096644>
- Hildebrandt, F., Attanasio, M., Otto, E., 2009. Nephronophthisis: Disease Mechanisms of a Ciliopathy. *J. Am. Soc. Nephrol.* 20, 23–35. <https://doi.org/10.1681/ASN.2008050456>
- Hildebrandt, F., Otto, E., Rensing, C., Nothwang, H.G., Vollmer, M., Adolphs, J., Hanusch, H., Brandis, M., 1997a. A novel gene encoding an SH3 domain protein is mutated in nephronophthisis type 1. *Nat. Genet.* 17, 149–153. <https://doi.org/10.1038/ng1097-149>
- Hildebrandt, F., Singh-Sawhney, I., Schnieders, B., Centofante, L., Omran, H., Pohlmann, A., Schmaltz, C., Wedekind, H., Schubotz, C., Antignac, C., Weber, J.L., Brandis, M., 1993. Mapping of a gene for familial juvenile nephronophthisis: Refining the map and defining flanking markers on chromosome 2. *Am. J. Hum. Genet.* 53, 1256–1261.
- Hildebrandt, F., Strahm, B., Nothwang, H.-G., Gretz, N., Schnieders, B., Singh-Sawhney, I., Kutt, R., Vollmer, M., Brandis, M., Members of the APN Study Group, 1997b. Molecular genetic identification of families with juvenile nephronophthisis type 1: Rate of progression to renal failure. *Kidney Int.* 51, 261–269.  
<https://doi.org/10.1038/ki.1997.31>
- Hildebrandt, F., Zhou, W., 2007. Nephronophthisis-Associated Ciliopathies. *J. Am. Soc. Nephrol.* 18, 1855–1871. <https://doi.org/10.1681/ASN.2006121344>
- Hoefele, J., Sudbrak, R., Reinhardt, R., Lehrack, S., Hennig, S., Imm, A., Muerb, U., Utsch, B., Attanasio, M., O’Toole, J.F., Otto, E., Hildebrandt, F., 2005. Mutational analysis of the NPHP4 gene in 250 patients with nephronophthisis. *Hum. Mutat.* 25, 411–411.  
<https://doi.org/10.1002/humu.9326>

- Hoff, S., Halbritter, J., Epting, D., Frank, V., Nguyen, T.-M.T., van Reeuwijk, J., Boehlke, C., Schell, C., Yasunaga, T., Helmstädter, M., Mergen, M., Filhol, E., Boldt, K., Horn, N., Ueffing, M., Otto, E.A., Eisenberger, T., Elting, M.W., van Wijk, J.A.E., Bockenbauer, D., Sebire, N.J., Rittig, S., Vyberg, M., Ring, T., Pohl, M., Pape, L., Neuhaus, T.J., Elshakhs, N.A.S., Koon, S.J., Harris, P.C., Grahammer, F., Huber, T.B., Kuehn, E.W., Kramer-Zucker, A., Bolz, H.J., Roepman, R., Saunier, S., Walz, G., Hildebrandt, F., Bergmann, C., Lienkamp, S.S., 2013. ANKS6 is a central component of a nephronophthisis module linking NEK8 to INVS and NPHP3. *Nat. Genet.* 45, 951–956. <https://doi.org/10.1038/ng.2681>
- Horsfield, J., Ramachandran, A., Reuter, K., LaVallie, E., Collins-Racie, L., Crosier, K., Crosier, P., 2002. Cadherin-17 is required to maintain pronephric duct integrity during zebrafish development. *Mech. Dev.* 115, 15–26. [https://doi.org/10.1016/S0925-4773\(02\)00094-1](https://doi.org/10.1016/S0925-4773(02)00094-1)
- Howe, K., Clark, M.D., Torroja, C.F., Torrance, J., Berthelot, C., Muffato, M., Collins, J.E., Humphray, S., McLaren, K., Matthews, L., McLaren, S., Sealy, I., Caccamo, M., Churcher, C., Scott, C., Barrett, J.C., Koch, R., Rauch, G.-J., White, S., Chow, W., Kilian, B., Quintais, L.T., Guerra-Assunção, J.A., Zhou, Y., Gu, Y., Yen, J., Vogel, J.-H., Eyre, T., Redmond, S., Banerjee, R., Chi, J., Fu, B., Langley, E., Maguire, S.F., Laird, G.K., Lloyd, D., Kenyon, E., Donaldson, S., Sehra, H., Almeida-King, J., Loveland, J., Trevanion, S., Jones, M., Quail, M., Willey, D., Hunt, A., Burton, J., Sims, S., McLay, K., Plumb, B., Davis, J., Clee, C., Oliver, K., Clark, R., Riddle, C., Elliott, D., Threadgold, G., Harden, G., Ware, D., Begum, S., Mortimore, B., Kerry, G., Heath, P., Phillimore, B., Tracey, A., Corby, N., Dunn, M., Johnson, C., Wood, J., Clark, S., Pelan, S., Griffiths, G., Smith, M., Glithero, R., Howden, P., Barker, N., Lloyd, C., Stevens, C., Harley, J., Holt, K., Panagiotidis, G., Lovell, J., Beasley, H., Henderson, C., Gordon, D., Auger, K., Wright, D., Collins, J., Raisen, C., Dyer, L., Leung, K., Robertson, L., Ambridge, K., Leongamornlert, D., McGuire, S., Gilderthorp, R., Griffiths, C., Manthavadi, D., Nichol, S., Barker, G., Whitehead, S., Kay, M., Brown, J., Murnane, C., Gray, E., Humphries, M., Sycamore, N., Barker, D., Saunders, D., Wallis, J., Babbage, A., Hammond, S., Mashreghi-Mohammadi, M., Barr, L., Martin, S., Wray, P., Ellington, A., Matthews, N., Ellwood, M., Woodmansey, R., Clark, G., Cooper, J.D., Tromans, A., Grafham, D., Skuce, C., Pandian, R., Andrews, R., Harrison, E., Kimberley, A., Garnett, J., Fosker, N., Hall, R., Garner, P., Kelly, D., Bird, C., Palmer, S., Gehring, I., Berger, A., Dooley, C.M., Ersan-Ürün, Z., Eser, C., Geiger, H., Geisler, M., Karotki, L., Kirn, A., Konantz, J., Konantz, M., Oberländer, M., Rudolph-Geiger, S., Teucke, M., Lanz, C., Raddatz, G., Osoegawa, K., Zhu, B., Rapp, A., Widaa, S., Langford, C., Yang, F., Schuster, S.C., Carter, N.P., Harrow, J., Ning, Z., Herrero, J., Searle, S.M.J., Enright, A., Geisler, R., Plasterk, R.H.A., Lee, C., Westerfield, M., de Jong, P.J., Zon, L.I., Postlethwait, J.H., Nüsslein-Volhard, C., Hubbard, T.J.P., Crollius, H.R., Rogers, J., Stemple, D.L., 2013. The zebrafish reference genome sequence and its relationship to the human genome. *Nature* 496, 498–503. <https://doi.org/10.1038/nature12111>
- Howe, K.L., Achuthan, P., Allen, James, Allen, Jamie, Alvarez-Jarreta, J., Amode, M.R., Armean, I.M., Azov, A.G., Bennett, R., Bhai, J., Billis, K., Boddu, S., Charkhchi, M., Cummins, C., Da Rin Fioretto, L., Davidson, C., Dodiya, K., El Houdaigui, B., Fatima, R., Gall, A., Garcia Giron, C., Grego, T., Guijarro-Clarke, C., Haggerty, L., Hemrom, A., Hourlier, T., Izuogu, O.G., Juettemann, T., Kaikala, V., Kay, M., Lavidas, I., Le, T., Lemos, D., Gonzalez Martinez, J., Marugán, J.C., Maurel, T., McMahan, A.C., Mohanan, S., Moore, B., Muffato, M., Oheh, D.N., Paraschas, D., Parker, A., Parton, A., Prosovetskaia, I., Sakthivel, M.P., Salam, A.I.A., Schmitt, B.M., Schuilenburg, H., Sheppard, D., Steed, E., Szpak, M., Szuba, M., Taylor, K., Thormann, A., Threadgold, G., Walts, B., Winterbottom, A., Chakiachvili, M., Chaubal, A., De Silva, N., Flint, B., Frankish, A., Hunt, S.E., Iisley, G.R., Langridge, N., Loveland, J.E., Martin, F.J., Mudge,

- J.M., Morales, J., Perry, E., Ruffier, M., Tate, J., Thybert, D., Trevanion, S.J., Cunningham, F., Yates, A.D., Zerbino, D.R., Flicek, P., 2021. Ensembl 2021. *Nucleic Acids Res.* 49, D884–D891. <https://doi.org/10.1093/nar/gkaa942>
- Hoy, W.E., Bertram, J.F., Denton, R.D., Zimanyi, M., Samuel, T., Hughson, M.D., 2008. Nephron number, glomerular volume, renal disease and hypertension. *Curr. Opin. Nephrol. Hypertens.* 17, 258–265. <https://doi.org/10.1097/MNH.0b013e3282f9b1a5>
- Hsu, P.D., Lander, E.S., Zhang, F., 2014. Development and Applications of CRISPR-Cas9 for Genome Engineering. *Cell* 157, 1262–1278. <https://doi.org/10.1016/j.cell.2014.05.010>
- Hu, P., Zhao, X., Zhang, Q., Li, W., Zu, Y., 2018. Comparison of Various Nuclear Localization Signal-Fused Cas9 Proteins and Cas9 mRNA for Genome Editing in Zebrafish. *G3 GenesGenomesGenetics* 8, 823–831. <https://doi.org/10.1534/g3.117.300359>
- Huang, S., Hirota, Y., Sawamoto, K., 2009. Various facets of vertebrate cilia: motility, signaling, and role in adult neurogenesis. *Proc. Jpn. Acad. Ser. B* 85, 324–336. <https://doi.org/10.2183/pjab.85.324>
- Hwang, W.Y., Fu, Y., Reyon, D., Maeder, M.L., Tsai, S.Q., Sander, J.D., Peterson, R.T., Yeh, J.-R.J., Joung, J.K., 2013. Efficient genome editing in zebrafish using a CRISPR-Cas system. *Nat. Biotechnol.* 31, 227–229. <https://doi.org/10.1038/nbt.2501>
- Izant, J.G., Weintraub, H., 1985. Constitutive and conditional suppression of exogenous and endogenous genes by anti-sense RNA. *Science* 229, 345–352. <https://doi.org/10.1126/science.2990048>
- Jansen, Ruud., Embden, Jan.D.A. van, Gaastra, Wim., Schouls, Leo.M., 2002. Identification of genes that are associated with DNA repeats in prokaryotes. *Mol. Microbiol.* 43, 1565–1575. <https://doi.org/10.1046/j.1365-2958.2002.02839.x>
- Jensen, V.L., Li, C., Bowie, R.V., Clarke, L., Mohan, S., Blacque, O.E., Leroux, M.R., 2015. Formation of the transition zone by Mks5/Rpgr1L establishes a ciliary zone of exclusion (CIZE) that compartmentalises ciliary signalling proteins and controls PIP2 ciliary abundance. *EMBO J.* 34, 2537–2556. <https://doi.org/10.15252/embj.201488044>
- Jiang, F., Doudna, J.A., 2017. CRISPR-Cas9 Structures and Mechanisms. *Annu. Rev. Biophys.* 46, 505–529. <https://doi.org/10.1146/annurev-biophys-062215-010822>
- Jinek, M., Chylinski, K., Fonfara, I., Hauer, M., Doudna, J.A., Charpentier, E., 2012. A Programmable Dual-RNA-Guided DNA Endonuclease in Adaptive Bacterial Immunity. *Science*. <https://doi.org/10.1126/science.1225829>
- Joung, J.K., Sander, J.D., 2013. TALENs: a widely applicable technology for targeted genome editing. *Nat. Rev. Mol. Cell Biol.* 14, 49–55. <https://doi.org/10.1038/nrm3486>
- Karlsson, J., von Hofsten, J., Olsson, P.E., 2001. Generating transparent zebrafish: a refined method to improve detection of gene expression during embryonic development. *Mar. Biotechnol. N. Y. N* 3, 522–527. <https://doi.org/10.1007/s1012601-0053-4>
- Kayser, N., Zaiser, F., Veenstra, A.C., Wang, H., Göcmen, B., Eckert, P., Franz, H., Köttgen, A., Walz, G., Yakulov, T.A., 2022. Clock genes rescue nphp mutations in zebrafish. *Hum. Mol. Genet.* [ddac160](https://doi.org/10.1093/hmg/ddac160). <https://doi.org/10.1093/hmg/ddac160>
- Kelly, D.M., Anders, H.-J., Bello, A.K., Choukroun, G., Coppo, R., Dreyer, G., Eckardt, K.-U., Johnson, D.W., Jha, V., Harris, D.C.H., Levin, A., Lunney, M., Luyckx, V., Marti, H.-P., Messa, P., Mueller, T.F., Saad, S., Stengel, B., Vanholder, R.C., Weinstein, T., Khan, M., Zaidi, D., Osman, M.A., Ye, F., Tonelli, M., Okpechi, I.G., Rondeau, E., 2021. International Society of Nephrology Global Kidney Health Atlas: structures, organization, and services for the management of kidney failure in Western Europe. *Kidney Int. Suppl.* 11, e106–e118. <https://doi.org/10.1016/j.kisu.2021.01.007>
- Khoshdel Rad, N., Aghdami, N., Moghadasali, R., 2020. Cellular and Molecular Mechanisms of Kidney Development: From the Embryo to the Kidney Organoid. *Front. Cell Dev. Biol.* 8.



- Kim, B.H., Zhang, G., 2020. Generating Stable Knockout Zebrafish Lines by Deleting Large Chromosomal Fragments Using Multiple gRNAs. *G3 GenesGenomesGenetics* 10, 1029–1037. <https://doi.org/10.1534/g3.119.401035>
- Kok, F.O., Shin, M., Ni, C.-W., Gupta, A., Grosse, A.S., van Impel, A., Kirchmaier, B.C., Peterson-Maduro, J., Kourkoulis, G., Male, I., DeSantis, D.F., Sheppard-Tindell, S., Ebarasi, L., Betsholtz, C., Schulte-Merker, S., Wolfe, S.A., Lawson, N.D., 2015. Reverse genetic screening reveals poor correlation between Morpholino-induced and mutant phenotypes in zebrafish. *Dev. Cell* 32, 97–108. <https://doi.org/10.1016/j.devcel.2014.11.018>
- Korbie, D.J., Mattick, J.S., 2008. Touchdown PCR for increased specificity and sensitivity in PCR amplification. *Nat. Protoc.* 3, 1452–1456. <https://doi.org/10.1038/nprot.2008.133>
- Kramer-Zucker, A.G., Olale, F., Haycraft, C.J., Yoder, B.K., Schier, A.F., Drummond, I.A., 2005. Cilia-driven fluid flow in the zebrafish pronephros, brain and Kupffer's vesicle is required for normal organogenesis. *Development* 132, 1907–1921. <https://doi.org/10.1242/dev.01772>
- Kurochkina, N., Guha, U., 2012. SH3 domains: modules of protein–protein interactions. *Biophys. Rev.* 5, 29–39. <https://doi.org/10.1007/s12551-012-0081-z>
- Labun, K., Montague, T.G., Krause, M., Torres Cleuren, Y.N., Tjeldnes, H., Valen, E., 2019. CHOPCHOP v3: expanding the CRISPR web toolbox beyond genome editing. *Nucleic Acids Res.* 47, W171–W174. <https://doi.org/10.1093/nar/gkz365>
- Ledford, H., Callaway, E., 2020. Pioneers of revolutionary CRISPR gene editing win chemistry Nobel. *Nature* 586, 346–347. <https://doi.org/10.1038/d41586-020-02765-9>
- Lee, P.Y., Costumbrado, J., Hsu, C.-Y., Kim, Y.H., 2012. Agarose Gel Electrophoresis for the Separation of DNA Fragments. *JoVE J. Vis. Exp.* e3923. <https://doi.org/10.3791/3923>
- Levine, M., Davidson, E.H., 2005. Gene regulatory networks for development. *Proc. Natl. Acad. Sci.* 102, 4936–4942. <https://doi.org/10.1073/pnas.0408031102>
- Lieschke, G.J., Currie, P.D., 2007. Animal models of human disease: zebrafish swim into view. *Nat. Rev. Genet.* 8, 353–367. <https://doi.org/10.1038/nrg2091>
- Lindström, N.O., McMahon, J.A., Guo, J., Tran, T., Guo, Q., Rutledge, E., Parvez, R.K., Saribekyan, G., Schuler, R.E., Liao, C., Kim, A.D., Abdelhalim, A., Ruffins, S.W., Thornton, M.E., Basking, L., Grubbs, B., Kesselman, C., McMahon, A.P., 2018. Conserved and Divergent Features of Human and Mouse Kidney Organogenesis. *J. Am. Soc. Nephrol.* 29, 785–805. <https://doi.org/10.1681/ASN.2017080887>
- Lüllmann-Rauch, R., Asan, E., 2019. Harnorgane, in: Lüllmann-Rauch, R., Asan, E. (Eds.), *Taschenlehrbuch Histologie*. Georg Thieme Verlag. <https://doi.org/10.1055/b-006-163361>
- Luo, F., Tao, Y.-H., 2018. Nephronophthisis: A review of genotype–phenotype correlation. *Nephrology* 23, 904–911. <https://doi.org/10.1111/nep.13393>
- Lykke-Andersen, S., Jensen, T.H., 2015. Nonsense-mediated mRNA decay: an intricate machinery that shapes transcriptomes. *Nat. Rev. Mol. Cell Biol.* 16, 665–677. <https://doi.org/10.1038/nrm4063>
- Mahuzier, A., Gaudé, H.-M., Grampa, V., Anselme, I., Silbermann, F., Leroux-Berger, M., Delacour, D., Ezan, J., Montcouquiol, M., Saunier, S., Schneider-Maunoury, S., Vesque, C., 2012. Dishevelled stabilization by the ciliopathy protein Rpgrip11 is essential for planar cell polarity. *J. Cell Biol.* 198, 927–940. <https://doi.org/10.1083/jcb.201111009>
- Makarova, K.S., Wolf, Y.I., Alkhnbashi, O.S., Costa, F., Shah, S.A., Saunders, S.J., Barrangou, R., Brouns, S.J.J., Charpentier, E., Haft, D.H., Horvath, P., Moineau, S., Mojica, F.J.M., Terns, R.M., Terns, M.P., White, M.F., Yakunin, A.F., Garrett, R.A., van der Oost, J., Backofen, R., Koonin, E.V., 2015. An updated evolutionary classification of CRISPR–Cas systems. *Nat. Rev. Microbiol.* 13, 722–736. <https://doi.org/10.1038/nrmicro3569>

- Marlow, F.L., 2010. Maternal Control of Development in Vertebrates, No. 1. ed, Maternal Control of Development in Vertebrates: My Mother Made Me Do It!, Colloquium Series on Developmental Biology. Morgan & Claypool Life Sciences.
- McConnachie, D.J., Stow, J.L., Mallett, A.J., 2021. Ciliopathies and the Kidney: A Review. *Am. J. Kidney Dis.* 77, 410–419. <https://doi.org/10.1053/j.ajkd.2020.08.012>
- McMahon, A.P., 2016. Development of the Mammalian Kidney. *Curr. Top. Dev. Biol.* 117, 31–64. <https://doi.org/10.1016/bs.ctdb.2015.10.010>
- Mochizuki, T., Saijoh, Y., Tsuchiya, K., Shirayoshi, Y., Takai, S., Taya, C., Yonekawa, H., Yamada, K., Nihei, H., Nakatsuji, N., Overbeek, P.A., Hamada, H., Yokoyama, T., 1998. Cloning of inv, a gene that controls left/right asymmetry and kidney development. *Nature* 395, 177–181. <https://doi.org/10.1038/26006>
- Mojica, F.J.M., Díez-Villaseñor, C., García-Martínez, J., Almendros, C.Y., 2009. Short motif sequences determine the targets of the prokaryotic CRISPR defence system. *Microbiology* 155, 733–740. <https://doi.org/10.1099/mic.0.023960-0>
- Mojica, F.J.M., Díez-Villaseñor, C., García-Martínez, J., Soria, E., 2005. Intervening Sequences of Regularly Spaced Prokaryotic Repeats Derive from Foreign Genetic Elements. *J. Mol. Evol.* 60, 174–182. <https://doi.org/10.1007/s00239-004-0046-3>
- Mollet, G., Salomon, R., Gribouval, O., Silbermann, F., Bacq, D., Landthaler, G., Milford, D., Nayir, A., Rizzoni, G., Antignac, C., Saunier, S., 2002. The gene mutated in juvenile nephronophthisis type 4 encodes a novel protein that interacts with nephrocystin. *Nat. Genet.* 32, 300–305. <https://doi.org/10.1038/ng996>
- Mollet, G., Silbermann, F., Delous, M., Salomon, R., Antignac, C., Saunier, S., 2005. Characterization of the nephrocystin/nephrocystin-4 complex and subcellular localization of nephrocystin-4 to primary cilia and centrosomes. *Hum. Mol. Genet.* 14, 645–656. <https://doi.org/10.1093/hmg/ddi061>
- Morales, E.E., Wingert, R.A., 2017. Zebrafish as a Model of Kidney Disease, in: Miller, R.K. (Ed.), *Kidney Development and Disease, Results and Problems in Cell Differentiation*. Springer International Publishing, Cham, pp. 55–75. [https://doi.org/10.1007/978-3-319-51436-9\\_3](https://doi.org/10.1007/978-3-319-51436-9_3)
- Morgan, D., Eley, L., Sayer, J., Strachan, T., Yates, L.M., Craighead, A.S., Goodship, J.A., 2002. Expression analyses and interaction with the anaphase promoting complex protein Apc2 suggest a role for inversin in primary cilia and involvement in the cell cycle. *Hum. Mol. Genet.* 11, 3345–3350. <https://doi.org/10.1093/hmg/11.26.3345>
- Moulton, J.D., 2017a. Using Morpholinos to Control Gene Expression. *Curr. Protoc. Nucleic Acid Chem.* 68, 4.30.1-4.30.29. <https://doi.org/10.1002/cpnc.21>
- Moulton, J.D., 2017b. Making a Morpholino Experiment Work: Controls, Favoring Specificity, Improving Efficacy, Storage, and Dose, in: Moulton, H.M., Moulton, J.D. (Eds.), *Morpholino Oligomers: Methods and Protocols, Methods in Molecular Biology*. Springer, New York, NY, pp. 17–29. [https://doi.org/10.1007/978-1-4939-6817-6\\_2](https://doi.org/10.1007/978-1-4939-6817-6_2)
- Nakayama, T., Blitz, I.L., Fish, M.B., Odeleye, A.O., Manohar, S., Cho, K.W.Y., Grainger, R.M., 2014. Chapter Seventeen - Cas9-Based Genome Editing in *Xenopus tropicalis*, in: Doudna, J.A., Sontheimer, E.J. (Eds.), *Methods in Enzymology, The Use of CRISPR/Cas9, ZFNs, and TALENs in Generating Site-Specific Genome Alterations*. Academic Press, pp. 355–375. <https://doi.org/10.1016/B978-0-12-801185-0.00017-9>
- Nasevicius, A., Ekker, S.C., 2000. Effective targeted gene ‘knockdown’ in zebrafish. *Nat. Genet.* 26, 216–220. <https://doi.org/10.1038/79951>
- Nauli, S.M., Alenghat, F.J., Luo, Y., Williams, E., Vassilev, P., Li, X., Elia, A.E.H., Lu, W., Brown, E.M., Quinn, S.J., Ingber, D.E., Zhou, J., 2003. Polycystins 1 and 2 mediate mechanosensation in the primary cilium of kidney cells. *Nat. Genet.* 33, 129–137. <https://doi.org/10.1038/ng1076>

- Nowak, M.A., Boerlijst, M.C., Cooke, J., Smith, J.M., 1997. Evolution of genetic redundancy. *Nature* 388, 167–171. <https://doi.org/10.1038/40618>
- Oates, A.C., Bruce, A.E.E., Ho, R.K., 2000. Too Much Interference: Injection of Double-Stranded RNA Has Nonspecific Effects in the Zebrafish Embryo. *Dev. Biol.* 224, 20–28. <https://doi.org/10.1006/dbio.2000.9761>
- Otto, E., Hoefele, J., Ruf, R., Mueller, A.M., Hiller, K.S., Wolf, M.T.F., Schuermann, M.J., Becker, A., Birkenhäger, R., Sudbrak, R., Hennies, H.C., Nürnberg, P., Hildebrandt, F., 2002. A Gene Mutated in Nephronophthisis and Retinitis Pigmentosa Encodes a Novel Protein, Nephroretinin, Conserved in Evolution. *Am. J. Hum. Genet.* 71, 1161–1167. <https://doi.org/10.1086/344395>
- Otto, E.A., Schermer, B., Obara, T., O’Toole, J.F., Hiller, K.S., Mueller, A.M., Ruf, R.G., Hoefele, J., Beekmann, F., Landau, D., Foreman, J.W., Goodship, J.A., Strachan, T., Kispert, A., Wolf, M.T., Gagnadoux, M.F., Nivet, H., Antignac, C., Walz, G., Drummond, I.A., Benzing, T., Hildebrandt, F., 2003. Mutations in INVS encoding inversin cause nephronophthisis type 2, linking renal cystic disease to the function of primary cilia and left-right axis determination. *Nat. Genet.* 34, 413–420. <https://doi.org/10.1038/ng1217>
- Parichy, D.M., 2015. Advancing biology through a deeper understanding of zebrafish ecology and evolution. *eLife* 4, e05635. <https://doi.org/10.7554/eLife.05635>
- Pelegri, F., 2003. Maternal factors in zebrafish development. *Dev. Dyn.* 228, 535–554. <https://doi.org/10.1002/dvdy.10390>
- Perantoni, A.O., 2003. Renal development: perspectives on a Wnt-dependent process. *Semin. Cell Dev. Biol., Kidney Development* 14, 201–208. [https://doi.org/10.1016/S1084-9521\(03\)00022-3](https://doi.org/10.1016/S1084-9521(03)00022-3)
- Perner, B., Englert, C., Bollig, F., 2007. The Wilms tumor genes *wt1a* and *wt1b* control different steps during formation of the zebrafish pronephros. *Dev. Biol.* 309, 87–96. <https://doi.org/10.1016/j.ydbio.2007.06.022>
- Praetorius, H.A., Spring, K.R., 2001. Bending the MDCK Cell Primary Cilium Increases Intracellular Calcium. *J. Membr. Biol.* 184, 71–79. <https://doi.org/10.1007/s00232-001-0075-4>
- Pyati, U.J., Cooper, M.S., Davidson, A.J., Nechiporuk, A., Kimelman, D., 2006. Sustained Bmp signaling is essential for cloaca development in zebrafish. *Dev. Camb. Engl.* 133, 2275–2284. <https://doi.org/10.1242/dev.02388>
- Reinard, T., 2021. *Molekularbiologische Methoden 2.0*, 3rd ed. Verlag Eugen Ulmer, Stuttgart.
- Rhoads, A.R., Friedberg, F., 1997. Sequence motifs for calmodulin recognition. *FASEB J.* 11, 331–340. <https://doi.org/10.1096/fasebj.11.5.9141499>
- Robu, M.E., Larson, J.D., Nasevicius, A., Beiraghi, S., Brenner, C., Farber, S.A., Ekker, S.C., 2007. p53 activation by knockdown technologies. *PLoS Genet.* 3, e78. <https://doi.org/10.1371/journal.pgen.0030078>
- Roepman, R., Letteboer, S.J.F., Arts, H.H., Beersum, S.E.C. van, Lu, X., Krieger, E., Ferreira, P.A., Cremers, F.P.M., 2005. Interaction of nephrocystin-4 and RPGRIP1 is disrupted by nephronophthisis or Leber congenital amaurosis-associated mutations. *Proc. Natl. Acad. Sci.* 102, 18520–18525. <https://doi.org/10.1073/pnas.0505774102>
- Rossi, A., Kontarakis, Z., Gerri, C., Nolte, H., Hölper, S., Krüger, M., Stainier, D.Y.R., 2015. Genetic compensation induced by deleterious mutations but not gene knockdowns. *Nature* 524, 230–233. <https://doi.org/10.1038/nature14580>
- Rothschild, S.C., Francescato, L., Drummond, I.A., Tombes, R.M., 2011. CaMK-II is a PKD2 target that promotes pronephric kidney development and stabilizes cilia. *Development* 138, 3387–3397. <https://doi.org/10.1242/dev.066340>
- Sang, L., Miller, J.J., Corbit, K.C., Giles, R.H., Brauer, M.J., Otto, E.A., Baye, L.M., Wen, X., Scales, S.J., Kwong, M., Huntzicker, E.G., Sfakianos, M.K., Sandoval, W., Bazan, J.F.,

- Kulkarni, P., Garcia-Gonzalo, F.R., Seol, A.D., O'Toole, J.F., Held, S., Reutter, H.M., Lane, W.S., Rafiq, M.A., Noor, A., Ansar, M., Devi, A.R.R., Sheffield, V.C., Slusarski, D.C., Vincent, J.B., Doherty, D.A., Hildebrandt, F., Reiter, J.F., Jackson, P.K., 2011. Mapping the NPHP-JBTS-MKS Protein Network Reveals Ciliopathy Disease Genes and Pathways. *Cell* 145, 513–528. <https://doi.org/10.1016/j.cell.2011.04.019>
- Schön, P., Tsuchiya, K., Lenoir, D., Mochizuki, T., Guichard, C., Takai, S., Maiti, A.K., Nihei, H., Weil, J., Yokoyama, T., Bouvagnet, P., 2002. Identification, genomic organization, chromosomal mapping and mutation analysis of the human INV gene, the ortholog of a murine gene implicated in left-right axis development and biliary atresia. *Hum. Genet.* 110, 157–165. <https://doi.org/10.1007/s00439-001-0655-5>
- Sedgwick, S.G., Smerdon, S.J., 1999. The ankyrin repeat: a diversity of interactions on a common structural framework. *Trends Biochem. Sci.* 24, 311–316. [https://doi.org/10.1016/s0968-0004\(99\)01426-7](https://doi.org/10.1016/s0968-0004(99)01426-7)
- Serluca, F.C., Fishman, M.C., 2001. Pre-pattern in the pronephric kidney field of zebrafish. *Dev. Camb. Engl.* 128, 2233–2241.
- Seroby, V., Kontarakis, Z., El-Brolosy, M.A., Welker, J.M., Tolstenkov, O., Saadeldein, A.M., Retzer, N., Gottschalk, A., Wehman, A.M., Stainier, D.Y., 2020. Transcriptional adaptation in *Caenorhabditis elegans*. *eLife* 9, e50014. <https://doi.org/10.7554/eLife.50014>
- Simons, M., Gloy, J., Ganner, A., Bullerkotte, A., Bashkurov, M., Krönig, C., Schermer, B., Benzing, T., Cabello, O.A., Jenny, A., Mlodzik, M., Polok, B., Driever, W., Obara, T., Walz, G., 2005. Inversin, the gene product mutated in nephronophthisis type II, functions as a molecular switch between Wnt signaling pathways. *Nat. Genet.* 37, 537–543. <https://doi.org/10.1038/ng1552>
- Slanchev, K., Pütz, M., Schmitt, A., Kramer-Zucker, A., Walz, G., 2011. Nephrocystin-4 is required for pronephric duct-dependent cloaca formation in zebrafish. *Hum. Mol. Genet.* 20, 3119–3128. <https://doi.org/10.1093/hmg/ddr214>
- Smith, K.A., Uribe, V., 2021. Getting to the Heart of Left–Right Asymmetry: Contributions from the Zebrafish Model. *J. Cardiovasc. Dev. Dis.* 8, 64. <https://doi.org/10.3390/jcdd8060064>
- Soliman, N.A., Hildebrandt, F., Otto, E.A., Nabhan, M.M., Allen, S.J., Badr, A.M., Sheba, M., Fadda, S., Gawdat, G., El-Kiky, H., 2012. Clinical Characterization and NPHP1 Mutations in Nephronophthisis and Associated Ciliopathies: A Single Center Experience. *Saudi J. Kidney Dis. Transplant. Off. Publ. Saudi Cent. Organ Transplant. Saudi Arab.* 23, 1090–1098. <https://doi.org/10.4103/1319-2442.100968>
- Song, Z., Zhang, X., Jia, S., Yelick, P.C., Zhao, C., 2016. Zebrafish as a Model for Human Ciliopathies. *J. Genet. Genomics* 43, 107–120. <https://doi.org/10.1016/j.jgg.2016.02.001>
- Spence, R., Gerlach, G., Lawrence, C., Smith, C., 2008. The behaviour and ecology of the zebrafish, *Danio rerio*. *Biol. Rev.* 83, 13–34. <https://doi.org/10.1111/j.1469-185X.2007.00030.x>
- Srivastava, S., Molinari, E., Raman, S., Sayer, J.A., 2018. Many Genes—One Disease? Genetics of Nephronophthisis (NPHP) and NPHP-Associated Disorders. *Front. Pediatr.* 5.
- Stainier, D.Y.R., Kontarakis, Z., Rossi, A., 2015. Making Sense of Anti-Sense Data. *Dev. Cell* 32, 7–8. <https://doi.org/10.1016/j.devcel.2014.12.012>
- Sternberg, S.H., Redding, S., Jinek, M., Greene, E.C., Doudna, J.A., 2014. DNA interrogation by the CRISPR RNA-guided endonuclease Cas9. *Nature* 507, 62–67. <https://doi.org/10.1038/nature13011>
- Stokman, M., Lilien, M., Knoers, N., 2016. Nephronophthisis, GeneReviews® [Internet]. University of Washington, Seattle.
- Sztaf, T.E., Stainier, D.Y.R., 2020. Transcriptional adaptation: a mechanism underlying genetic robustness. *Development* 147, dev186452. <https://doi.org/10.1242/dev.186452>

- Thisse, B., Thisse, C., 2014. In Situ Hybridization on Whole-Mount Zebrafish Embryos and Young Larvae, in: Nielsen, B.S. (Ed.), *In Situ Hybridization Protocols, Methods in Molecular Biology*. Springer, New York, NY, pp. 53–67. [https://doi.org/10.1007/978-1-4939-1459-3\\_5](https://doi.org/10.1007/978-1-4939-1459-3_5)
- Tory, K., Rousset-Rouvière, C., Gubler, M.-C., Morinière, V., Pawtowski, A., Becker, C., Guyot, C., Gié, S., Frishberg, Y., Nivet, H., Deschênes, G., Cochat, P., Gagnadoux, M.-F., Saunier, S., Antignac, C., Salomon, R., 2009. Mutations of NPHP2 and NPHP3 in infantile nephronophthisis. *Kidney Int.* 75, 839–847. <https://doi.org/10.1038/ki.2008.662>
- Truebestein, L., Leonard, T.A., 2016. Coiled-coils: The long and short of it. *Bioessays* 38, 903–916. <https://doi.org/10.1002/bies.201600062>
- Tuladhar, R., Yeu, Y., Tyler Piazza, J., Tan, Z., Rene Clemenceau, J., Wu, X., Barrett, Q., Herbert, J., Mathews, D.H., Kim, J., Hyun Hwang, T., Lum, L., 2019. CRISPR-Cas9-based mutagenesis frequently provokes on-target mRNA misregulation. *Nat. Commun.* 10, 4056. <https://doi.org/10.1038/s41467-019-12028-5>
- Urnov, F.D., Rebar, E.J., Holmes, M.C., Zhang, H.S., Gregory, P.D., 2010. Genome editing with engineered zinc finger nucleases. *Nat. Rev. Genet.* 11, 636–646. <https://doi.org/10.1038/nrg2842>
- Veelken, R., Ditting, T., 2018a. Aufgaben der Niere, in: Arastéh, K., Baenkler, H.-W., Bieber, C., Brandt, R., Chatterjee, T.T., Dill, T., Ditting, T., Duckert, M., Eich, W., Ernst, S., Fischer-Rasokat, U., Fischli, S., Fleck, R., Fritze, D., Fießl, H., Hahn, J.-M., Hamm, C., Harenberg, J., Hengstmann, J.H., Herzog, W., Hinkelbein, J., Hofmann, T., Holstege, A., Huck, K., Kähler, J., Keller, M., Kim, W.-K., Klingmüller, D., Knaevelsrud, I., Köster, R., Kuck, K.-H., Liebetrau, C., Löwe, B., Loßnitzer, N., Mann, W.A., Matzdorff, A., Müller-Tasch, T., Nienaber, C.A., Nikendei, C., Nürnberg, M., Pausch, J., Petzsch, M., Pfeifer, M., Rösch, W., Sauer, N., Schäfer, J., Scherbaum, H., Scheurich, C., Schlehofer, B., Schmidt, M., Schneider, H., Schöffauer, M., Schork, J., Schuchert, A., Schwab, M., Schweikert, H.-U., Spannagl, M., Stern, H., Stocker, H., Usadel, K.-H., Veelken, R., Voll, R.E., Wahl, P., Wißner, E., Zastrow, A., Zeuzem, S., Ziegler, R., Zipfel, S. (Eds.), *Duale Reihe Innere Medizin*. Georg Thieme Verlag KG. <https://doi.org/10.1055/b-005-145255>
- Veelken, R., Ditting, T., 2018b. Chronische/terminale Niereninsuffizienz, in: Arastéh, K., Baenkler, H.-W., Bieber, C., Brandt, R., Chatterjee, T.T., Dill, T., Ditting, T., Duckert, M., Eich, W., Ernst, S., Fischer-Rasokat, U., Fischli, S., Fleck, R., Fritze, D., Fießl, H., Hahn, J.-M., Hamm, C., Harenberg, J., Hengstmann, J.H., Herzog, W., Hinkelbein, J., Hofmann, T., Holstege, A., Huck, K., Kähler, J., Keller, M., Kim, W.-K., Klingmüller, D., Knaevelsrud, I., Köster, R., Kuck, K.-H., Liebetrau, C., Löwe, B., Loßnitzer, N., Mann, W.A., Matzdorff, A., Müller-Tasch, T., Nienaber, C.A., Nikendei, C., Nürnberg, M., Pausch, J., Petzsch, M., Pfeifer, M., Rösch, W., Sauer, N., Schäfer, J., Scherbaum, H., Scheurich, C., Schlehofer, B., Schmidt, M., Schneider, H., Schöffauer, M., Schork, J., Schuchert, A., Schwab, M., Schweikert, H.-U., Spannagl, M., Stern, H., Stocker, H., Usadel, K.-H., Veelken, R., Voll, R.E., Wahl, P., Wißner, E., Zastrow, A., Zeuzem, S., Ziegler, R., Zipfel, S. (Eds.), *Duale Reihe Innere Medizin*. Georg Thieme Verlag KG. <https://doi.org/10.1055/b-005-145255>
- Warburton-Pitt, S.R.F., Jauregui, A.R., Li, C., Wang, J., Leroux, M.R., Barr, M.M., 2012. Ciliogenesis in *Caenorhabditis elegans* requires genetic interactions between ciliary middle segment localized NPHP-2 (inversin) and transition zone-associated proteins. *J. Cell Sci.* 125, 2592–2603. <https://doi.org/10.1242/jcs.095539>
- Westerfield, M., 1995. *The zebrafish book: A guide for the laboratory use of zebrafish (Danio rerio)*, 3rd ed. University of Oregon Press, Eugene, OR.
- Wiedenheft, B., Sternberg, S.H., Doudna, J.A., 2012. RNA-guided genetic silencing systems in bacteria and archaea. *Nature* 482, 331–338. <https://doi.org/10.1038/nature10886>

- Williams, C.L., Li, C., Kida, K., Inglis, P.N., Mohan, S., Semenc, L., Bialas, N.J., Stupay, R.M., Chen, N., Blacque, O.E., Yoder, B.K., Leroux, M.R., 2011. MKS and NPHP modules cooperate to establish basal body/transition zone membrane associations and ciliary gate function during ciliogenesis. *J. Cell Biol.* 192, 1023–1041. <https://doi.org/10.1083/jcb.201012116>
- Wingert, R.A., Davidson, A.J., 2008. The zebrafish pronephros: A model to study nephron segmentation. *Kidney Int.* 73, 1120–1127. <https://doi.org/10.1038/ki.2008.37>
- Wolf, M.T.F., Hildebrandt, F., 2011. Nephronophthisis. *Pediatr. Nephrol.* 26, 181–194. <https://doi.org/10.1007/s00467-010-1585-z>
- Wolf, M.T.F., Saunier, S., O’Toole, J.F., Wanner, N., Groshong, T., Attanasio, M., Salomon, R., Stallmach, T., Sayer, J.A., Waldherr, R., Griebel, M., Oh, J., Neuhaus, T.J., Josefiak, U., Antignac, C., Otto, E.A., Hildebrandt, F., 2007. Mutational analysis of the RPGRIP1L gene in patients with Joubert syndrome and nephronophthisis. *Kidney Int.* 72, 1520–1526. <https://doi.org/10.1038/sj.ki.5002630>
- Yasunaga, T., Hoff, S., Schell, C., Helmstädter, M., Kretz, O., Kuechlin, S., Yakulov, T.A., Engel, C., Müller, B., Bensch, R., Ronneberger, O., Huber, T.B., Lienkamp, S.S., Walz, G., 2015. The polarity protein Inturned links NPHP4 to Daam1 to control the subapical actin network in multiciliated cells. *J. Cell Biol.* 211, 963–973. <https://doi.org/10.1083/jcb.201502043>
- Yokoyama, T., Copeland, N.G., Jenkins, N.A., Montgomery, C.A., Elder, F.F.B., Overbeek, P.A., 1993. Reversal of Left-Right Asymmetry: a Situs Inversus Mutation. *Science.* <https://doi.org/10.1126/science.8480178>
- Zhang, Q., Fu, Y., Thakur, C., Bi, Z., Wadgaonkar, P., Qiu, Y., Xu, L., Rice, M., Zhang, W., Almutairy, B., Chen, F., 2020. CRISPR-Cas9 gene editing causes alternative splicing of the targeting mRNA. *Biochem. Biophys. Res. Commun.* 528, 54–61. <https://doi.org/10.1016/j.bbrc.2020.04.145>

## 8. Publication

The results of this thesis have partly been published in July 2022 by *Human Molecular Genetics* in the publication entitled “Clock genes rescue *nphp* mutations in zebrafish”. The corresponding Pubmed entry is:

Kayser N, Zaiser F, Veenstra AC, Wang H, Göcmen B, Eckert P, Franz H, Köttgen A, Walz G, Yakulov TA. Clock genes rescue *nphp* mutations in zebrafish. *Hum Mol Genet.* 2022 Jul 21;ddac160. doi: 10.1093/hmg/ddac160. Epub ahead of print. PMID: 35861640.

Authors: Nicolas Kayser<sup>1\*</sup>, Friedemann Zaiser<sup>1\*</sup>, Anna C. Veenstra<sup>1\*</sup>, Hui Wang<sup>1\*</sup>, Burulca Göcmen<sup>2</sup>, Priska Eckert<sup>1</sup>, Henriette Franz<sup>3</sup>, Anna Köttgen<sup>2</sup>, Gerd Walz<sup>1,4</sup> and Toma A. Yakulov<sup>1</sup>

<sup>1</sup>Renal Division, University Freiburg Medical Center, Faculty of Medicine, Hugstetter Str. 55, Freiburg 79106, Germany

<sup>2</sup>Institute of Genetic Epidemiology, Faculty of Medicine and Medical Center, University of Freiburg, Freiburg 79106, Germany

<sup>3</sup>Department of Biomedicine, University of Basel, Pestalozzistr. 20, Basel CH-4056, Switzerland

<sup>4</sup>Signalling Research Centres BIOSS and CIBSS, University of Freiburg, Albertstrasse 19, Freiburg 79104, Germany

\* Nicolas Kayser, Friedemann Zaiser, Anna C. Veenstra And Hui Wang share the first authorship.

## 9. Appendix

### 9.1 Abbreviations

<b>abbreviation</b>	<b>meaning</b>
aa	amino acid
ATL	ascending thin limb (of the loop of Henle)
bp	base pair
Cas9	CRISPR associated protein 9
cdh17	cadherin 17
CKD	chronic kidney disease
cldnb	claudin b
cm	centimeter
CRISPR	clustered regularly interspaced short palindromic repeats
crRNA	CRISPR RNA
DBS	double strand break
ddH <sub>2</sub> O	double distilled Water
DNA	desoxyribonucleic acid
dpf	days post fertilization
e.g.	exempli gratia
EGFP	enhanced green fluorescent protein
ENU	N-ethyl-N-nitrosurea
ESDR	end-stage renal disease
ESRD	end stage renal disease
GFP	green fluorescent protein
gRNA	guide RNA
HDR	homology-directed repair
hpf	hours post fertilization
JBS	Joubert syndrome
LB	lysogeny broth
LCA	Leber congenital amaurosis
MKS	Meckel-Gruber syndrome
MO	Morpholino
mRNA	messenger ribonucleic acid
NHEJ	non-homologous end-joining
NPH	nephronophthisis
Nphp	nephronophthisis protein
nphp	nephronophthisis protein gene
PAM	protospacer adjacent motif
PCR	polymerase chain reaction
RNA	ribonucleic acid
rpm	rounds per minute
SBM	splice blocking morpholino
sgRNA	single guide RNA
SLS	Senior-Løken syndrome
SOC	super optimal broth with catabolite repression
TAE	tris-acetat-EDTA-electrophoresis buffer
TALEN	trans-activator like effector nuclease



TBM	translation blocking morpholino
tracrRNA	trans-activating crRNA
UTR	untranslated region
wt	wild type
wt1b	WT1 transcription factor b
ZFN	zinc finger nuclease

## 9.2 List of tables

Table 1: List of chemicals.....	30
Table 2: List of enzymes and biological reagents.....	31
Table 3: List of bacteria.....	31
Table 4: List of kits.....	31
Table 5: List of consumables.....	31
Table 6: Ingredients for Danieau’s solution (30x).....	32
Table 7: Ingredients of Danieau’s solution (0.3x).....	32
Table 8: Ingredients of 1-phenyl-2-thiourea (PTU) solution.....	33
Table 9: Ingredients for 0.4% Tricaine solution.....	33
Table 10: Ingredients for Tris-HCL 1M, pH=7.5.....	33
Table 11: Recipe of Ethylenediaminetetraacetate (EDTA) 0.5M.....	33
Table 12: Ingredients for 50x TAE Buffer.....	34
Table 13: List of primers for PCR and sequencing.....	34
Table 14: List oligonucleotides used for sgRNA construction.....	35
Table 15: List of MOs.....	35
Table 16: List of hardware.....	35
Table 17: List of software.....	36
Table 18: List of transgenic zebrafish lines.....	39
Table 19: List of mutant fish lines and their transgenic outcrosses.....	39
Table 20: Settings for touchdown PCR.....	41
Table 21: Settings for PCR with KOD Hot Start DNA Polymerase.....	43
Table 22: Setting for Colony PCR.....	44
Table 23: Injection solutions for sgRNA microinjections.....	48

### 9.3 List of figures

Figure 1: Metanephric and pronephric nephrons share a similar segmentation pattern).....	11
Figure 2: Structures of conventional DNA and morpholino oligonucleotides .....	23
Figure 3: Gene knock-down by MOs.....	24
Figure 4: The CRISPR/Cas adaptive immune system .....	27
Figure 5: CRISPR/Cas9 target binding and cleavage, followed by endogenous repair mechanisms.....	29
Figure 6: Scheme of the zebrafish pairing strategy .....	53
Figure 7: Glomerular and cloaca cyst formation of F1 and F2 <i>nphp2</i> <sup>sa36157</sup> mutant fish.....	55
Figure 8: Ciliopathy associated phenotypes in F2 <i>nphp2</i> <sup>sa36157</sup> mutant fish .....	56
Figure 9: Glomerular and cloaca cyst formation of F1 and F2 <i>nphp4</i> <sup>sa41188</sup> mutant fish .....	58
Figure 10: Ciliopathy associated phenotypes in F2 <i>nphp4</i> <sup>sa41188</sup> mutant fish .....	59
Figure 11: Glomerular and cloaca cyst formation of F1 and F2 <i>nphp4</i> <sup>sa38686</sup> mutant fish .....	60
Figure 12: Ciliopathy associated phenotypes in F2 <i>nphp4</i> <sup>sa38686</sup> mutant fish .....	61
Figure 13: Glomerular and cloaca cyst formation of F1 and F2 <i>nphp8</i> <sup>sa24730</sup> mutant fish.....	63
Figure 14: Ciliopathy associated phenotypes in F2 <i>nphp8</i> <sup>sa10096</sup> mutant fish .....	64
Figure 15: Glomerular and cloaca cyst formation of F1 and F2 <i>nphp8</i> <sup>sa10096</sup> mutant fish.....	65
Figure 16: Ciliopathy associated phenotypes in F2 <i>nphp8</i> <sup>sa10096</sup> mutant fish .....	66
Figure 17: MO induced knockdown of <i>nphp4</i> <sup>sa41188</sup> in maternal zygotic mutants .....	68
Figure 18: MO-induced knockdown of <i>nphp4</i> <sup>sa38686</sup> in maternal zygotic mutants .....	70
Figure 19: Glomerular and cloaca cyst formation in F2 <i>nphp4-ex1-del5</i> mutant fish.....	72
Figure 20: Ciliopathy associated phenotypes in F2 <i>nphp4-ex1-del5</i> mutant fish.....	73
Figure 21: MO-induced knockdown of <i>nphp4-ex1-del5</i> in maternal zygotic mutants.....	75
Figure 22: Glomerular and cloaca cyst formation in F1 <i>nphp1-ex15-del4</i> mutant fish.....	77
Figure 23: sgRNA target selection for CRISPR/Cas9 mutation of <i>nphp2</i> .....	78
Figure 24: Electrophoresis gel showing PCR products of genomic DNA from sgRNA-injected embryos.....	80
Figure 25: Successful sgRNA directed deletion of <i>nphp2/invs</i> via CRISPR/Cas9 .....	81
Figure 26: Non-sense mediated decay (NMD) in heterozygous carriers of premature termination codons (PTCs).....	86
Figure 27: How to avoid transcriptional adaptation (TA) when designing loss-of-function alleles. ....	92

## **Lebenslauf**

Diese Seite enthält persönliche Daten. Sie ist deshalb nicht Bestandteil der Veröffentlichung.

## Eidesstattliche Versicherung

Eidesstattliche Versicherung gemäß § 8 Absatz 1 Nr. 3 der Promotionsordnung der Universität Freiburg für die Medizinische Fakultät

1. Bei der eingereichten Dissertation zu dem Thema

### **Characterization of zebrafish lines with mutations in the nephronophthisis-associated genes *nphp1*, *nphp2*, *nphp4* and *nphp8***

handelt es sich um meine eigenständig erbrachte Leistung.

2. Ich habe nur die angegebenen Quellen und Hilfsmittel benutzt und mich keiner unzulässigen Hilfe Dritter bedient. Insbesondere habe ich wörtlich oder sinngemäß aus anderen Werken übernommene Inhalte als solche kenntlich gemacht. Niemand hat von mir unmittelbar oder mittelbar geldwerte Leistungen für Arbeiten erhalten, die im Zusammenhang mit dem Inhalt der vorgelegten Dissertation stehen.
3. Die Dissertation oder Teile davon habe ich bislang nicht an einer Hochschule des In- oder Auslands als Bestandteil einer Prüfungs- oder Qualifikationsleistung vorgelegt.
4. Die Richtigkeit der vorstehenden Erklärungen bestätige ich.
5. Die Bedeutung der eidesstattlichen Versicherung und die strafrechtlichen Folgen einer unrichtigen oder unvollständigen eidesstattlichen Versicherung sind mir bekannt.

Ich versichere an Eides statt, dass ich nach bestem Wissen die reine Wahrheit erklärt und nichts verschwiegen habe.

Freiburg, den 01.03.2023

---

Ort und Datum

---

Unterschrift

## Erklärung zum Eigenanteil

### Dissertation

Die vorliegende Dissertation zur Erlangung des Medizinischen Doktorgrades wurde von mir, Nicolas Kayser, verfasst.

\*Einzelne Daten betreffend die Entwicklung der Kloakenregion in der F1 Generation wurden, zu Zwecken der Beurteilung von einer Kompensation zwischen den Generationen F1 und F2, aus der Dissertation von Friedemann Zaiser übernommen und im Text dementsprechend gekennzeichnet.

- Konzeption der Gesamtidee der Studie: Prof. Dr. G. Walz, PD Dr. T. A. Yakulov
- Betreuung der Arbeit: PD Dr. T. A. Yakulov
- Durchführung der Versuche: Nicolas Kayser, (Friedemann Zaiser\*)
- Technische Unterstützung bei den Laborversuchen: Annette Schmitt (MTA) und Carina Kramer (CTA)
- Datenerhebung und Ergebnisauswertung: Nicolas Kayser, (Friedemann Zaiser\*)
- Interpretation der Ergebnisse / Konzeption weiterer Versuche: PD Dr. T. A. Yakulov, Nicolas Kayser, Prof. Dr. G. Walz
- Literaturrecherche: Nicolas Kayser

### Publikation

Aus Bestandteilen der Daten dieser Dissertation ging eine Publikation mit dem Titel: „Clock genes rescue *nphp* mutations in zebrafish“ hervor. Diese wurde im Juli 2022 im Fachjournal *Human Molecular Genetics* veröffentlicht.

Die Studie wurde von Prof. Dr. G. Walz und PD Dr. T. A. Yakulov konzipiert.

Die Publikation wurde von PD Dr. T. A. Yakulov verfasst.

An der Publikation beteiligte Personen waren: Nicolas Kayser, Friedemann Zaiser, Anna C. Veenstra, Hui Wang, Burulca Göcmen, Priska Eckert, Prof. Dr. Anna Köttgen, Prof. Dr. Gerd Walz, PD Dr. Toma A. Yakulov.

Beiträge von Nicolas Kayser:

- Kreuzung, Aufzucht, phänotypische Beurteilung bezüglich Glomerulum Zysten und anschließende Genotypisierung von mutierten Zebrafischen in *nphp4* und *nphp8* (F1)  
(Daten für Abbildungen 2A(unten), 3A (rechts), 4A (rechts), 4D (rechts), 5A)
- Kreuzung, Aufzucht, phänotypische Beurteilung bezüglich Kloakenregion, Glomerulum Zysten und anschließende Genotypisierung von mutierten Zebrafischen in *nphp4* und *nphp8* (F2)  
(Daten für Abbildungen 2B, 3B-F, 4B, 4D (rechts), 4E)
- Morpholino Oligonukleotid Knockdown von *nphp4* mit phänotypischer Beurteilung von Kloakenregion und Glomerulum Zysten  
(Daten für Abbildung 5)
- phänotypische Beurteilung der Orientierung der Herzschleife, Perikardödem, Hydrozephalus und Körperkrümmung bei mutierten Zebrafischen in *nphp4* und *nphp8* (F2)  
(Bilder und Daten für Abbildung S2, S3)